DEVELOPMENT OF FUNCTIONAL XOR DNA-BASED LOGIC GATE IN ENZYME-FREE BIOLOGICAL CIRCUIT

PEERAPAT INTALUCK

**A THESIS SUBMITTED IN PARTIAL FULFILLMENT
OF THE REQUIREMENTS FOR THE DEGREE OF
DOCTOR OF PHILOSOPHY (BIOTECHNOLOGY)
FACULTY OF GRADUATE STUDIES
MAHIDOL UNIVERSITY
2014**

Thesis
entitled

DEVELOPMENT OF FUNCTIONAL XOR DNA-BASED LOGIC GATE IN ENZYME-FREE BIOLOGICAL CIRCUIT

.....
Mr. Peerapat Intaluck
Candidate

.....
Prof. Prasit Palittapongarnpim,
M.D.
Major advisor

.....
Prof. Watanalai Panbangred,
Dr.Eng
Co-advisor

.....
Lect. Boonsit Yimwadsana,
Ph.D.
Co-advisor

.....
Lect. Radeekorn Akkarawongsapat,
Ph.D.
Co-advisor

.....
Prof. Banchong Mahaisavariya,
M.D., Dip Thai Board of Orthopedics
Dean
Faculty of Graduate Studies
Mahidol University

.....
Assoc. Prof. Chuenchit Boonchird, Ph.D.
Program Director
Doctor of Philosophy Program in
Biotechnology
Faculty of Science , Mahidol University

Thesis
entitled

DEVELOPMENT OF FUNCTIONAL XOR DNA-BASED LOGIC GATE IN ENZYME-FREE BIOLOGICAL CIRCUIT

was submitted to the Faculty of Graduate Studies, Mahidol University
for the degree of Doctor of Philosophy (Biotechnology)
on
April 18, 2014

.....
Mr. Peerapat Intaluck
Candidate

.....	.....
Prof. Prasit Palittapongarnpim, Ph.D. Member	Asst. Prof. Sujinda Thanaphum, M.D. Chair
.....	.....
Prof. Watanalai Panbangred, Dr.Eng Member	Lect. Boonsit Yimwadsana, Ph.D. Member
.....	.....
Lect. Radeekorn Akkarawongsapat, Ph.D. Member	Lect. Anuttara Udomprasert, Ph.D. Member
.....	.....
Prof. Banchong Mahaisavariya, M.D., Dip Thai Board of Orthopedics Dean Faculty of Graduate Studies Mahidol University	Prof. Skorn Mongkolsuk, Ph.D. Dean Faculty of Science Mahidol University

ACKNOWLEDGEMENTS

The success of this thesis can be succeeded by the attentive support from Prof. Prasit Palittapongarnpim, Prof. Watanalai Panbangred, Dr. Boonsit Yimwadsana and Dr. Radeekorn Akkarawongsapat for precious knowledge and suggestions during my life as candidate of Doctor of Philosophy degree. I would like to gratefully thank to all supports from Microbiology department for space and facility in B611 room and also K410 members. I would like to thank to Dr. Praweenuch Penpassakarn for providing comfort treatment in many experimental skills. At last, I would like to thank to all committees in my thesis defense, Asst. Prof. Sujinda Thanaphum, Prof. Prasit Palittapongarnpim, Prof. Watanalai Panbangred, Dr. Boonsit Yimwadsana, Dr. Radeekorn Akkarawongsapat and Dr. Anuttara Udomprasert.

Peerapat Intaluck

DEVELOPMENT OF FUNCTIONAL XOR DNA-BASED LOGIC GATE IN ENZYME-FREE BIOLOGICAL CIRCUIT

PEERAPAT INTALUCK 4801130 SCBT/D

Ph.D. (BIOTECHNOLOGY)

THESIS ADVISORY COMMITTEE: PRASIT PALITTAPONGARNPIM, MD., WATANALAI PANBANGRED, Dr.Eng, BOONSIT YIMWADSANA, Ph.D., RADEEKORN AKKARAWONGSAPAT, Ph.D.

ABSTRACT

DNA computing is an emerging field in nanotechnology with the purpose of using DNA molecules to execute the computing processes as in conventional computer. Development of DNA computing shows the capability of DNA molecules for solving some kinds of mathematical problems; however, the universality for other kinds of problems is lacking. This thesis reports the development of signal synchronization system or "separator system" by utilizing the hairpin structure of DNA molecule in order to control the state of the input strand signal to be ON or OFF in enzyme-free condition. Two aspects of the separator system were analyzed: data leakage and activation level via separator strand. By optimizing lengths of various parts in the separator system (i.e. stem region, loop region, separator strand, and related downstream logic gate structure for cascading circuit application), we show that the length of 14 bases of the stem region is optimal for signal activation and data leakage prevention. The results also show an increase of activation level when a 4-extra-base-extended separator strand was applied to the hairpin structure with more than 14 bases the in loop region.

We also develop an XOR DNA-based logic gate, which is able to execute computing process correctly with cascading circuit design in an enzyme-free condition. According to our design, the optimization experiments suggest an extra seven bases as clamps for $X_{in}Y_{in}$ complex in order to prevent cross-activation reaction with the XOR logic gate up to 92.9%. Furthermore, full-adder DNA-based logic gate development for enzyme-free system is reported in this thesis. We introduce two methods for the full-adder system: 3-way-junction structure and non-assembly system. The results show the possibility of the non-assembly system to execute 1-bit full-adder operation and also suggest the possibility of multiple-bit circuit construction with the non-assembly system.

KEY WORDS: DNA COMPUTING / ENZYME-FREE CASCADING CIRCUIT / DNA SYNCHRONIZATION / XOR DNA-BASED LOGIC GATE / DNA-BASED FULL ADDER

105 pages

การสร้าง XOR DNA-Based Logic Gate เพื่อใช้งานในวงจรชีวภาพที่ปราศจากเอนไซม์
DEVELOPMENT OF FUNCTIONAL XOR DNA-BASED LOGIC GATE IN ENZYME-FREE BIOLOGICAL CIRCUIT

พีรภัทร์ อินทลักษ์ 4801130 SCBT/D

ปร.ด. (เทคโนโลยีชีวภาพ)

คณะกรรมการที่ปรึกษาวิทยานิพนธ์ : ประสิทธิ์ ผลิตผลการพิมพ์, MD., วัฒนาลัย ปานบ้านเกร็ด, Dr.Eng, บุญสิทธิ์ ยิ้มวาสนา, Ph.D., รดีกร อัครวงศาพัฒน์, Ph.D.

บทคัดย่อ

DNA computing เป็นศาสตร์ที่ถูกพัฒนาขึ้นมาในด้านนาโนเทคโนโลยี โดยมีจุดประสงค์เพื่อใช้สาย DNA ในการทำการคำนวณเพื่อแก้ปัญหาต่างๆ เช่นเดียวกับคอมพิวเตอร์ในยุคปัจจุบัน พัฒนาการของ DNA computing ได้แสดงให้เห็นถึงความสามารถของสาย DNA ที่สามารถทำการคำนวณ เพื่อแก้ปัญหาทางคณิตศาสตร์บางประเภทได้อย่างมีประสิทธิภาพ อย่างไรก็ตาม DNA computer ที่ถูกพัฒนาขึ้นยังขาดความสามารถในการทำงานที่หลากหลายไป

งานวิจัยชิ้นนี้ จึงทำการพัฒนาระบบ ที่ช่วยให้กระบวนการคำนวณใน DNA computing สามารถ ทำการคำนวณได้อย่างเป็นลำดับขั้นตอนมากขึ้น ด้วย separator system ซึ่งสามารถทำงานได้ในวงจรที่ปราศจากเอนไซม์ โดยระบบนี้ จะใช้ประโยชน์จากความสามารถในการเกิดโครงสร้าง hairpin ของสาย DNA ในการควบคุมภาวะของสัญญาณในวงจร ให้อยู่ในภาวะที่พร้อมทำงาน (ON) หรือ ไม่พร้อมทำงาน (OFF) เราได้ทำการตรวจวัดความสามารถของ separator system ในสองเรื่องด้วยกัน คือ การป้องกันสัญญาณรั่วไหลภายในวงจรและความสามารถในการเปลี่ยนภาวะของสัญญาณด้วย separator strand โดยการทดสอบด้วยการใช้ความยาวที่ต่างกันในส่วนของ stem และ ส่วนของ loop ของโครงสร้าง hairpin อีกทั้งทำการทดสอบการใช้ extended separator และโครงสร้างที่ต่างกันของ logic gate ที่อยู่ในขั้นตอนถัดไปภายในวงจรเดียวกัน ผลการทดลองแสดงให้เห็นว่า ความยาว 14 เบส เป็นความยาวที่เหมาะสมสำหรับ stem ในการป้องกันการรั่วไหลของสัญญาณได้อย่างมีประสิทธิภาพ อีกทั้งช่วยให้ separator strand สามารถทำงานในการเปลี่ยนภาวะของสัญญาณได้อย่างเหมาะสม นอกจากนี้ การใช้ extended separator ที่มีความยาวพิเศษ 4 เบสจาก separator ปกติ สามารถช่วยให้การเปลี่ยนภาวะของสัญญาณทำได้ดีขึ้น เมื่อโครงสร้าง hairpin มีความยาวของ loop มากขึ้น

นอกจากนี้ เราได้พัฒนา XOR logic gate จากสาย DNA ที่สามารถทำงานได้อย่างถูกต้องในวงจรชีวภาพที่ปราศจากเอนไซม์ ผลการทดลองแสดงให้เห็นว่า การออกแบบของเรานั้นต้องการ 7 เบสที่หัวและท้ายของ $X_{in}Y_{in}$ complex สำหรับทำหน้าที่ป้องกันการลัดวงจร กับ XOR logic gate ได้ถึง 92.9%

ท้ายสุดนี้ เราได้รายงานถึงการออกแบบโครงสร้าง full-adder โดยแนะนำการออกแบบ 2 วิธี คือ โครงสร้าง 3-way-junction และ ระบบ non-assembly ผลการทดลองได้แสดงให้เห็นถึงความเป็นไปได้ของระบบ non-assembly ในการทำงาน การบวกเลขฐานสอง 1 หลักได้อย่างถูกต้องในระบบที่ปราศจากเอนไซม์ อีกทั้งแสดงให้เห็นถึงความเป็นไปได้ในการออกแบบวงจร ที่สามารถทำการบวกเลขฐานสองหลายหลักได้

105 หน้า

CONTENTS

CONTENTS (cont.)

CONTENTS (cont.)

LIST OF TABLES

LIST OF FIGURES

LIST OF FIGURES (cont.)

LIST OF FIGURES (cont.)

LIST OF FIGURES (cont.)

LIST OF FIGURES (cont.)

LIST OF ABBREVIATIONS

Abbreviation	
^{o}C	Degree celcius
A	Adenine
bit(s)	Binary digit(s)
bps	base pairs
C	Cytosine
DNA	Deoxyribonuclic acid
EDTA	Ethylenediaminetetraacetic acid
G	Guanine
MFE	Minimum Free Energy
NP-complete	Non-deterministic polynomial time
PAGE	Polyacrylamide gel electrophoresis
rpm	round per minute
SAT problem	satisfaction problem
T	Thymine
TAE	Tris acetate EDTA
TE	Tris EDTA
T_m	Melting temperature
U	Uracil
UV	Ultraviolet
µM	Micromolar
µL	Microlitre

CHAPTER I
INTRODUCTION

1.1 Deoxyribonucleic acid

Discovery of deoxyribonucleic acid (DNA) was firstly reported by Friedrich Miescher in 1878 and called as "nuclein" [1]. Later, five nitrogenous bases and phosphate-deoxyribose backbone were identified [2][3]. In 1953, James Watson and Francis Crick revealed a double-helix model of the DNA structure based on X-ray diffraction image [4]. The model was demonstrated to be valid as several reports published in the same year were shown to support the Watson-Crick DNA double-helix model [5-9].

Deoxyribonucleic acid (DNA) is a molecule that is composed of five essential elements: Carbon (C), Hydrogen (H), Oxygen (O), Nitrogen (N) and Phosphorus (P). Each DNA molecule can be divided into two parts: phosphate-deoxyribose backbone and nitrogenous base. Phosphate-deoxyribose backbone is a polymer chain of pentose (five-carbon) sugars in the form of furanose ring with phosphate group (PO_4^{3-}). The phosphate-deoxyribose sugars are linked by phosphodiester bonds between the hydroxyl group of the fifth carbon position of former sugar (5') and the phosphate group at the third position of the latter sugar (3') (Figure 1.1).

Nitrogenous base is a non-polar heterocyclic aromatic compound that links to the phosphate-deoxyribose backbone at the first carbon position (1'). There are two types of nitrogenous bases: pyrimidine and purine. Pyrimidine is a heterocyclic compound of four carbon atoms and two nitrogen atoms. There are two pyrimidine derivatives found in DNA: cytocine (C) and thymine (T), and one derivative, uracil (U), in RNA. Purine is a heterocyclic aromatic compound consisting of pyrimidine ring and imidazole ring. There are two purine derivative compounds found in natural nucleic acids: adenine (A) and guanine (G) (Figure 1.2).

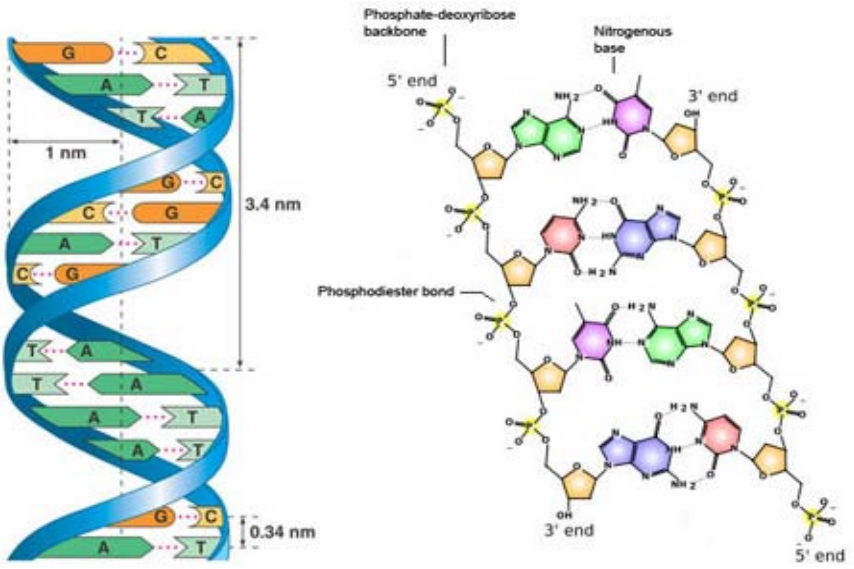

Figure 1.1 The DNA structure. (Left) Illustration of DNA double helix [10]. (Right) The chemical structure illustration of phosphate-deoxyribose backbone linked with phosphodiester bonds and base pairing with hydrogen bonds between nitrogenous bases with adjacent strand [11].

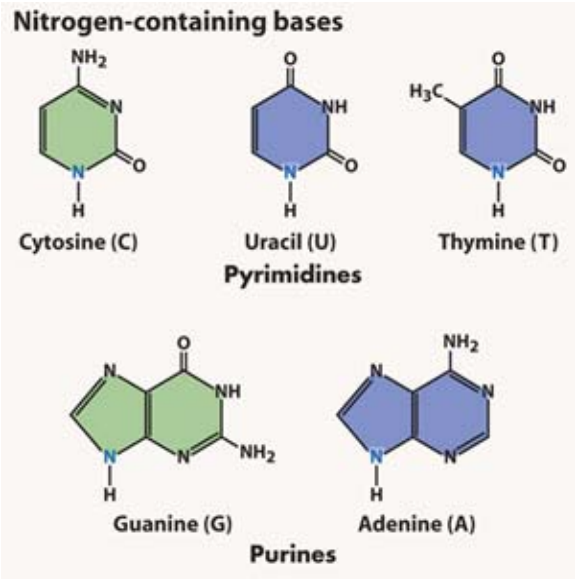

Figure 1.2 Chemical structures of natural DNA purines (A and G) and pyrimidines (C and T) and RNA purines (A and U) and pyrimidines (C and G) nitrogenous bases [12].

1.1.1 Formation of double-stranded DNA

In nature, DNA molecule is mostly found in pairs. The pairs of DNA molecule are arranged in an anti-parallel direction, one from 5' end to 3' end and another from 3' end to 5' end. These two DNA strands form into right-handed double-helix structure (B-DNA) which primarily is stabilized by hydrogen bonds between nucleotides and nitrogen base-stacking. The double helix structure size is 10 Å in radius and 34 Å in length for each turn of helix (Figure 1.1). Each turn of helix can be divided into major groove and minor groove with groove width of 22 Å and 12 Å, respectively. However, there are variations on helical structure formation of DNA. A-DNA is a right-handed helix DNA similar to common B-DNA but wider in radius and shorter in length per turn. The A-DNA can be found in low humidity and high salt concentration condition. There is also a left-handed helix DNA called Z-DNA. Z-DNA can be occurred in many conditions such as high torsional strain during transcription and high salt concentration condition. The geometry characteristics of alternative structures are shown in Figure 1.3 and Table 1.1.

Table 1.1 Characteristics of alternative double-helix DNA structure.

Attribute	A-DNA	B-DNA	Z-DNA
Helix turn	Right-handed	Right-handed	Left-handed
Repeating unit	1 bp	1 bp	2 bp
bp/turn	11	10.5	12
Length per turn	28.2 Å	33.2 Å	45.6 Å
Diameter	23 Å	20 Å	18 Å

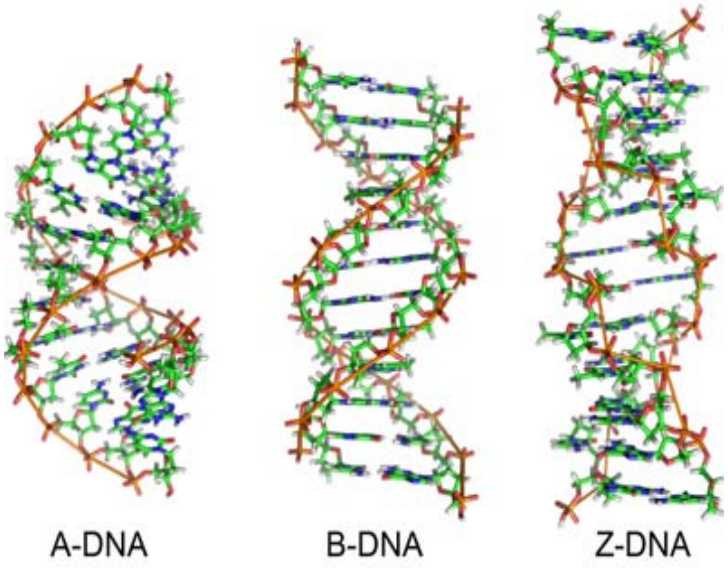

Figure 1.3 Alternative double-helix DNA structures in different conditions. The right-handed B-DNA is found commonly in organisms. The right-handed A-DNA can be found in low humidity and high salt concentration condition. The left-handed Z-DNA can be rarely found during transcriptional process in organisms. It also can be found in high salt concentration condition [13].

The double helix DNA structure is stabilized by two chemical interactions: inter-strand base pairing and intra-strand base stacking. The base pairing is a hydrogen bond interaction between two bases on 2 distinct DNA strands. Hydrogen bond in base pairing occurs in specific arrangement, A-T and A-U base pairings form two hydrogen bonds and G-C base pairing forms three hydrogen bonds (Figure 1.4). As this base pairing is hydrogen bond, helix strand dissociation can be occurred. As a result, the double-stranded DNA is stable at room temperature especially with high GC content although the higher temperature will increase strand dissociation possibility. However, base pairing or GC content is not the only factor for DNA double helix stability, base stacking also plays a major role. Base stacking or so called "π- π stacking (pi stacking)" is an intra-strand interaction between bases in the same strand (Figure 1.4). Pi-stacking is the Van de Waals force between aromatic ring and its adjacent ring. The difference in neighbouring bases, therefore, will result in changes of helix stability even with the same length and bases. For example, double stranded DNA with

5'ATAT 3' - 3'TATA5' has free energy different from that with 5'AATT 3' - 3'TTAA5'.

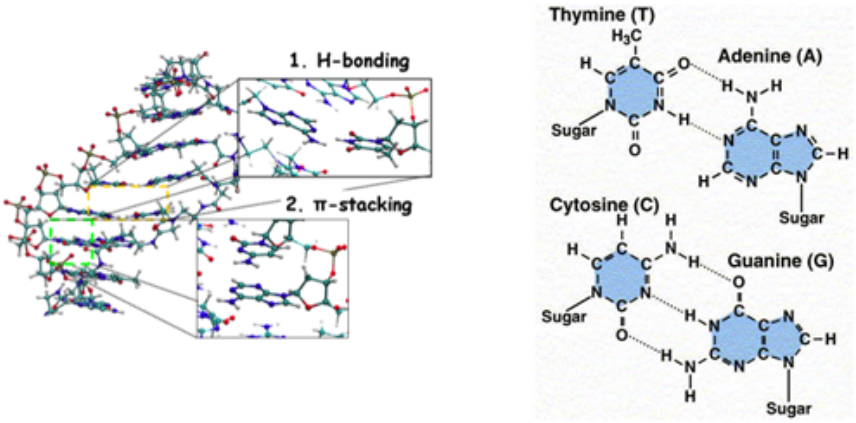

Figure 1.4 The chemical interaction within the double helix DNA structure. The inter-strand interaction "hydrogen bonding" and intra-strand interaction "π- π stacking" (left) [14]. The illustration of nitrogenous bases and their hydrogen bonding interactions between A-T and G-C (right) [15].

In order to measure DNA double helix stability, parameter called "melting temperature" or T_m was defined. The melting temperature is a parameter that indicates the temperature in which half of double-stranded DNA molecules turn into single-stranded DNA molecules. T_m depends on strand length and specific oligonucleotide sequence. Higher GC content, therefore, results in higher T_m value. The T_m parameter of a short DNA strand (14-20 bases) can be briefly approximate by the following equation.

$$T_m = 2(A + T) + 4(G + C)$$

A, T, C and G are the number of each nucleotide, Adenine, Thymine, Cytosine and Guanine, respectively.

In case of a long DNA strand or the DNA structure with complexity, a more accurate equation is necessary. The state of strand dissociation can be shown as the following equation.

$$AB \longleftrightarrow A + B$$

While A and B represent each strand of the double-stranded DNA. So, the equilibrium constant of this equation is $K = \frac{[A][B]}{[AB]}$. In order to calculate free energy of the AB structure of this two state equation. The Van´t Hoff equation is applied.

$$\Delta G^{o} = - RT\ln K$$

While R is ideal gas constant and T is temperature in Kelvin. So, the equation for strand dissociation is shown as the following equation.

$$\Delta G^{o} = - RT\ln \frac{[A][B]}{[AB]}$$

Since T_m is the state that half of [AB] turn into [A] and [B], the equation of this state is shown as the following equation.

$$\Delta G^{o} = - RT_m\ln \frac{\frac{[AB][AB]}{2 \quad 2}}{\frac{[AB]}{2}}$$

$$T_m = - \frac{\Delta G^{o}}{R\ln \frac{[AB]}{2}}$$

From this equation, when thermodynamics parameters, ΔG^{o} or ΔH^{o} and ΔS^{o}, is/are known, the melting temperatures of those strands can be predicted. However, these thermodynamics parameters for oligonucleotides were studied and estimated by Nearest-neighbour model.

The Nearest-neighbour model was introduced by Breslauer and colleagues in 1986 [16] and further developed by Santa Lucia and colleagues [17,18]. There are 10 possible Nearest-neighbour parameters for this model, AA/TT, AT/TA, TA/AT, CA/GT, GT/CA, CT/GA, GA/CT, CG/GC, GC/CG and GG/CC. These parameters are

studied and provided to the condition of 1M NaCl at 37 ºC. The Nearest-neighbour parameters are shown in Table 1.2.

Table 1.2 Thermodynamics parameter of base stacking estimated by The Nearest-neighbour model [17].

Propagation sequence	ΔH° (kcal mol^{-1})	ΔS° (e.u.)	ΔG°_{37} (kcal mol^{-1})
AA/TT	−7.6	−21.3	−1.00
AT/TA	−7.2	−20.4	−0.88
TA/AT	−7.2	−21.3	−0.58
CA/GT	−8.5	−22.7	−1.45
GT/CA	−8.4	−22.4	−1.44
CT/GA	−7.8	−21.0	−1.28
GA/CT	−8.2	−22.2	−1.30
CG/GC	−10.6	−27.2	−2.17
GC/CG	−9.8	−24.4	−2.24
GG/CC	−8.0	−19.9	−1.84
Initiation	+0.2	−5.7	+1.96
Terminal AT penalty	+2.2	+6.9	+0.05
Symmetry correction	0.0	−1.4	+0.43

In some DNA secondary structures, all oligonucleotides are not completely match and leave the excess bases at the end of the strand as the "dangling end". The free energy of DNA structure with dangling end, therefore, is necessary to be corrected. Since there are four bases A, T, C and G, so there are 32 Nearest-neighbour parameters for dangling end calculation. The Nearest-neighbour parameters for dangling ends at the condition of 1M NaCl at 37 ºC are shown in Table 1.3.

Table 1.3 Thermodynamics parameters of dangling bases estimated by The Nearest-neighbour model [17].

Dangling end sequence	X = A		X = C		X = G		X = T	
	ΔH°	ΔG°_{37}	ΔH°	ΔG°_{37}	ΔH°	ΔG°_{37}	ΔH°	ΔG°_{37}
5′-dangling ends								
XA/T	0.2	−0.51	0.6	−0.42	−1.1	−0.62	−6.9	−0.71
XC/G	−6.3	−0.96	−4.4	−0.52	−5.1	−0.72	−4.0	−0.58
XG/C	−3.7	−0.58	−4.0	−0.34	−3.9	−0.56	−4.9	−0.61
XT/A	−2.9	−0.50	−4.1	−0.02	−4.2	0.48	−0.2	−0.10
3′-dangling ends								
AX/T	−0.5	−0.12	4.7	0.28	−4.1	−0.01	−3.8	0.13
CX/G	−5.9	−0.82	−2.6	−0.31	−3.2	−0.01	−5.2	−0.52
GX/C	−2.1	−0.92	−0.2	−0.23	−3.9	−0.44	−4.4	−0.35
TX/A	−0.7	−0.48	4.4	−0.19	−1.6	−0.50	2.9	−0.29

As all of ΔG^o parameters have been approximated, the stability of DNA secondary structure can be estimated with the following equation.

$$\Delta G^o_{total} = \Delta G^o_{initiation} + \Delta G^o_{symmetry} + \sum \Delta G^o_{stack} + \Delta G^o_{terminal} + (\Delta G^o_{dangling})$$

$\Delta G^o_{initiation}$ is a constant value equal to 1.96

$\Delta G^o_{symmetry}$ is a value for self-complementary calculation equal to 0.43

$\sum \Delta G^o_{stack}$ is total ΔG^o of nucleotides and their adjacent nucleotides along the DNA strands

$\Delta G^o_{terminal}$ is a value for penalty of A/T termination at each end of a duplex equal to 0.05

$\Delta G^o_{dangling}$ is a value for dangling end calculation in case of DNA structure with dangling end

1.1.2 Complex structure of DNA

Rather than common double-helix structure, the nucleic acid molecules are able to form many alternative secondary structures as follows,

Stem-loop structure or so called "hairpin" is the secondary structure formed by a single-stranded nucleic acid. The hairpin structure is composed of two parts: the stem region and the loop region. The stem region is the double-stranded region while the loop region is the short single-stranded unpaired region. The stem-loop structure can be formed into a larger structure called "clover-leaf" which is the X-junction structure with three branches of hairpin. The clover-leaf structure is typically found in transfer RNA (tRNA) (Figure 1.5).

Holliday junction or so called "X-junction" is the secondary structure formed by four nucleic acid strands. These four strands bind together and form the 4-way junction structure with double-stranded branches. The Holliday junction structure can be found in organism during homologous segment exchange of chromatids in prophase of meiosis I. The Holliday junction structure is shown in Figure 1.6.

Triple-helix DNA is a secondary structure comprising of three nucleic acid strands. The triple-helix DNA is formed by the Hoogsteen base-pairing (variation of base-pairing) of the third strand to the major groove of Watson-Crick double-helix structure. The triple-helix DNA is occurred only with homopurine or homopyrimidine strand. There are two possible triple-helix DNA structures. The first one is formed by homopyrimidine third strand with Hoogsteen base-pairing in the parallel direction. The second one is formed by homopurine third strand with reverse Hoogsteen base-pairing in the anti-parallel direction. The base triads pairing of the triple-helix DNA is shown in Figure 1.7 [19].

G-quadruplex is a secondary structure formed by four guanine bases in the single-stranded region via Hoogsteen hydrogen-bonding. These guanine bases form into square planar structure called "guanine tetrad". Each guanine tetrad can stack each other and form into the G-quadruplex structure. The G-quadruplex structure can be found in telomeres which reduce telomerase activity. Schematic diagram of the G-quadruplex structure and guanine tetrad are shown in Figure 1.8.

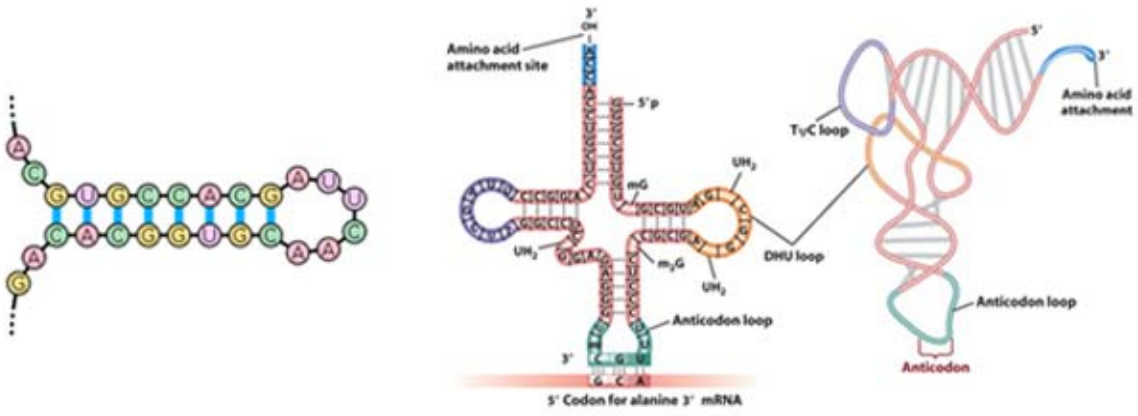

Figure 1.5 Nucleic acid stem-loop secondary structure or "hairpin" with stem region and loop region (left) [20]. The clover-leaf structure of transfer RNA (right) [21].

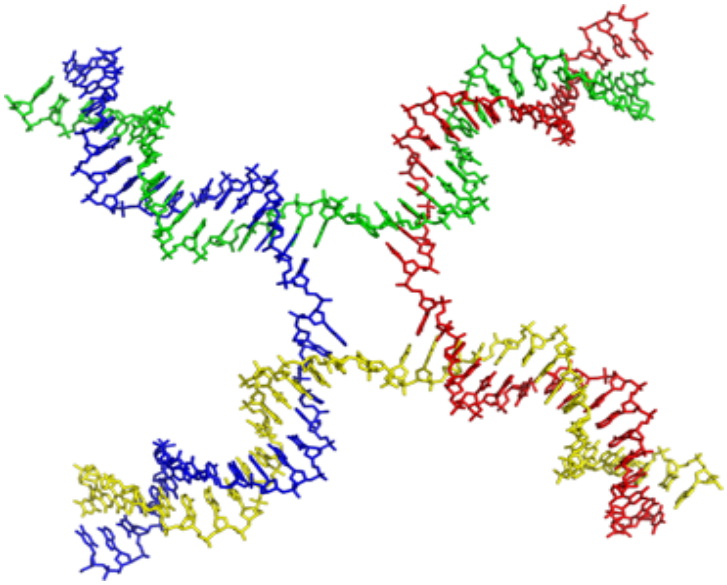

Figure 1.6 Holliday junction secondary structure or "X-junction" is the 4-way junction structure comprising of four nucleic acid strands as represented by different colors [22].

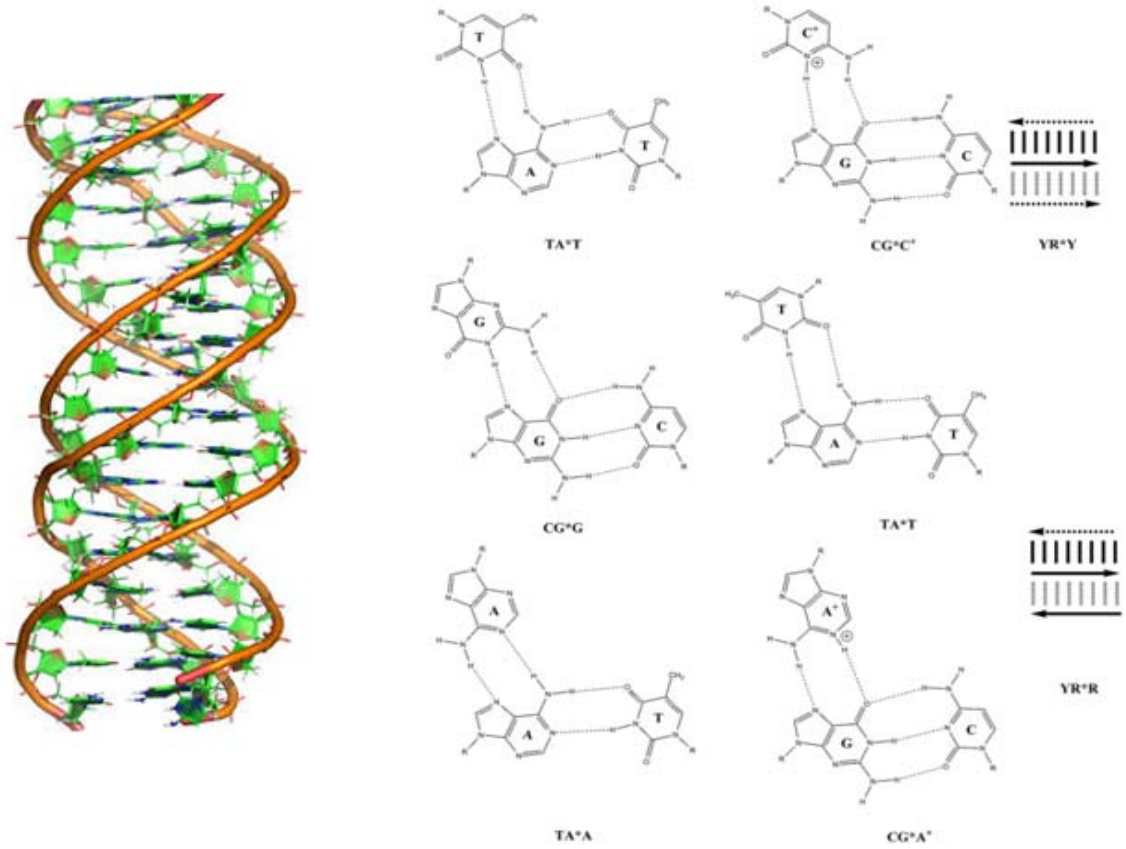

Figure 1.7 Schematic diagram of triple-helix DNA structure (left) [23]. Base triads pairing of triple-helix DNA with Hoogsteen or reverse Hoogsteen base-pairing (right) [24].

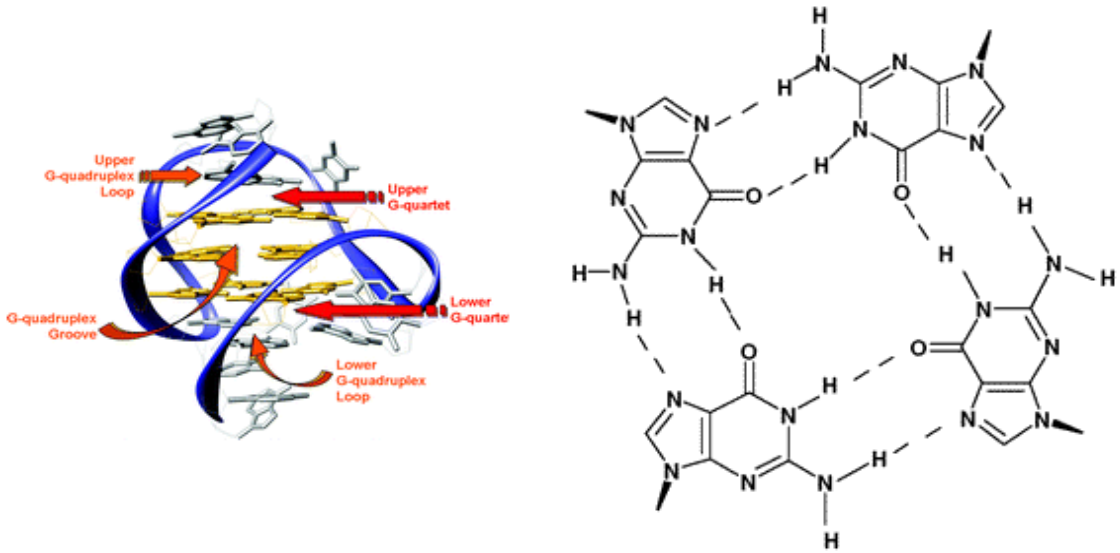

Figure 1.8. Schematic diagram of the G-quadruplex structure (left) [25]. The formation of four guanine bases as square planar or guanine tetrad (right) [26].

1.2 Introductory to DNA computing

DNA computing is a branch in the field of DNA nanotechnology. DNA computing focuses on using DNA as a major component of a computing unit instead of silicon-based computing unit in biological environment.

DNA molecule is known for long as a molecular unit involving in transcriptional process of organisms. The properties of DNA to act as a container of data for living things are recognized by the researchers to adapt the DNA molecule for use in computation. Since we consider DNA molecule as data, instead of "0" and "1" for Boolean logic in conventional silicon-based computer, the information content of single nucleotide can be A, T, C or G. In other words, only single nucleotide of DNA molecule contains 2 bits information instead of 1 bit compare to Boolean logic binary number.

The development in the field of DNA computing was initiated in year 1994 by Leonard Adleman to solve the mathematical problem called "Hamiltonian path problem" [27]. This problem is a category of graph theory question with seven vertices which the answer is to find the possible pathways that all vertices have been passed started from vertex 0 and ended with vertex 6 (Figure 1.9). Hamiltonian path problem is considered as a Non-deterministic polynomial time problem (NP-complete problem), one of the hardest types of mathematical problems, which the time required to solve this problem is increased exponentially when the problem is even more complex. However, there is no known algorithm on traditional silicon-based computer to solve this problem efficiently rather than fundamental method called "trial-error algorithm" which means the problem is challenged repeatedly until it is solved. This algorithm is, therefore, considered as "sequential computation". However, Adleman introduced the method utilizing base pairing and ligation in computing method. Since all of DNA strands, all vertices, are presented and challenged at the same time in computing solution, this method can be considered as "parallel computation". The answers are then monitored by PCR amplification and gel electrophoresis to separate the answer strands.

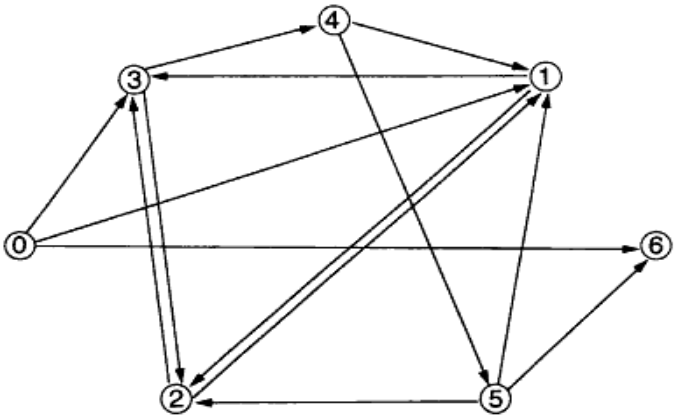

Figure 1.9 Schematic picture of seven vertices "Hamiltonian path problem" starting from vertex "0" and end with vertex "6". The possible paths are shown as arrows.

The success of Adleman's work suggests a possibility of using biological molecules, DNA in this case, to perform computation in the same manner as silicon-based computer. The results also suggest the superiority of DNA computing to perform "parallel computation". After Adleman's DNA computation work has been published, the use of DNA molecule to solve mathematical problem becomes interested by many researchers. In 1995, Lipton introduced the Aleman's method to solve another type of NP-complete problem called "satisfaction problem (SAT)" [28]. In 2000, Sakamoto and colleagues introduced the possibility of using hairpin structure formation to solve 6-variable SAT problem [29]. In 2004, Braich and colleagues demonstrated the power of DNA molecule to solve 20-variable SAT problem with 2^{20} or 1,048,576 possible truth assignments [30].

1.2.1 Boolean logic algebra

Although Adelman has introduced the method on solving mathematical problem by using DNA, the method is considered to be too specific on only a kind of problem. However, Lipton also introduced diverse computing algorithm by adjusting DNA molecule to handle binary numbers and solve mathematical problem with Boolean logic circuit in the same tradition as silicon-based computer [28]. The Boolean logic circuit is based on the Boonlean algebra which is binary computation system encoded with "1" and "0", TRUE or FALSE, to solve the question.

The Boolean logic circuit is composed of three units: input, operation and output. The input is a truth value, TRUE or FALSE, in the form of binary digits number or called "bits" which the value is "1" or "0" respectively. These inputs will be analyzed by the operation unit. The operation unit is a mathematical condition which those inputs will be considered logically. So the operation unit may be called as "logic gate" for the Boolean logic circuit in traditional computer. The result of analyzed input unit by the operation unit will be transmuted into the output unit which also is in the form of bits. The basic operations and logic gates of Boolean algebra are shown in Table 1.4 and Figure 1.10.

Table 1.4 Basic operations of Boolean algebra with truth table value.

Operations	Logic symbol	Truth table		
		Input A	Input B	Output
AND	$\wedge$	0	0	0
		0	1	0
		1	0	0
		1	1	1
OR	$\vee$	0	0	0
		0	1	1
		1	0	1
		1	1	1
NOT	$\neg$	0	-	1
		1	-	0

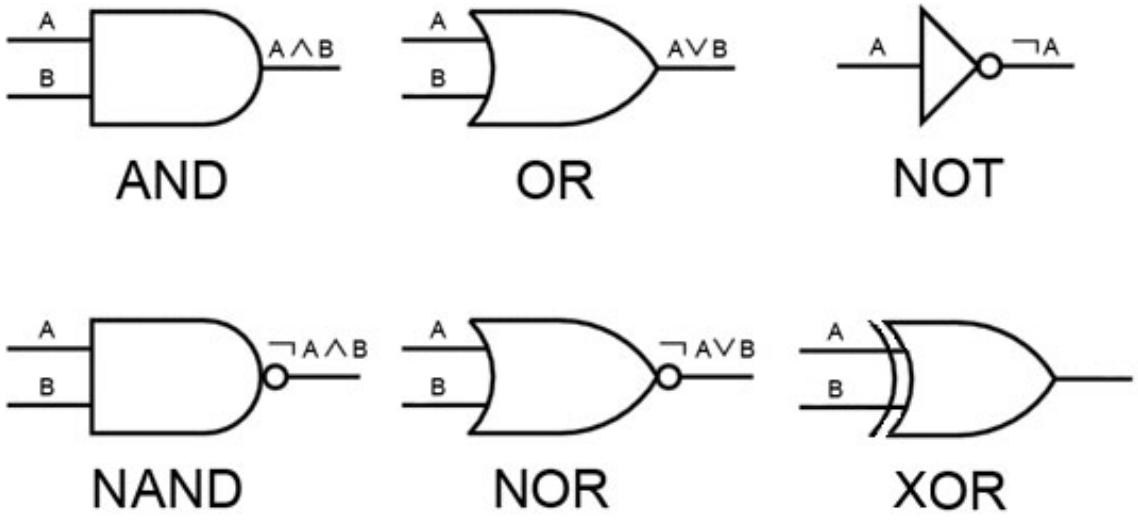

Figure 1.10 The symbol of logic gates in Boolean logic circuit. AND, OR and NOT are the simple logic gates whereas NAND, NOR and XOR are examples of complex logic gates.

Any complex propositional logic clause in Boolean algebra can be written from simple operations AND, OR and NOT. For instance, XOR is the complex logic gate which can be simplified into simple propositional logic clause as shown in the following,

$$A \text{ XOR } B = (\neg A \wedge B) \vee (A \wedge \neg B)$$

The XOR logic gate simplification is shown in Figure 1.11.

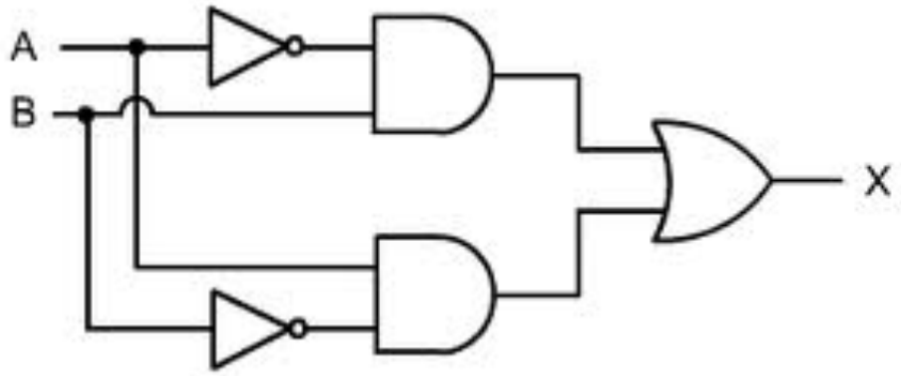

Figure 1.11 The simplified Boolean logic circuit of the complex XOR logic gate. The XOR logic gate can be simplified into a circuit of simple logic gates. A XOR B = (¬A ∧ B) ∨ (A ∧ ¬B).

1.2.2 DNA-based computation in enzyme-free system

The DNA computation based on Boolean logic was further demonstrated in 2002 by Stojanovic and colleagues [31]. In this paper, deoxyribozyme-based logic gate system, the first enzyme-free system, was introduced. The deoxyribozymes or "DNAzymes" are DNA molecules with catalytic action. Furthermore, the DNA branch migration was used in computational process and the deoxyribozyme system labeled with fluorescent dye was used to monitor the method. When all input strands were already added to the computing solution, the input strands changed the deoxyribozyme-based logic gate structure. Then, the deoxyribozyme was added in order to cleave DNA output strand at specific catalytic site and, therefore, turned into fluorescent output signal. Overall mechanism of AND deoxyribozyme-based logic gate is shown in Figure 1.12.

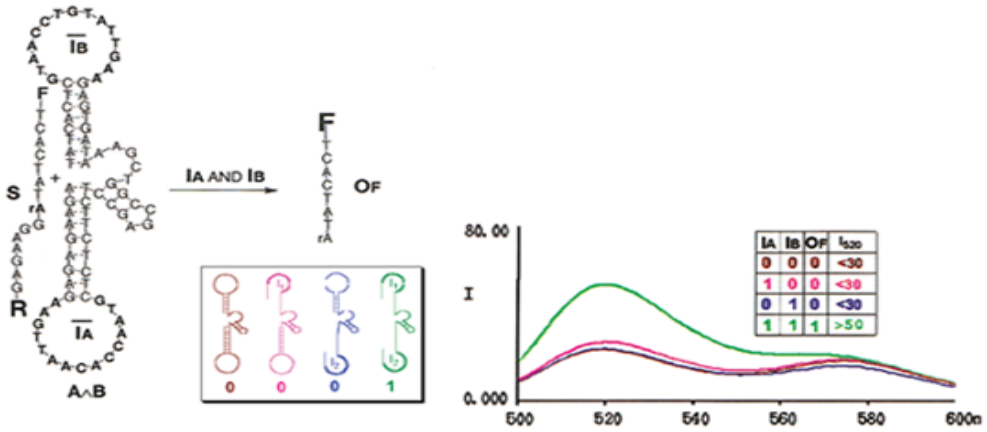

Figure 1.12 AND deoxyribozyme-based logic gate. IA and IB DNA strands function as inputs of the AND gate. Binding of IA and IB strands result in structural change of the AND gate, allowing the S strand to bind with AND gate. The deoxyribozyme, then, cleaves the S strand at catalytic site, resulting in blockage of fluorescence resonance energy transfer (FRET) within the S strand. The change of fluorescence emission wavelength is detected [31].

The deoxyribozyme-based logic gate system suggests a possibility of enzyme-free system; however, the interactions between the deoxyribozyme-based logic gates within the same circuit are troublesome since cross activation between logic gates can be occurred.

In comparative to the enzymatic DNA computing system, the enzyme-free system suggests many advantages. First, the enzymatic DNA computing system requires the specific condition in order to allow the enzyme to function properly. Second, since this system involves with the enzyme, the limitation to construct the large circuit which contains many enzymes is a major problem. So, here we are going to introduce development of DNA computation in the scope of enzyme-free system.

In 2008, Fedichkin and colleagues developed a DNA-based XOR logic gate which was able to function in enzyme-free condition [32]. They utilized the ability of DNA strand to form hairpin structure by designing their DNA-based XOR logic gate to initially form a hairpin structure. If both input strands that complemented to the sequence in the loop of the hairpin structure were added, the gate would be changed into stretched structure. However, if only one input strand was added, the gate structure remained unchanged. Although this DNA-based XOR logic gate was successful to function in the enzyme-free condition, it was unable to construct into large circuit. Since there was no output strand released, and the gate itself still formed the hairpin structure, it was difficult to connect this gate to a downstream DNA-based logic gate. The XOR hairpin DNA-based logic gate computing process is shown in Figure 1.13.

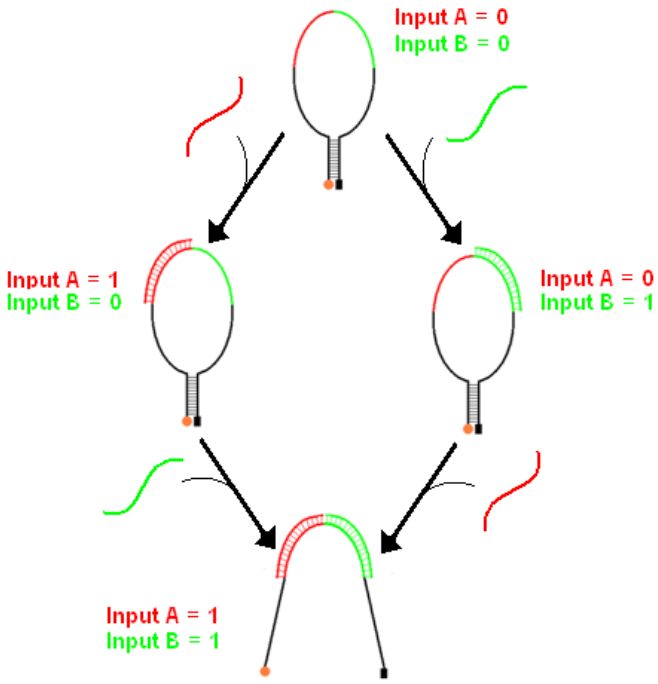

Figure 1.13 XOR hairpin DNA-based logic gate computing process. The input strands, A and B, are able to bind with complementary sequences inside the loop region of the hairpin structure. The binding of both input A and input B strands result in breakage of hairpin structure and release of fluorescence signal.

In the same year, Voelcker and colleagues also developed a DNA-based XOR logic gate [33]. They utilized the property of DNA sequence complementary. If both input strands of DNA-based XOR logic gate were presented, the DNA input strands would bind with each other. As a consequence, the computing process would not happen with significant probability. Voelcker's DNA-based XOR logic gate computing process is shown in Figure 1.14.

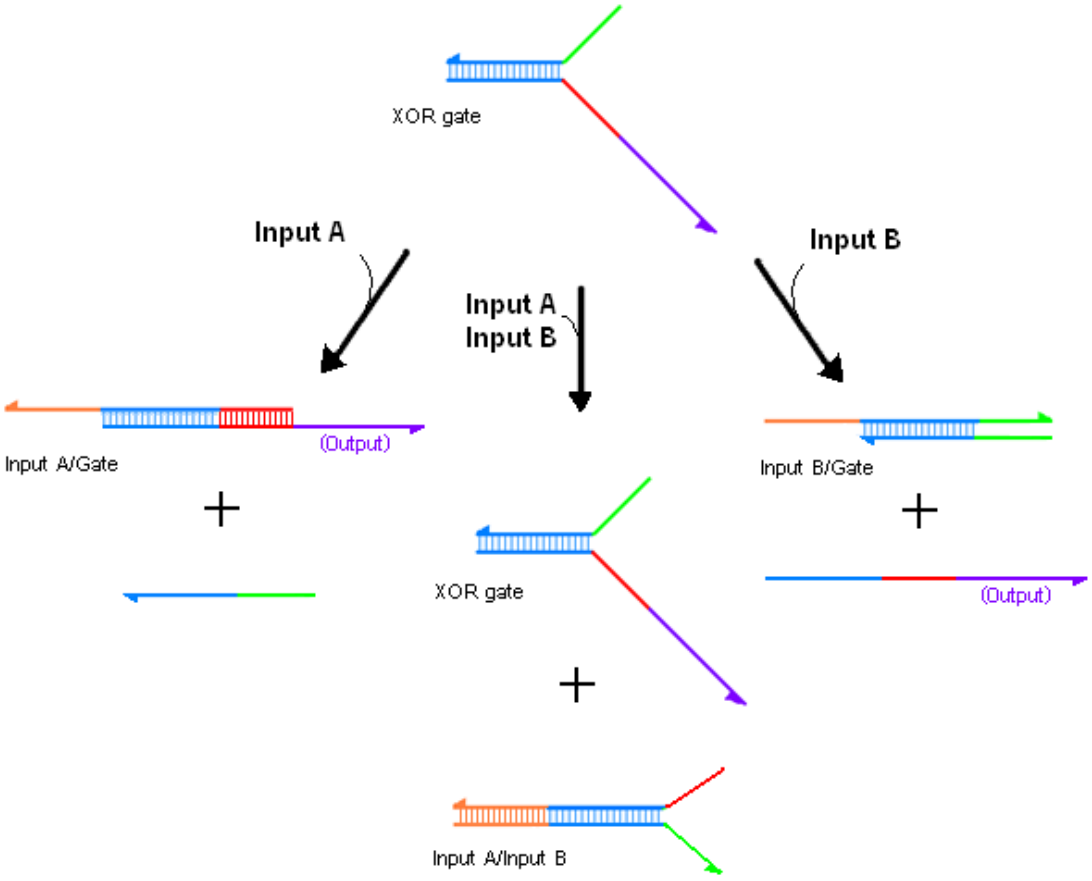

Figure 1.14 Voelcker's DNA-based XOR logic gate computing process. Toehold binding region of input A is shown in red. Toehold binding region of input B is shown in green.

Although Voelchker's DNA-based XOR logic gate produces an output strand, the strand cannot react with another DNA-based logic gate as an input right after the reaction from the first gate. This is because of the cross activation between DNA-based logic gates. In order to avoid the cross activation between DNA-based logic gates, the toe-hold bind motif of the output strand (purple part on DNA-based XOR logic gate) must be concealed (Figure 1.14).

1.2.3 DNA branch migration

As we consider the underlying mechanisms of reaction of any introduced algorithms, all mechanisms involve with the processes of DNA strand association and strand dissociation. In 1970, Lee and colleagues studied about this process of DNA *in vitro* and suggested sequential states of branch migration process [34] (Figure 1.15). Reynaldo and colleagues also studied about blunt end strand displacement in kinetics terms [35]. The result showed the effect of temperature, strand length and strand concentration on strand displacement process. In 1989, Quartin and colleagues studied the DNA branch migration with overhangs on DNA strands and compared to DNA branch migration with blunt end strands [36-37]. Results suggested effectiveness of overhang strands in DNA branch migration process. Application of DNA branch migration in DNA computing field was reported by Yurke and colleagues who introduced the term "toehold" to call the overhangs region (Figure 1.16) and also studied kinetics of toehold region with variation in lengths (Figure 1.17) [38-39]. In 2009, Zhang and Winfree reported quantitative thermodynamics kinetics of binding toehold(n) and invading toehold(m) and also reported saturation of branch migration kinetics of toehold length of 7 bases and more (Figure 1.18) [40].

The mechanisms that drive the branch migration process via toehold region is related to Gibbs free energy or the change of free energy during DNA structural change (ΔG). The Gibbs free energy parameter can be calculated by the following equation

$$\Delta G^{o} = \Delta G^{o}_{after} - \Delta G^{o}_{before}$$

ΔG^{o}_{before} parameter is the state that toehold region is a free single-stranded region

ΔG^{o}_{after} parameter is the state that toehold region binds with input strand

The binding of toehold region causes more hydrogen bonding and π- π stacking which lower the free energy of the structure. Since ΔG^{o} value is negative, the reaction is spontaneous.

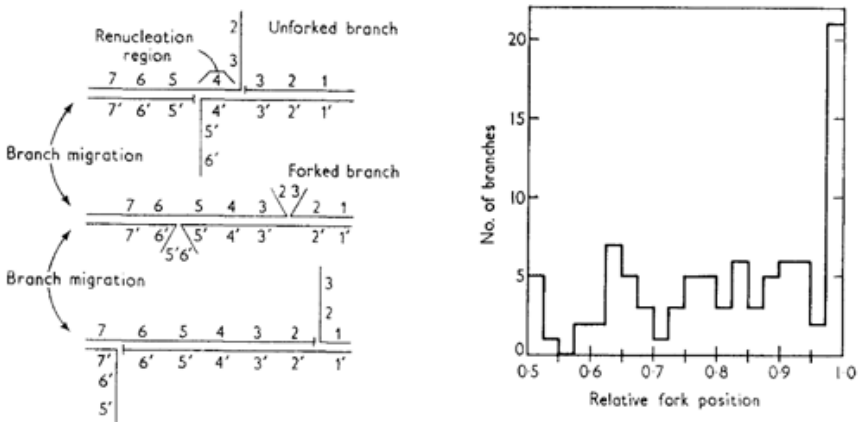

Figure 1.15 Schematic diagram of branch migration process model (left). Relative fork position of 91 repetitious branches was observed at 25 ºC. The longer branch was measured which 1.0 means the complete linear strand while 0.5 means the fork is in the middle of the branch. The results suggest the continuous process of branch migration (right) [34].

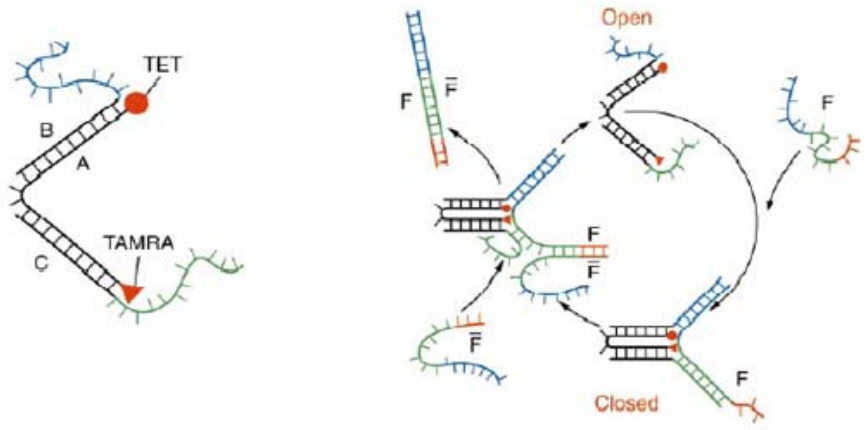

Figure 1.16 The application of DNA migration and overhang strands in DNA-based computation. The hybridization of tweezer strand A with overhang strand B and C (left). Overall mechanism of molecular tweezer interacted with fuel strand F via overhang on strand B (blue) and C (green) (right) [38].

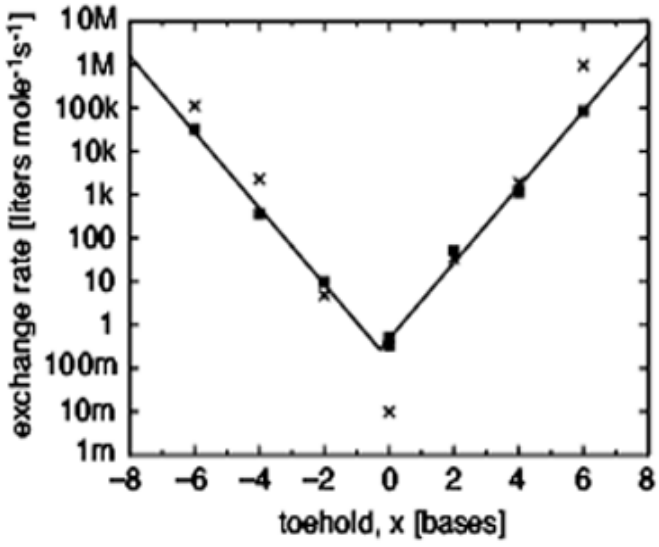

Figure 1.17 The kinetics of branch migration process with different lengths of toehold region of 2, 4 and 6 bases. The result suggests the increase of strand exchange rate due to the increase of toehold length [39].

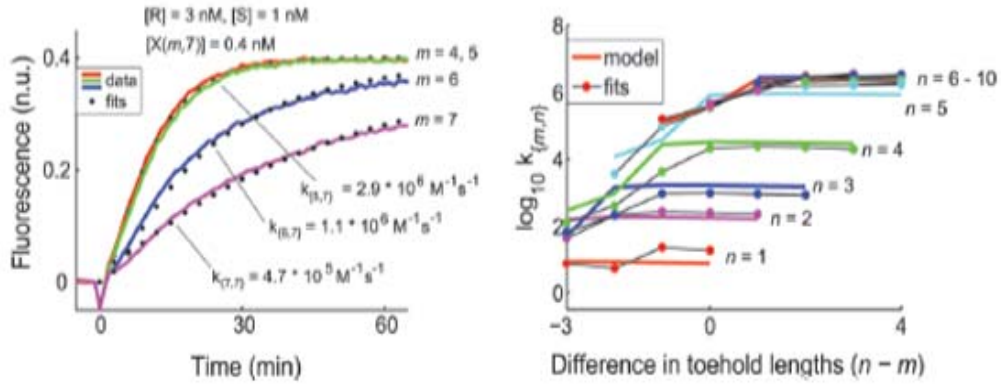

Figure 1.18 The kinetics of different toehold lengths. *m* is the length of invading toehold, double-stranded region complementary to input strand, while *n* is the length of binding toehold, single-stranded region complementary to input strand. The toehold invading length (*m*) was varied from 4 to 7 bases with the fixed 7 bases of toehold binding length (*n*) (left). The observation of kinetics saturation with toehold binding length varied from 1-10 bases. The result shows the saturation of branch migration speed with $n \geq 6$ and longer toehold binding region is necessary to the increase of toehold invading region length (right) [41].

The discovery of branch migration process via toehold region has a significant impact on the development of enzyme-free DNA-based computation. In 2003, Turberfield and colleagues developed a simple DNA-based circuit with catalytic fuel strand, a single-stranded DNA with substrate-recycling ability, based on DNA hybridization and branch migration [41]. This work suggests a possibility to construct a large-scale circuit with only nucleic acid molecules (Figure 1.19). Since then, many enzyme-free DNA-based systems have been developed. In 2004, Dirks and colleagues developed the DNA-based chain reaction with hairpin structure (Figure 1.20) [42]. Yin and colleagues also developed autonomous system of bipedal walkers utilizing hairpin structure [43].

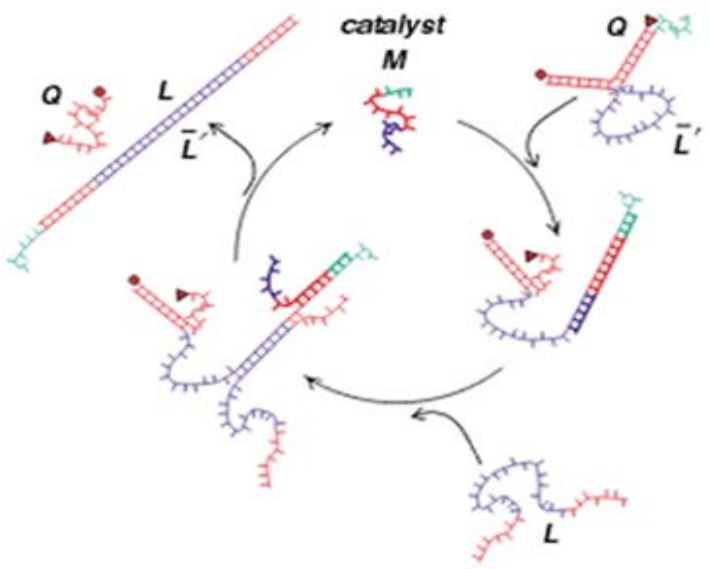

Figure 1.19 The loop circuit system with DNA fuel. The DNA catalyst strand M function as initiator of reaction, allowing strand L to bind with L' strand. The catalyst strand M is, then, released [41].

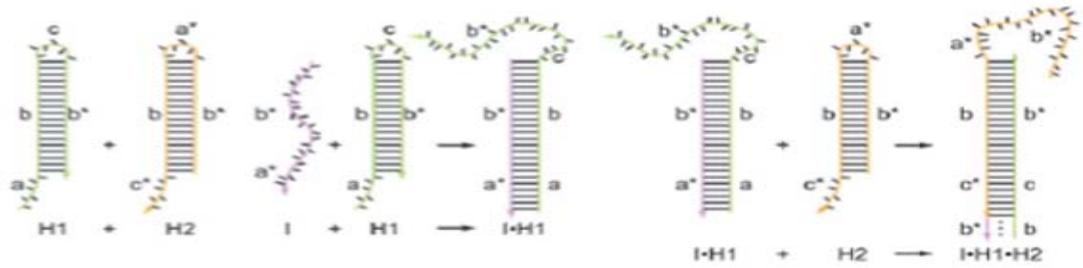

Figure 1.20 The hybridization chain reaction with hairpin structure. Strand I functions as initiator of the chain reaction [42].

In 2006, Seelig and colleagues introduced the enzyme-free DNA-based cascading circuit which input and output are in the same form of single-stranded nucleic acids. [44]. Since input and output are single-stranded nucleic acids with unrelated sequence, the output of upstream logic gate is able to function as input for downstream logic gate and the large scale cascading circuit is possible (Figure 1.21).

In 2009, Quan and Winfree developed dual-rail seesaw cascading circuit [45]. Each unit of seesaw gate is composed of input, threshold motif, and fuel. The input strand binds to toehold binding region and displace output strand. The fuel strand, then, displaces the input strand. The input strand, therefore, is active again for the next threshold motif (Figure 1.22). The advantage of dual-rail seesaw cascading circuit is unique. Any logic gates, simple and complex logic gates, can be derived into dual-rail seesaw circuit (Figure 1.23). However, a limitation of this system is cross-activation within the circuit since most of the units share the same sequences but only toehold region. In 2011, Quan and Winfree reported the scaling up of dual-rail seesaw cascading circuit with 32 seesaw gates to calculate the integer of square-root operation of counting number 1-8 (Figure 1.24) [46].

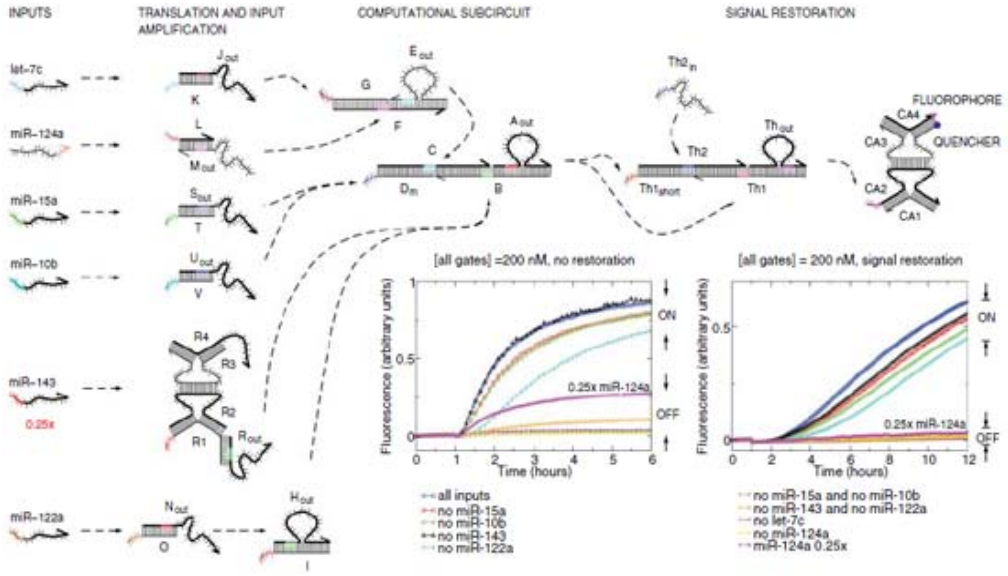

Figure 1.21 The enzyme-free DNA-based cascading circuit. The miRNAs are used as first layer input and the DNA molecules are released as output and function as input strand for the second layer logic gates. The AND and OR logic gates are demonstrated within the cascading circuit [44].

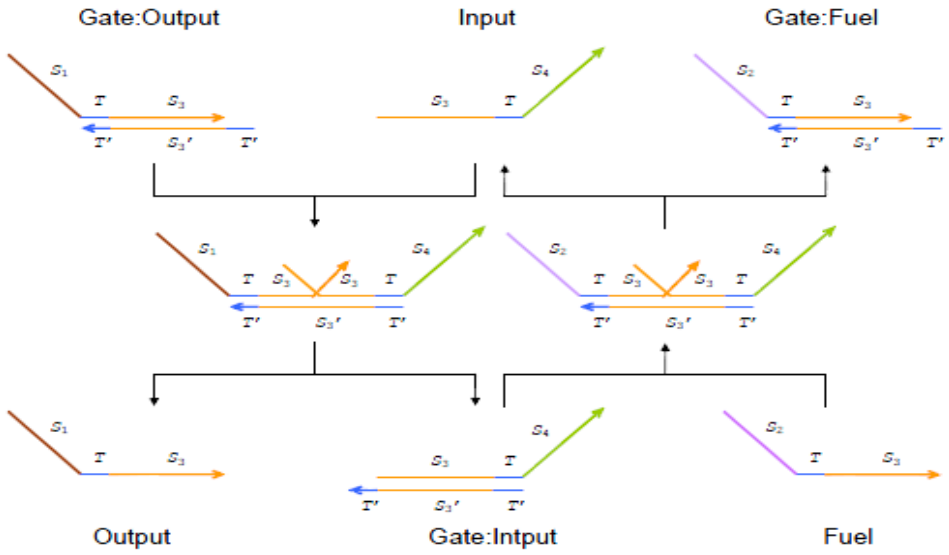

Figure 1.22 The unit of Seesaw gate, composing of input, threshold motif and fuel [45].

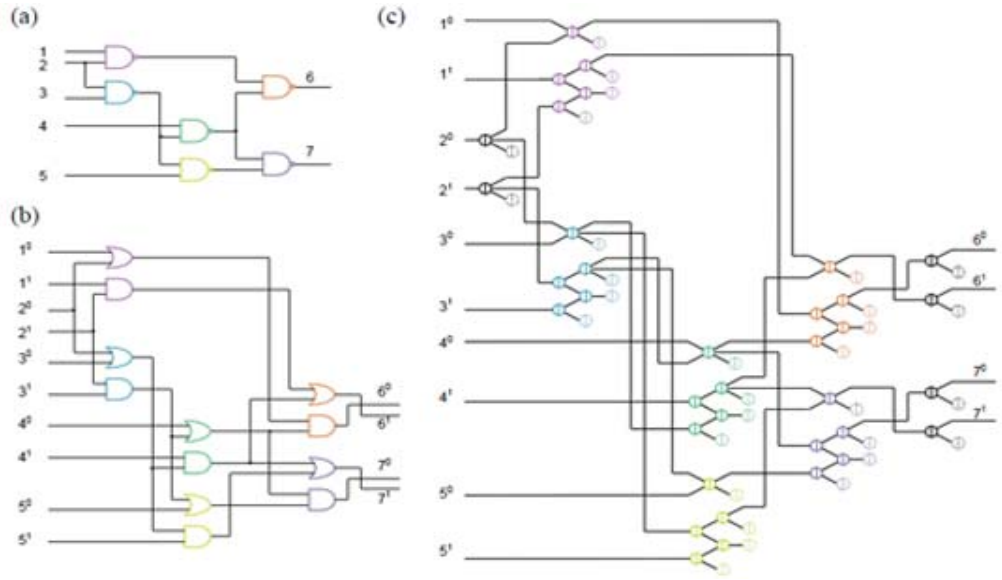

Figure 1.23 An example of circuit comprising of 6 NAND gates (a). The derived circuit from 6 NAND gates circuits into 6 couples of AND and OR gates (b). The derived dual-rail circuit with 36 seesaw gates (c) [45].

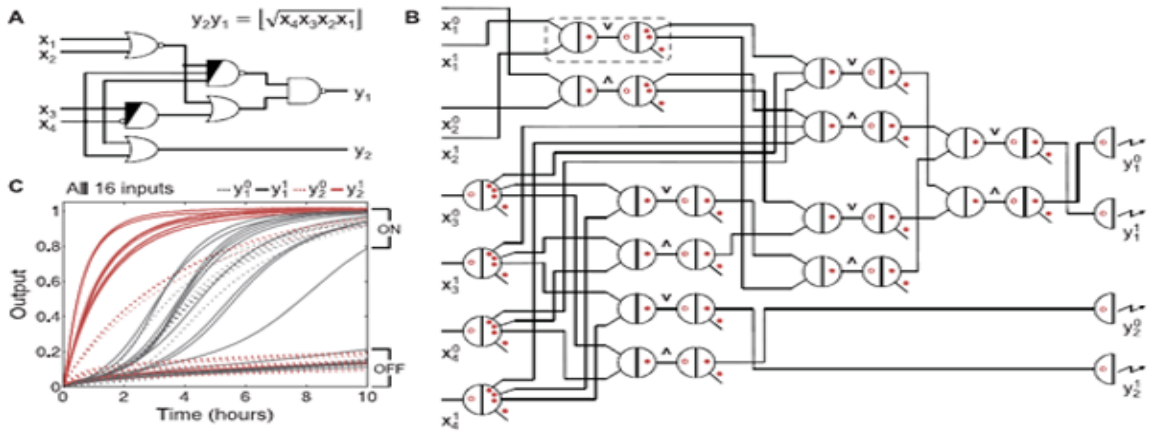

Figure 1.24 The logic circuit for 4-bit square-root (a). The dual-rail seesaw cascading circuit with 32 seesaw gates to solve square-root of 4-bit numbers task (b). The kinetics result of all 4-bit number 0000 to 1111 [46].

To date, the development of DNA computing in enzyme-free system focus on the purpose to design even more complex circuits in order to solve the harder tasks as mentioned in many reports. However, these circuit designs still are based on the simple principle of Boolean logic gates. So, we are interested to develop the simple tools which still are incomplete for variation in circuit designs.

First, we introduce the system called "separator system" (Chapter 2). Since many logic circuits require the control on computation state, for example XOR logic gate. So we develop the separator system as a tool with controlling function on the state of input as demand.

In Chapter 3, we furthermore, introduce the development of "XOR logic gate" which is able to function correctly in the cascading circuit (Chapter 3) and also development of full adder system with addition function based on the separator system (Chapter 4).

CHAPTER II
DNA SIGNAL SYNCHRONIZATION BY HAIRPIN STRUCTURE IN DNA-BASED LOGIC CIRCUIT

2.1 Introduction to signal synchronization

The development of DNA-based logic gates is still in an early stage similar to when digital electronics were first invented. We relate digital DNA-based circuit to the digital silicon-based circuit and realize that controlled communication among logic gates inside a digital system must also be invented. Our work focuses on the development of synchronized system which relies heavily on the use of clock signaling. All interactions of DNA strands in our scope are based on strand displacement processes called "branch migration". Normally, the cascading of output signal from one logic gate to the next logic gate happens naturally within a system based on our so-called DNA separation and annealing kinetics. However, controlling a signal to interact only at a specific time in a situation that many logic gates are presented together in a circuit system is a major challenge. This problem can be found in XOR logic gate, for example, when the XOR gate has to wait for a specific amount of time to ensure that all inputs are given enough time to be presented before the gate execution.

The use of DNA hairpin structure in DNA computing has been reported. In 2000, Sakamoto and colleagues used DNA hairpin structures to solve combinatorial problems in enzymatic reactions [29]. In 2008, Yin and colleagues developed a DNA hairpin self-assembly system which totally based on free energy of DNA structure [43]. In our work, we demonstrate the utilization of a hairpin structure mentioned briefly in [40] and [42], designated as a separator system, to control DNA molecule released in sequential computation. The separator system operates based on DNA branch migration process which involves the partial binding of an external DNA strand called, the separator, to the assigned toehold to separate the bonding of the stem region of a DNA hairpin structure. The binding continues until the separator strand

linearizes the hairpin structure and forms into a new duplex. The utilization of a hairpin structure has been demonstrated on secondary structure hybridization chain reaction [42], the possibility of the hairpin structure application in molecular computation also has reported [29, 31, 43]. We believe that suitable design of kinetic pathway is necessary in order to drive the computation system in cascading fashion properly similar to that of conventional electronic circuits [44].

2.2 Signal synchronization system design

In our design, it is assumed that our process is a process in a cascading chain of a complete logic circuit operation. The input of our process is, in fact, an output from a prior process. We call the input strand of our process as "controlled input strand" since we would like to hold, inactivate or control the operation between the output of the prior process (or we can view it as the input of the current process) and the subsequent downstream gate such that the operation can only happen when we trigger or activate it with a signal (by using our "separator" DNA strand) resembling the clock operation of digital circuits in conventional computers. We call our inactivated input strand as the “controlled input strand” that has a hairpin structure such that the controlled input strand cannot prematurely engage in any reaction with any downstream gates. The controlled strand is said to be in an inactive state when it is in the form of hairpin structure because the DNA input data segment carrying the actual DNA input data for the downstream gate, supposed to be interacting with the downstream gate as an input of the gate, is placed inside the loop region of the hairpin structure (Figure 2.1). The input DNA segment will effectively interact with the downstream gate if the input strand segment is not contained in the loop region [40]. In order to release the input DNA segment outside the hairpin loop, the stem of the hairpin structure of the controlled input strand must be broken which will linearize the hairpin structure without the hairpin loop (Figure 2.2). We design a basic single-stranded DNA called “separator” whose sequences match entirely with the left side of the stem region as shown in Figure 2.1. When the separator strand is introduced to the system, the separator will completely invade the stem region of the controlled input strand and perform branch migration with the controlled strand to become a partially

duplexed DNA as shown in Figure 2.2. This results in the activation of the controlled strand (active input) exposing the DNA input segment to interact with subsequent downstream gate.

We, herewith, investigate the feasibility of our concept of the separator system using a double-stranded DNA reporter to represent the downstream gate.

2.3 Sequence design of separator system

DNA sequences of the controlled input strand were randomly generated based on thermodynamic nearest-neighbor model for DNA [17] with some basic constraints. Two "GC" base pairs were placed at both duplex ends and all junctions to reduce duplex fraying. Three base repetitions were avoided. The toehold-binding region (4 bases) for the downstream gate was placed right next to the stem region of the controlled input strand (Figure 2.1). The separator was designed to complement to the 4-base-long toehold segment and the entire length of the stem (Figure 2.1). The downstream gate used to verify our system concept (so-called “reporter gate”) was designed to be complementary to the entire loop encoding the input DNA data segment as well as a part of the stem different from the binding site of the separator mentioned earlier. All randomly generated sequences were carefully selected to minimize unintended secondary structure formation and minimize cross activation due to unintended alignment with other sequences by MFE reduction method. The sequences were discarded if they contained 3-base repetition or any unintended secondary structure at the concentration of 0.25 μM and 25 ^{o}C in the absence of any ion. The sequence of all oligonucleotides are shown in Table 2.5.

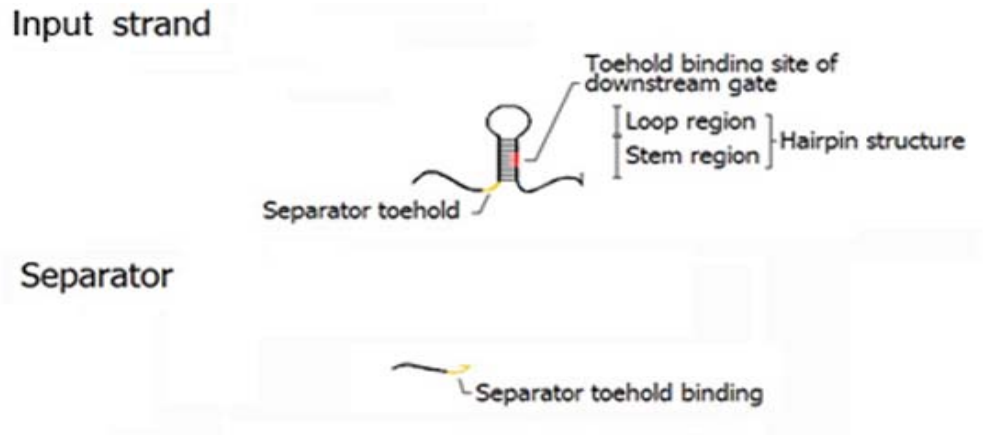

Figure 2.1 Illustration of components in signal synchronization system or so called "separator system". The inactive or controlled input strand (C) and the separator strand (S) are illustrated. Separator toehold is represented in yellow. Toehold-binding site for the downstream gate is represented in red.

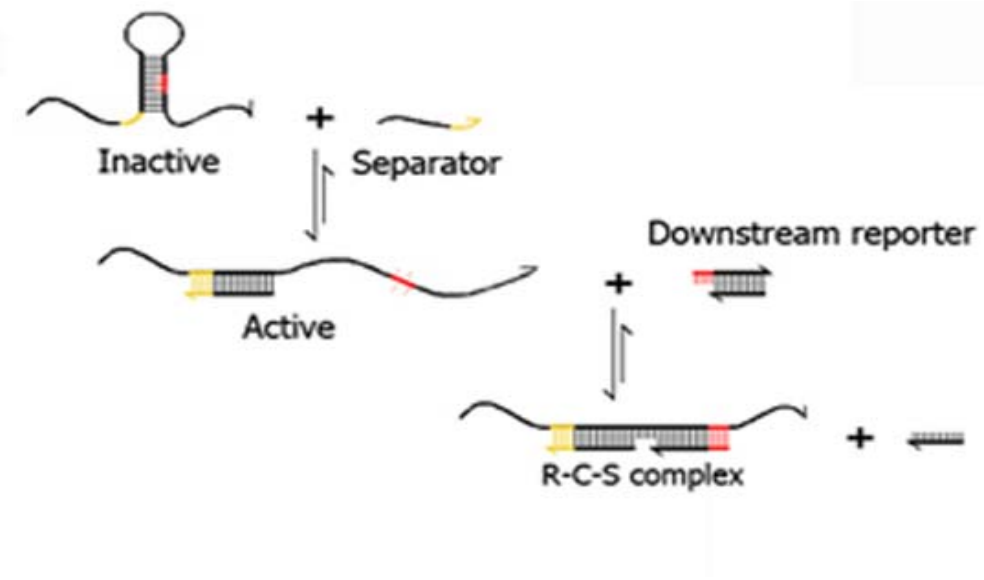

Figure 2.2 The proposed mechanism of the separator system. The separator toehold-binding region binds to the separator toehold region on the inactive input strand. The controlled input strand is consequently linearized, exposing toehold-binding site of a downstream reporter to function as input for the downstream reporter, thus, leading to R-C-S complex formation.

2.4 Materials and methods of separator system

Strand preparation: All DNA oligonucleotides are synthesized by Pacific Science Co., Ltd (Thailand). Oligonucleotides are purified by denaturing polyacrylamide gel electrophoresis (16% PAGE, 7 M Urea). The purified oligonucleotides are stored in TE buffer (0.04 M Tris base, 1 mM EDTA) as stock solution at 100 µM. The stock solutions are kept at - 20 ^{o}C.

Gate formation: The downstream reporter gate single-stranded DNA (Gate up-strand and down-strand) at 2.5 µM concentration are incubated in TE buffer at 20 µL total volume. The solution is heated up to 90 ^{o}C for 5 minutes and slowly cooled down with a constant rate of 1 ^{o}C/min to 15 ^{o}C. The assembled reporter gates can be stored at 4 ^{o}C for couple weeks with efficient function.

Gate function analysis: The reporter gate, controlled strands and separator are incubated at 25 ^{o}C for 15 minutes. Then, the reaction mixture is analyzed by non-denaturing polyacrylamide gels electrophoresis (non-denaturing PAGE) with 10% acrylamide-bis 19:1 gel. PAGE result shows gate structure and interaction between gate and input strands. The input strand and separator strand concentrations are 1 µM. The concentration reporter gate is 0.25 µM. For each set of experiment, three reaction scenarios were performed in three different tubes. The first tube contained only the downstream reporter (R), which served as our control or monitored variable. The second tube contained the inactive controlled input strand (C) with the downstream reporter (R). This tube allows us to evaluate the unintended cross reaction between the two circuit components (controlled input and gate) commonly known in conventional computing community as “data leakage”. The third tube contained the controlled input strand (C), the downstream reporter (R) and the separator strand (S). This tube is used to demonstrate the operation of our proposed system. In an effective separator system, the interaction between the inactivated controlled input strand (C) and the separator strand (S) would activate the controlled input strand (C), enabling it to interact with the downstream reporter (R). As a result, substantial reduction in the concentration of the downstream reporter (R) and the separator strand (S) would be observed whereas the concentration of the new molecule (R-C-S complex) would be increased. All experiments were done in triplicate. All reactions were incubated for 15 minutes at room temperature in TE buffer. The results of the reactions were subjected

to non-denaturing polyacrylamide gel electrophoresis (PAGE; 10% acrylamide-bis 19:1), which was run for 90 minutes at 120 V at room temperature in TAE buffer (0.04 M Tris Acetate, 1 mM EDTA). The non-denaturing gels were stained in ethidium bromide, visualized under UV light and photographed by G:box (SYNGENE, UK) (Figure 2.4). The DNA band intensity was measured by GENETOOLS software (SYNGENE, UK), normalized to the control (reporter only) and compared as appropriate by student t-test.

Ladder marker: GeneRuler Ultra Low Range DNA Ladder (Thermo Scientific) is used as marker in all experiments. The ladder contains the band of double-stranded DNA with lengths varying from 10-300 base pairs. The pattern of GeneRuler Ultra Low Range DNA Ladder is shown in Figure 2.3

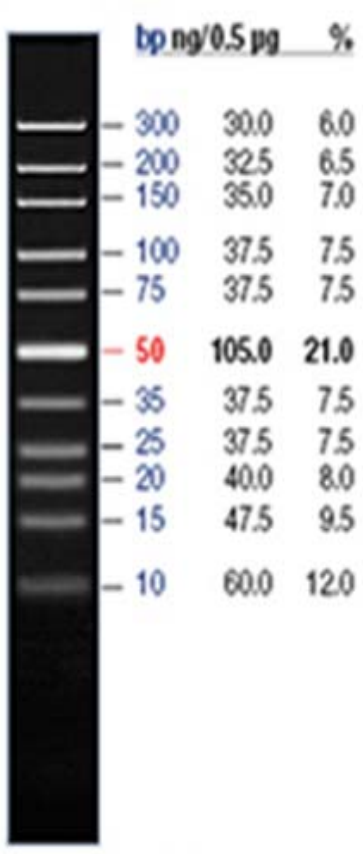

Figure 2.3 The eletrophoretic pattern of GeneRuler Ultra Low Range DNA Ladder in 1X TBE at 5cm/V for 1 hour. The Brightest band indicates the 50 bps position.

Table 2.1 Oligonucleotides for all DNA strands use in the study. Abbreviation; C = Inactive Controlled strand, S = Separator, R = Reporter, B = bulge , s = stem length, l = loop length, u = up-strand of reporter, d = down-strand of reporter, e = extended base length, Number = length of bases of letter in the front. Stem region is indicated with underline.

Strand Name	Bases
Cs8l6	5'-ACTCTGATGGATACACCTAACTGAAGGTGTATGGTAGTCTAA -3'
Cs10l6	5'-ACTCTGATGGCATACACCTGAACTGACAGGTGTATGGGTAGTCTAA -3'
Cs12l6	5'-ACTCTGATGGTCATACACCTGTAACTGAACAGGTGTATGAGGTAGTCTAA -3'
Cs14l6	5'-ACTCTGATGGATCATACACCTGTCAACTGAGACAGGTGTATGATGGTAGTCTAA -3'
Cs16l6	5'-ACTCTGATGGTATCATACACCTGTCGAACTGACGACAGGTGTATGATAGGTAGTCTAA -3'
Cs18l6	5'-ACTCTGATGGTTATCATACACCTGTCGGAACTGACCGACAGGTGTATGATAAGGTAGTCTAA -3'
Cs14l14	5'-ACTCTGATGGATCATACACCTGTCCGCTGAGTCAGATCGACAGGTGTATGATGGTAGTCTAA -3'
Cs14l20	5'-ACTCTGATGGATCATACACCTGTCCGCTGAGTCAGATCGTTAGTGACAGGTGTATGATGGTAGTCTAA -3'
Cs18l20	5'-ACTCTGATGGTTATCATACACCTGTCGGCAGTCTCTCATATCGTTCGTCCGACAGGTGTATGATAAGGTAGTCTAA -3'
Ss8	5'- AGGTGTATCCAT -3'
Ss10	5'- CAGGTGTATGCCAT -3'
Ss12	5'- ACAGGTGTATGACCAT -3'
Ss14	5'- GACAGGTGTATGATCCAT -3'
Ss16	5'- CGACAGGTGTATGATACCAT -3'
Ss18	5'- CCGACAGGTGTATGATAACCAT -3'
Ss14e2	5'- CGGACAGGTGTATGATCCAT -3'
Ss14e4	5'- AGCGGACAGGTGTATGATCCAT -3'
Ss14e6	5'- TCAGCGGACAGGTGTATGATCCAT -3'
Ss18e2	5'- TGCCGACAGGTGTATGATAACCAT -3'
Ss18e4	5'- ACTGCCGACAGGTGTATGATAACCAT -3'

Table 2.1 Oligonucleotides for all DNA strands use in the study (cont.). Abbreviation; C = Inactive Controlled strand, S = Separator, R = Reporter, B = bulge , s = stem length, l = loop length, u = up-strand of reporter, d = down-strand of reporter, e = extended base length, Number = length of bases of letter in the front. Stem region is indicated with underline.

Ss14e2	5'- CGGACAGGTGTATGATCCAT -3'
Ss14e4	5'- AGCGGACAGGTGTATGATCCAT -3'
Ss14e6	5'- TCAGCGGACAGGTGTATGATCCAT -3'
Ss18e2	5'- TGCCGACAGGTGTATGATAACCAT -3'
Ss18e4	5'- ACTGCCGACAGGTGTATGATAACCAT -3'
Ss18e2	5'- TGCCGACAGGTGTATGATAACCAT -3'
Ss18e4	5'- ACTGCCGACAGGTGTATGATAACCAT -3'
Rs8l6u	5'- ACACCTTCAGTT -3'
Rs8l6d	5'- AACTGAAG -3'
Rs10l6u	5'- ACACCTGTCAGTT -3'
Rs10l6d	5'- AACTGACAG -3'
Rs12l6u	5'- ACACCTGTTCAGTT -3'
Rs12l6d	5'- AACTGAACAG -3'
Rs14l6u	5'- ACACCTGTCTCAGTT -3'
Rs14l6d	5'- AACTGAGACAG -3'
Rs16l6u	5'- ACACCTGTCGTCAGTT -3'
Rs16l6d	5'- AACTGACGACAG -3'
Rs18l6u	5'- ACACCTGTCGGTCAGTT -3'
Rs18l6d	5'- AACTGACCGACAG -3'
Rs14l14u	5'- ACACCTGTCGATCTGACTCAGCG -3'
Rs14l14d	5'-CGCTGAGTCAGATCGACAG -3'
Rs14l14ue	5'- ACACCTGTCGATCTGACTC -3'
Rs14l14de	5'- GAGTCAGATCGACAG -3'
Rs14l20ue	5'- ACACCTGTCACTAACGATCTGACTCAG -3'
Rs14l20de	5'- CTGAGTCAGATCGTTAGTGACAG -3'
Rs18l20ue	5'- ACACCTGTCGGACGAACGATATGAGAG -3'
Rs18l20de	5'- CTCTCATATCGTTCGTCCGACAG -3'
Rs14l20ueB	5'- ACACCTGTCACTAACGATCTGACTCAG -3'
Rs14l20deB	5'- CTGAGTCAGATAAAAAACGTTAGTGACAG -3'

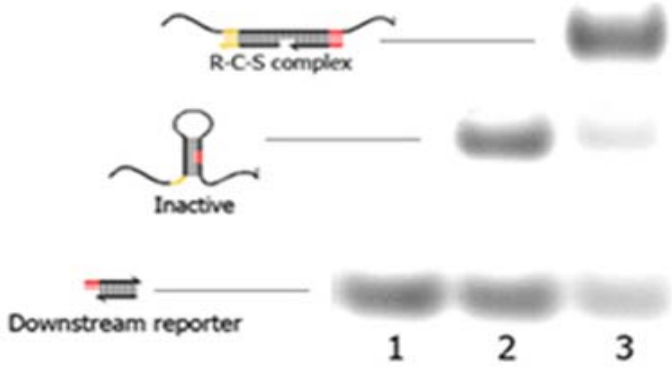

Figure 2.4 The ideal electrophoretic patterns of the separator and the downstream reporter from three different combinations. Lane 1 contains only the downstream reporter (R). Lane 2 contains the controlled strand and the reporter without the separator (R+C). Addition of the separator strand (R+C+S) leads to the formation of the R-C-S complex and reduction of the concentrations of both the controlled strand (C), and the downstream reporter (R) as shown in lane 3.

2.5 Experimental results of separator system

The experiments were demonstrated in order to observe separator system in two aspects, data blockage and separator activation level.

2.5.1 Optimization of hairpin stem length

Since the separator function is based on DNA branch migration [40], the separator's toehold-binding region, by our design, will bind to the inactivated controlled input strand's toehold region for the separator (next to the left stem of the hairpin shown in Figure 2.1), allowing the separator strand to continue to invade the stem region of the hairpin structure in the controlled input strand (Figure 2.1) and restructure the controlled input strand into a partial duplex molecule (Figure 2.2). The successful operation of the separator was demonstrated and verified by the interaction between the active input strand, whose DNA input strand is no longer contained in the hairpin loop, and a downstream reporter gate, which is designed to accept the DNA input strand (Figure 2.2). Each experiment is designed to observe three different scenarios in different tubes, which respectively contain the reporter only (R), the

reporter and the inactive controlled input strand (R+C), and the reporter, the inactive controlled input strand and the separator (R+C+S) (Figure 2.4). Without the presence of the separator strand (in the R and R+C tubes), the toehold-binding region of DNA input data for downstream reporter gate, originally located in the stem of the hairpin loop not bind with the separator, is prevented or blocked from binding with the downstream gate's toehold. Thus, no R-C-S complex is. The results shown in Figure 2.4 and 2.5 prove our design concept. Next, we focused on the effectiveness and limitation of our separator system. We look at the data-leakage blocking ability of the separator system and the separation process by the separator. Firstly, we hypothesize that the data-leakage blocking ability could be improved if the stem region is larger due to the increase in the stability of the hairpin structure. We then varied the length of the stem region from 8 to 18 base-pairs (S8 to S18). Note that the length of the separator must match the length of the stem as mentioned in the previous section. The DNA input segment in the hairpin loop was fixed to 6 bases (L6). The results of this experiment are shown in Figure 2.5 indicating that the longer the stem, the less the data leakage. We also found that if the stem length is too long, the reaction efficiency between the activated controlled input strand and the reporter gate is reduced. For the DNA input segment of 6 bases, the 14-bp-long stem showed the most effective activation of the controlled input strand (96.7%). The controlled input strand with 16- or 18-bp-long stem did not respond well to the separators even though they efficiently block the data leakage (Figure 2.5). The bar graph shows band intensity ratio data of reporter gate from triplicate results. The band intensity ratio is the ratio of the indicating experiment compares to control (the first lane of each set of experiment). The band intensity ratio of control lane is 1. The data leakage value and activation level value are calculated by the relative reduction of band intensity ratio in R+C lane and R+C+S lane, respectively, compares to control lane. The data leakage value and activation level value are reported in percentage.

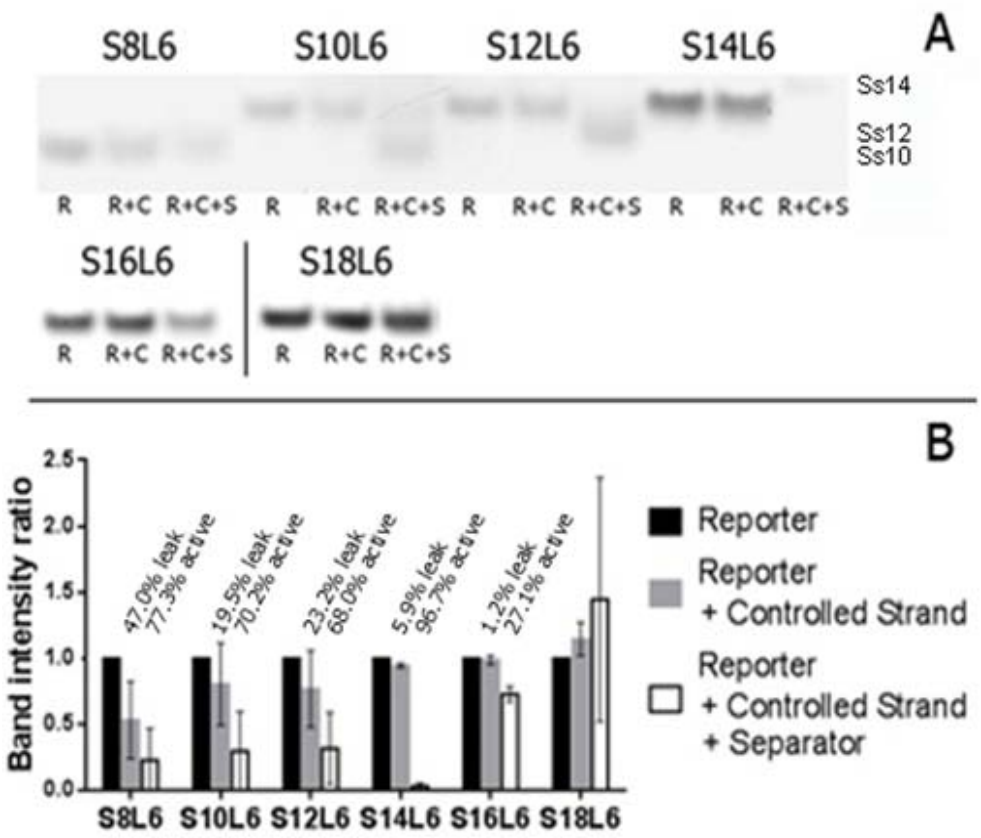

Figure 2.5 The effect of stem length on the performance of the separator functions, prevention of data leakage and the efficiency of separation. [A] The loop was six-base long in all inactive controlled strands (C) while the length of the stem ranged from 8 to 18. For each stem length, the bands of the reporter from three conditions are shown: with only the reporter (R), with the controlled input strand (R+C), and with the controlled input strand and the separator (R+C+S). The R:C:S molar ratio used was 1:2:2. 10% non-denaturing polyacrylamide gel electrophoresis was used to observed data leakage and activation level by monitoring the reporter gate band intensity (R) on various stem length of the controlled strand (C). Decrease of the intensities in Lane R+C reflected the intrinsic data leakage of the controlled strand without the separator, while further decrease of the intensities in Lane R+C+S reflected the efficiency of the separator system. [B] Chart representing the intensities of the reporter bands in various conditions compared to the intensities of the reporters in Lane R. The error bars were shown according to the results of three experiments. Reporter gate concentration is 2 μM, inactive controlled strand concentration is 2 μM and separator strand concentration is 2 μM.

2.5.2 Optimization of the separator system with long loop

In some applications, the controlled input strand needs to carry large input data for downstream gates. This could result in large hairpin loop size in the controlled input strand. To determine whether our design can deal with large DNA input data, we designed experiments with different loop size from 14 to 20 bases while the stem length was fixed at 14 bps (which previously showed that the activation efficiency is maximum based on our design model). Results of the experiments are shown in Figure 2.6. The 14-bp-long stem and 14-base-long loop controlled strand (S14L14) efficiently prevented data leakage (6.5% leakage). However, activation efficiency was very low using the separator of 18 (4+14) bases according to our original design (only 31.4% of the original reporters were exhausted) (Figure 2.6B and 2.6C). Since the activation efficiency was low for large hairpin loop length, we hypothesize that our current design of the separator may be insufficient to break the bonding of the long stem of the hairpin structure of the controlled input strand. We therefore choose to conduct additional experiments by extending the length of the separator with additional 4 bases (called Ss14e4 or E4 separator) to invade the hairpin structure further inside the loop region. The 22-base-long separator, resulting from the addition of original 18-base separator and 4 extra bases, contained an additional sequence complementary to the 3' end of the loop region in the controlled strand (Figure 2.6A). The separation efficiency measured from the E4 separator system (S14L14e) increased considerably to 87.5% (Figure 2.6B and 2.6C), suggesting the usefulness of the extended separator in our separator system with large-loop controlled input strand.

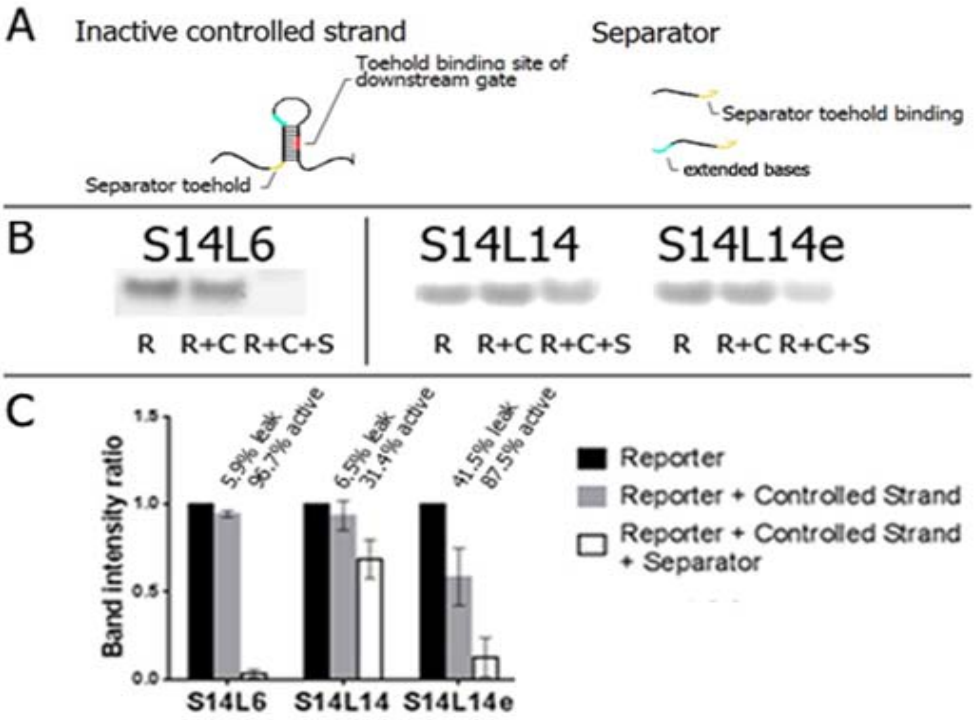

Figure 2.6 The effect of loop length on the performance of the separator functions. [A] Illustration of inactive controlled strand (C), normal separator (S) and separator with 4 bases extension (blue). The stem was 14 base pairs long in all inactive controlled strands. Thus, the normal separator (Ss14) together with the toehold binding region is 18 bases long whereas the 4-base extended separator (Ss14e) is 22 bases long. [B] Polyacrylamide gel electrophoresis of the reporters (R) with the inactive controlled strand (C) and separator (S). The bands of the reporters from three conditions (R, R+C and R+C+S) with the R:C:S molar ratio of 1:2:2 are shown. Decrease of the intensities of R in Lane R+C implies the data leakage while further decrease of the intensities of R in Lane R+C+S implies the efficiency of the separator system. [C] The chart represents the intensities of the reporter bands in various conditions compared to the intensities of the reporters in Lane R. The error bars were shown according to the results of three experiments. While the controlled strand with 6-base-long loop provided satisfactory performance. It is envisaged that many applications may require a longer loop length which appears to decrease the efficiency of the separator system. The efficiency can be improved satisfactory for the controlled strand with 14-bp-long stem by adding four more bases to the 5' end of the separator strand (S14L14e). Reporter gate concentration is 2 µM, inactive controlled strand concentration is 2 µM and separator strand concentration is 2 µM.

By the way, there are circumstances that downstream reporter gate may need to use large DNA input strand for some circuit operations. Large DNA input strand leads to large hairpin loop size of the controlled input strand which may affect the operation of our separator system. We investigate this condition by selecting a controlled input strand with the loop size of 20 bases for testing, given that the stem length was still fixed at 14 base pairs. Two extended separators with additional two and four bases invading the hairpin loop (E2 and E4 separators) were used in the experiments. Figure 2.7A shows that the separator E4 performed better than separator E2 yielding 41.2% and 18.8% activation level respectively. The activation level of the system between the E2 and E4 separators is even more obvious when the concentration of the separator was 4 times as much as the concentration of downstream reporter and 2 times as much as the concentration of controlled input strand. The effectiveness of the separator was less noticeable when the concentration of the separator was low compared to the concentration of the downstream reporter and controlled input strand. In an attempt to improve the separator system of L20 controlled strand, we tried to apply the 18-bp-long stem region (S18) together with 4-bp extended separator to investigate the separation efficiency (Figure 2.7B). As expected from previous results, the longer stem results in reduced efficiency of the separation system. More separator concentration or longer extended separators could be applied to yield better separation efficiency.

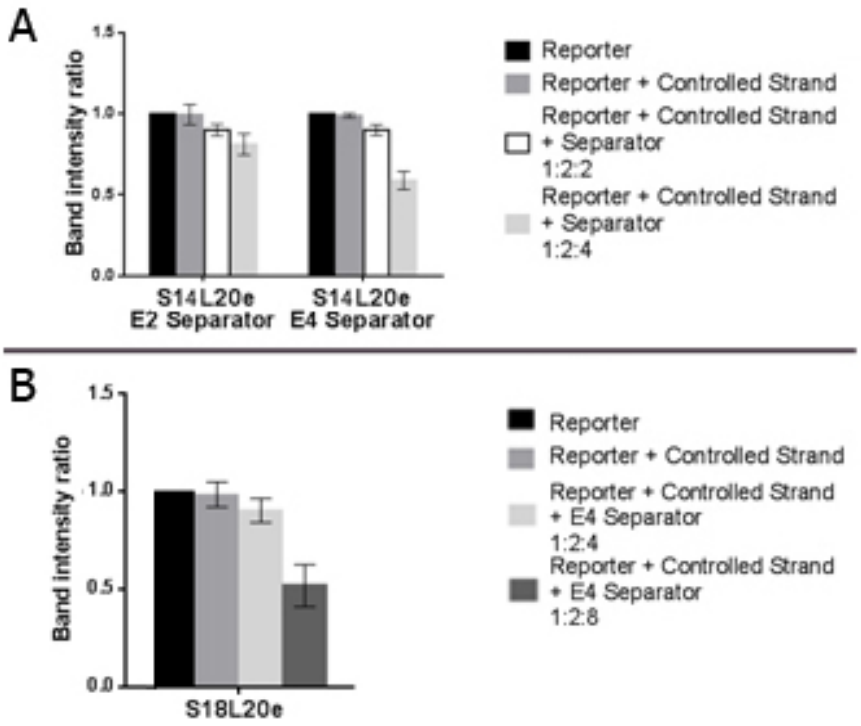

Figure 2.7 Efforts to improve the performance of the separator strand with 20-base-long loop (S14L20). [A] Extension of the separator length by 2 (E2) and 4 bases (E4) using different concentrations of the separator. R:C:S molar ratios are 1:2:2 and 1:2:4. [B] Extended separator function with 18-bp-long stem region in the controlled strand. Separator functions were analyzed for data leaked blockage and separation efficiency. E4 separator function was observed in two different conditions: R:C:S concentration ratios are 1:2:4 and 1:2:8. Reporter gate concentration is 2 µM, inactive controlled strand concentration is 2 µM and separator strand concentration is 2 µM.

The E6 separator was also tested in the S14L20 controlled strand but the result suggested insignificant increase in separator function compared to E4 separator (Figure 2.8). The downstream logic gate structure was studied. The bulge reporter with 6-A bases bulge in the middle of double-stranded DNA is compared with common linear reporter with a 14-base-stem 14-base-loop controlled strand. Result shows the detection of leaked band of C-S complex in lane 3 with unpredicted separating function (Figure 2.9).

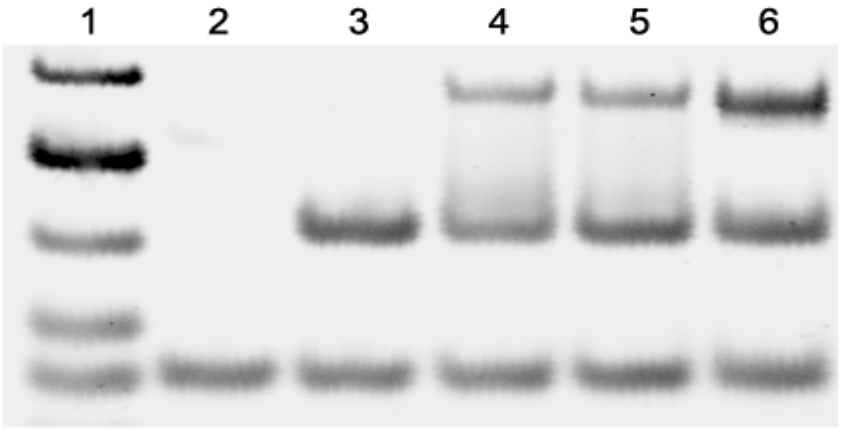

Figure 2.8 Efforts to improve the performance of the separator strand with 20-base-long loop (S14L20). R:C:S molar ratios1:2:2. Separator functions were analyzed. The E2, E4 and E6 separator function were observed for data leaked blockage and separation efficiency. [Reporter] = 2 µM, [Controlled strand] = 2 µM, [separator] = 2 µM.

Lane 1 = Ladder Marker

Lane 2 = Reporter (Rs14l20e)

Lane 3 = Reporter + Cs14l20

Lane 4 = Reporter + Cs14l20 + Ss14e2

Lane 5 = Reporter + Cs14l20 + Ss14e4

Lane 6 = Reporter + Cs14l20 + Ss14e6

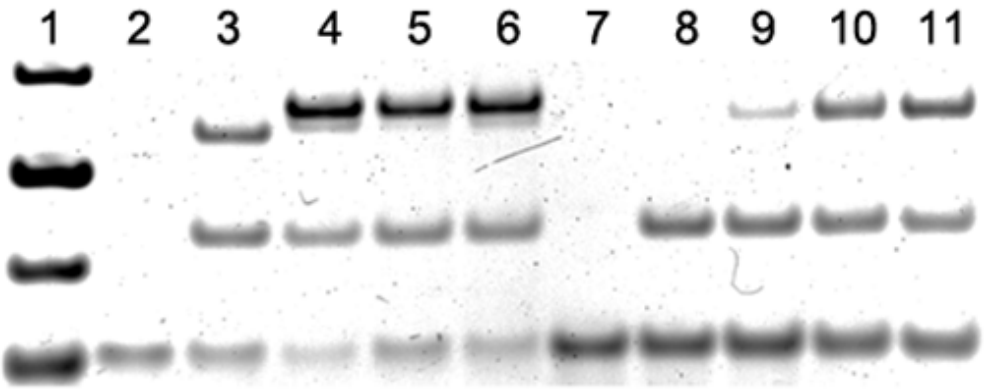

Figure 2.9 Effect of downstream structure to separator system. The 6-A bulge reporter and complete linear reporter were compared in term of function. The leaked band of R-C complex is detected in lane 3. [Reporter] = 2 µM, [Controlled strand] = 2 µM, [separator] = 2 µM.

Lane 1 = Ladder Marker

Lane 2 = Bulge Reporter (Rs14l20eB)

Lane 3 = Bulge Reporter + Cs14l20

Lane 4 = Bulge Reporter + Cs14l20 + Ss14e2

Lane 5 = Bulge Reporter + Cs14l20 + Ss14e4

Lane 6 = Bulge Reporter + Cs14l20 + Ss14e6

Lane 7 = Reporter (Rs14l20)

Lane 8 = Reporter + Cs14l20

Lane 9 = Reporter + Cs14l20 + Ss14e2

Lane 10 = Reporter + Cs14l20 + Ss14e4

Lane 11 = Reporter + Cs14l20 + Ss14e6

2.6 Discussion of separator system

Here we introduced a system to synchronize the operations of DNA computation by keeping an input sequence representing data inactive, in a hairpin loop, until another signal, the separator, is added to the system in order to trigger the inactive hairpin structure DNA molecule to reveal the DNA input sequence to the downstream gate for next circuit operation. In the context of conventional electronic circuit, the separator therefore functions as the clock signaling the system to be ready for the next subsequent operation. The successful demonstration of this concept will allow us to construct a cascading DNA-based logic circuits that resemble those of logic circuits used in conventional computers (with the only exception that the gate cannot go back to its original state once it has performed an execution). In our design of DNA-based logic circuit, the circuit will consist of multiple stages of cascading logic gate operations. Each cascade gate operation will only happen when there is a triggering signal (normally carried by the clock signal) specific to each operation to start the execution of the input in order to maintain order of circuit operations. Thus, circuit pathway can be designed and controlled. DNA-based software programs similar to conventional silicon-based software programs could be written to direct the path of circuit operations. The triggering signal in our DNA-based logic gate is carried by the separator specific to each controlled DNA input strand. When the separator changes the controlled input strand from hairpin structure to linear partial duplex structure (activation), the DNA input segment, originally contained in the hairpin loop, is exposed to the downstream gate allowing reaction between the downstream gate and the DNA input segment to happen (Figure 2.1). The reaction could produce yet another output strand that has the same format as the controlled input strand to be ready for the next cascading operation. By carefully designing the controlled input strands of all gate operations, one can achieve any complex circuit similar to conventional computer circuits.

Our experiment shown in the result section confirms that our concept is feasible and effective. For the loop size of 6 bases and toehold of 4 bases, we find that the controlled input strand in hairpin structure containing DNA input segment in the loop of the hairpin could not efficiently react to the downstream gate unless there is a

separator that breaks the bonding of the stem of the hairpin structure of the controlled input strand (Figure 2.2).

However, there are limitation to our system as we investigated further. For the loop size of 6 bases, the length of the stem that produces the highest level of activation of controlled input strand is 14 base pairs. Controlled input strands with stem length greater or lower than 14 base pairs yield activation level lower than the strand with stem length of 14 base pairs. It is worth noting that the stem region must be strong enough to prevent signal leakage; otherwise, some proportions of the output strand will accidentally bind with the output toehold region of the downstream gates. Further, we investigate the effect of the loop length on the data leakage (premature reaction between the controlled input strand and the downstream reporter gate) and the activation efficiency. We found that, for the stem length of 14 base pairs, as the loop length becomes larger, data leakage performance is similar to that of the loop length of 6, but the activation performance is lower. This could be because of the fact that when the loop length is long, the activated input strand could go back to inactivated state easily due to the increase in flexibility of DNA strand movement. To test this hypothesis, we extended the length of the separator into the hairpin loop region of the hairpin structure of the controlled input strand in order to make stem binding a bit more difficult and run the same experiment again. We find that our hypothesis is true as seen in Figure 2.7C. The activation performance of the system improved when the extended separator was used. Figure 2.6 shows that 4-base extension of the separator into the hairpin loop region improves the activation performance of the separator. We also show in Figure 2.8 that higher concentration of separator could help drive the activation of the controlled input strand.

Regarding the application of our separator system, the controlled input strand, which may be received from previous operation of upstream logic gates (or circuits), is designed to be inactive until, at designated time within a circuit execution cycle, all logic operations are ready for the next execution round. At this time, separators for each inactive input strands for this round will activate the input strands resulting in the next cascaded circuit operation. This operation is commonly used in conventional computer called “clock synchronization” in order to ensure that all inputs are ready for the next circuit operation round.

Synchronization is extremely important in many logic operations. For instance, an XOR logic gate requires exactly only one input (A or B) but not both, to activate the XOR logic gate operation to produce an output. If two active inputs arrive at the XOR logic gate but at different times, the gate may be activated by the first input resulting in an incorrect operation. In contrast, if the inputs are designed to be originally inactive, the XOR logic gate operation can be waited until it is certain that both inputs have arrived. Once ready, the inactive inputs will be activated by the addition of appropriate separators, resulting in an efficient XOR logic gate operation. Choosing the appropriate time is, therefore, necessary for the correct operation of synchronized DNA-based circuit system and the separator system can provide a basis of a timing device (e.g. via micro- or nano-scale fluidic devices).

Our separator system can also be applied to a biological detection system as an encoder used for detecting a variety of objects or data patterns or a DNA-based computer. The encoder for aptamer detection system could be developed to demonstrate this concept. A controlled strand in hairpin structure containing aptamer matching sequence in the hairpin loop could be deployed in a system to detect aptamer. For example, aptamer sequence of adenosine molecule inside the loop region forms a complex structure with two adenosine molecules. The release of extended separator strand from upstream computing process will separate the controlled strand and impede the complex formation with adenosine molecules. The adenosine molecules are therefore released for downstream detection system (Figure 2.10).

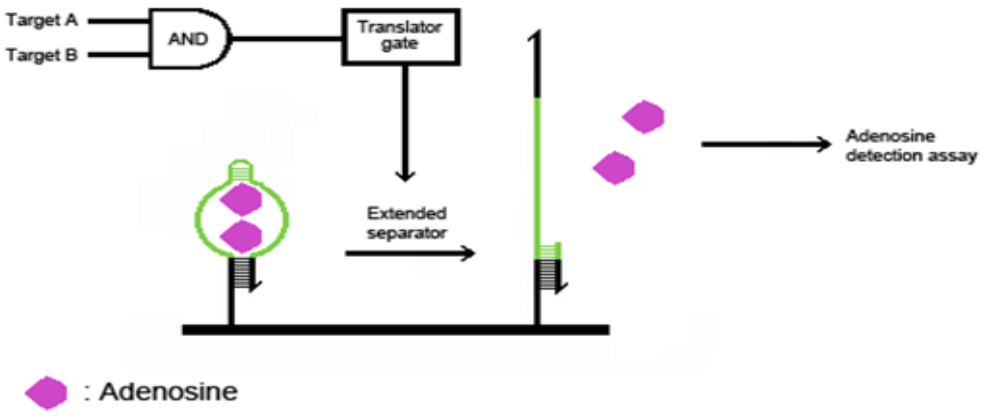

Figure 2.10 Schematic picture of separator application on detection system. Target A and Target B are two DNA sequences of interest in this detection. Two targets are computed with AND gate then AND output is released and translated into extended separator with the translator gate. In this case, the extended separator performs separating process and also disturbs structure formation between aptamer and adenosine molecules. The adenosine molecules are released for downstream detection process.

CHAPTER III
DEVELOPMENT OF FUNCTIONAL XOR DNA-BASED LOGIC GATE IN ENZYME-FREE BIOLOGICAL CIRCUIT

3.1 Enzyme-free DNA-based circuit

The enzyme-free DNA-based system underlying with Boolean logic algebra was firstly introduced by Stojanovic and colleagues [31]. Instead of using enzyme, the single-stranded DNA called "DNAzymes" are used. However, the DNAzymes-based system could not be linked together into the large scale circuit. In 2006, Seelig and colleagues introduced the enzyme-free DNA-based cascading circuit whose input and output are in the same form of single-stranded nucleic acids. According to Seelig' s model, the large scale circuit is possible. Since complex circuit can be designed, it is possible to solve problems or perform digital logic operations in the same way that the circuit of silicon-based computer performs. One of those common circuits is half-adder circuit.

Half-adder circuit is the circuit with the function of 1-bit addition. The circuit is composed of an XOR logic gate and an AND logic gate (Figure 3.1). The input A and input B represent two binary numbers used in the addition operation while the two outputs represent the sum of input A and input B binary numbers and the carry in (input C) from the previous bit addition operation. The addition operation of 1-bit number is demonstrated in Figure 3.2.

Since the half-adder circuit can only perform addition operation of two one-bit inputs, two half-adder circuit can be joined together with slight modification to perform addition operation with carry-in bit or so called "Full-adder" circuit. The full-adder circuit can be cascaded to perform multiple-bit addition. The CARRY output of the first full-adder circuit will be used as the CARRY input for the second half-adder circuit. The full-adder circuit is shown in Figure 3.3.

Since each full-adder circuit is composed of 3 inputs, there are $2^3 = 8$ possible conditions. Full-adder’s truth table is shown in Table 3.1.

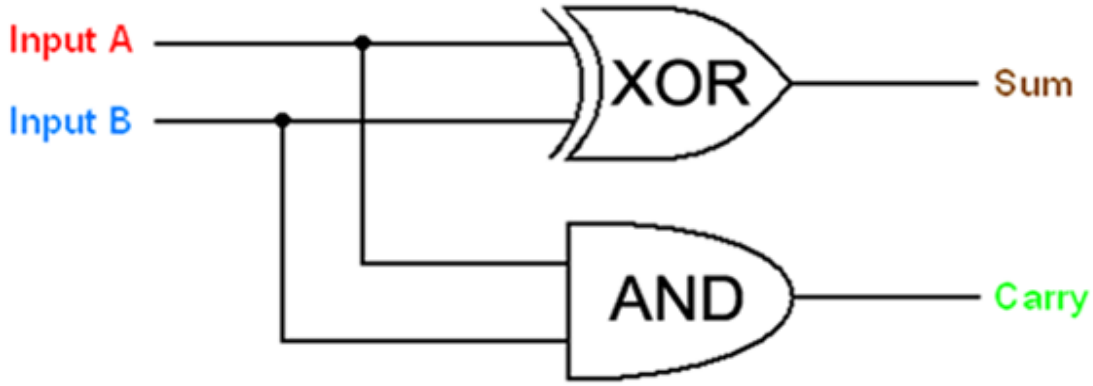

Figure 3.1 Schematic diagram of half-adder logic circuit. The circuit is composed of two inputs, A and B, two logic gates, XOR and AND, and two outputs, SUM and CARRY.

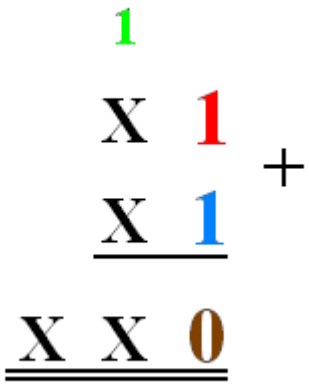

Figure 3.2 Addition operation of 1-bit binary number. For example, Input A (red) = 1, Input B (blue) = 1, XOR output (sum number, brown) = 0 and AND output (carry number, green) = 1.

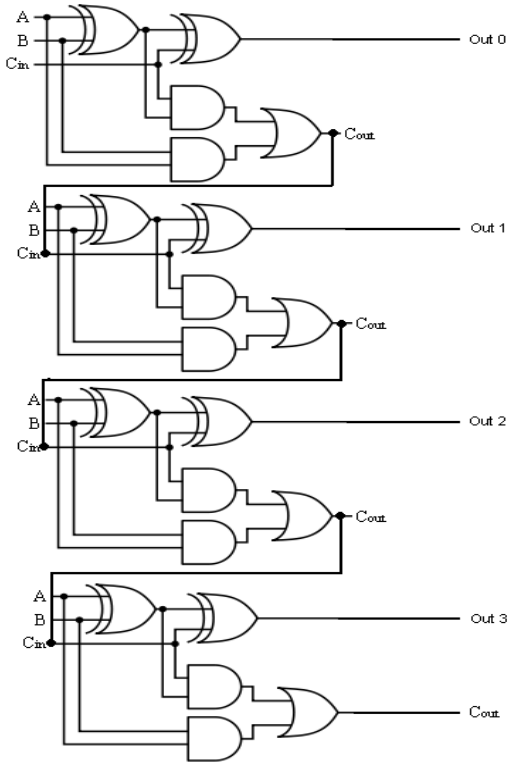

Figure 3.3 The 4-bit full-adder circuit. SUM = (A XOR B) XOR C. CARRY = (A XOR B) ∧ C ∨ (A ∧ B)

Table 3.1 The Full-adder's truth table.

Input			**Output**	
A_{in}	**B_{in}**	**C_{in}**	**SUM**	**CARRY**
0	0	0	0	0
1	0	0	1	0
0	1	0	1	0
0	0	1	1	0
1	1	0	0	1
1	0	1	0	1
0	1	1	0	1
1	1	1	1	1

In order to construct a circuit capable of performing complex operations similar to the conventional, silicon-based, Boolean logic circuit, the output strand must be able to function as an input strand for the next downstream DNA-based logic gate. Therefore, the DNA-based logic gates are designed in such a way that they can be cascaded allowing the construction of a large DNA-based circuit. Hence, Seelig's cascading circuit model is a suitable model. They reported success in the development of AND, OR and NOT DNA-based logic gates which are able to function together into large cascading-circuits. In addition, an amplifier gate is also implemented in order to amplify input signals in the circuit so that the probability of forward reaction is high. However, XOR DNA-based logic gate which is another important fundamental logic gate was not reported in this paper. Therefore, we firstly focus on XOR DNA-based logic gate design which would be suitable in enzyme-free cascading circuit.

3.2 Design of XOR DNA-based logic gate

DNA-based XOR logic gate requires that both inputs must be different in order to produce an output value of true. Since we use the existence of the object as the notion of true, the operation of the DNA-based logic gate depends on the concentration of both inputs. If there is a significant amount of only one of the two inputs the DNA-based XOR logic gate will release the output (Table 3.2). In order to detect only one input, but not two inputs, the DNA-based XOR logic gate should be designed in such a way that both input receptors (or detectors) should function in the same manner when either one of the inputs is detected but not both of the inputs together. We notice that a palindromic sequence fulfill this specification.

A palindromic sequence is a nucleotide sequence with sequence arrangement reading from 5’ to 3’ on both complementary strands are identical; example is 5’-GTCGAC-3’/ 3’-CAGCTG-5’. The DNA-based XOR logic gate with palindromic motifs and DNA input strands were designed as shown in Figure 3.4 and Figure 3.5 respectively. The XOR truth table is shown in Table 3.2.

Table 3.2 The truth table of XOR Boolean logic operation.

A_{in}	B_{in}	Output
0	0	0
0	1	1
1	0	1
1	1	0

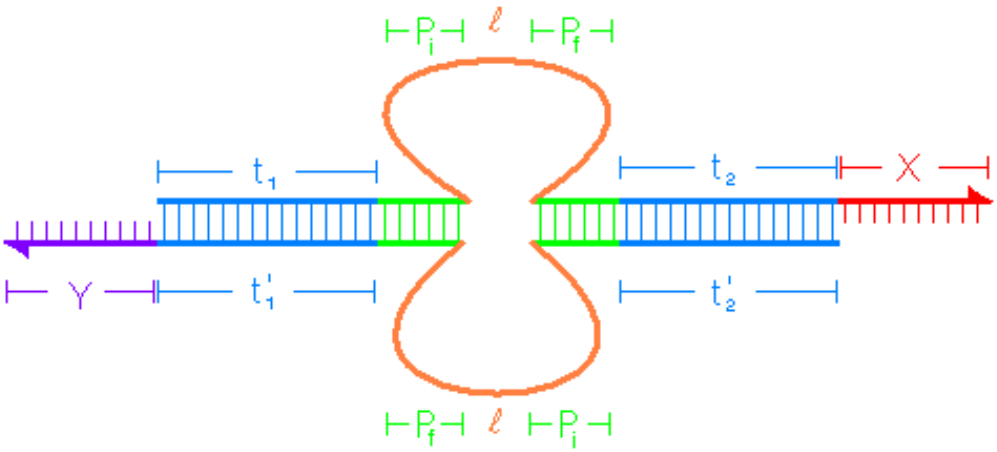

Figure 3.4 Design of DNA-based XOR logic gate with palindromic motifs (P_i and P_f) (see descriptions in the text).

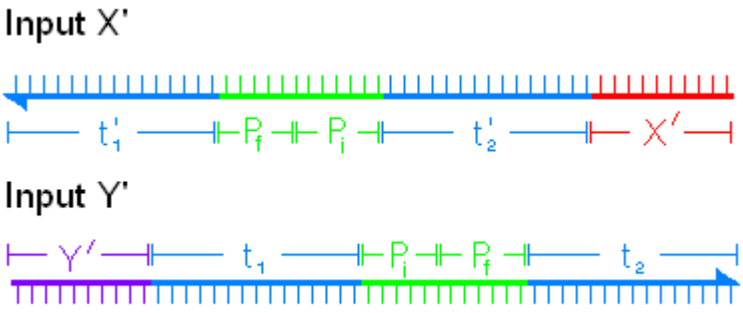

Figure 3.5 Design of DNA input strands for XOR DNA logic gate. (see descriptions in the text).

The design of DNA-based XOR logic gate (Figure 3.4) consists of 4 motifs:

Toe-hold motifs (X (red) and Y (purple)): 10-base long. Toe-hold motifs are single-stranded regions that function as recognition regions for specific inputs (input X' and Y').

Clamp motifs (t_1/t^I_1 and t_2/t^I_2 (blue)): 10-base-pair long. Clamp motifs are double-stranded regions adjacent to the toe-hold motif. Clamp motifs function as recognition regions for specific inputs and strong holding region during gate formation process.

Palindromic motifs (P_i and P_f (green)): 6-base-pair long. Palindromic motifs are double-stranded regions containing palindromic sequence that flanks the loop motif. Palindromic motifs function as recognition regions for specific inputs. Palindromic motifs are important regions for XOR computing process and its sequence is essential for downstream computing process.

Loop motif (ℓ (orange)): 20-base long. Loop motif is a single-stranded region. Loop motif plays no role in XOR computing process but its specific sequence is used as a part of input sequence for downstream computing process.

The overall of DNA-based XOR logic gate computing process is shown in Figure 3.6. The function of DNA-based XOR logic gate is based on entropy-driven mechanism. In the presence of one DNA input strand (Input X or Input Y), it binds to the corresponding toehold motif on the DNA-based XOR logic gate (Gate strand X or Gate strand Y), resulting in strand displacement. As a consequence, another single-stranded gate strand (Gate strand Y or Gate strand X, respectively) is released as an output (Figure 3.6, condition 2 and 3). If two DNA input strands are present at the same time, the input strands, with palindromic sequence, will bind each other, and the DNA-based XOR logic gate is intact (Figure 3.6, condition 4).

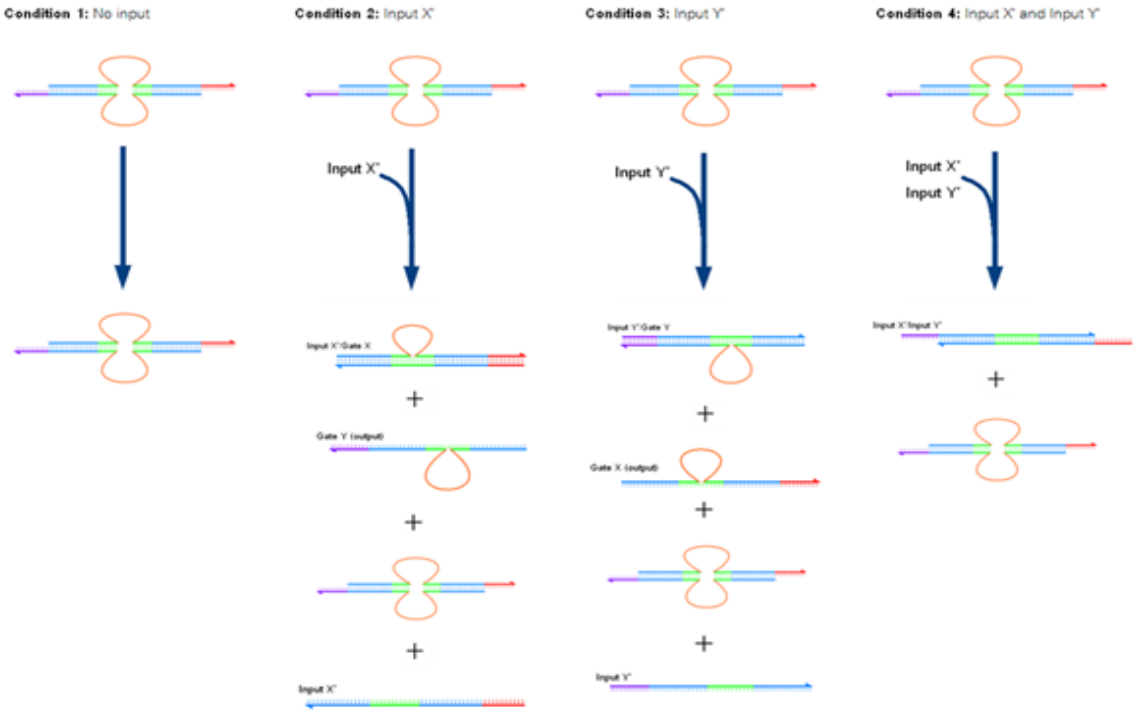

Figure 3.6 The overall process of DNA-based XOR logic gate in all four conditions.

3.3 Sequence design of DNA-based XOR logic gate

Since the structure of our DNA-based XOR logic gate contains palindromic motifs, the intended secondary structure along with other unintended structure will be formed (hairpin structure with stem region contains palindromic motifs). Our task is to reduce the occurrence probability of other secondary structures and unintended cross-activation.

Primary sequences are designed *in silico* by the "DNACodeDesigner" program developed by Dr. Boonsit Yimwadsana. The purpose of this algorithm is to design sequences of each strand with minimum crosstalk and unintended secondary structures. This algorithm divides the structure into parts. According to the design, the structure of the DNA-based XOR logic gate is divided into 5 parts: Toehold Y, Clamp T_1, Loop, Clamp T_2 and Toehold X. The sequence of Toehold X part was, then, randomly generated *in silico*. Any generated sequence that contains four or more repeated bases especially Guanine is not allowed in order to prevent G-quartet structure formation. The generated sequences that were compatible with the sequence design constraints were subjected to calculated for total ΔG value of Toehold X/Toehold X structure for all possible hybridization outcome. Those sequences with total ΔG value of any structure lesser than -3.0 kcal/mole were discarded. The sequences that agreed with all designing process constraints were recorded for further sequence assembly. Then, Clamp T_2 sequence was generated with the same process as done with Toehold X. Total ΔG value of Toehold X/Clamp $T_2$and Clamp T_2/Clamp T_2 were calculated for the Clamp T_2 sequences. Those sequences with total ΔG value lesser than -3.0 kcal/mole were discarded. Then, the sequences of the remaining parts were generated.

After the sequences of all five parts were generated, they were assembled into a new whole strand. Finally, the sequence for palindromic motif was generated with restriction that the palindromic sequence must not be able to hybridize with any other part of the whole strand sequence. The palindromic sequence was, then, inserted into the whole strand and become the complete strand. The overall sequence design process of "DNACodeDesigner" for XOR DNA-based logic gate is shown in Figure 3.7.

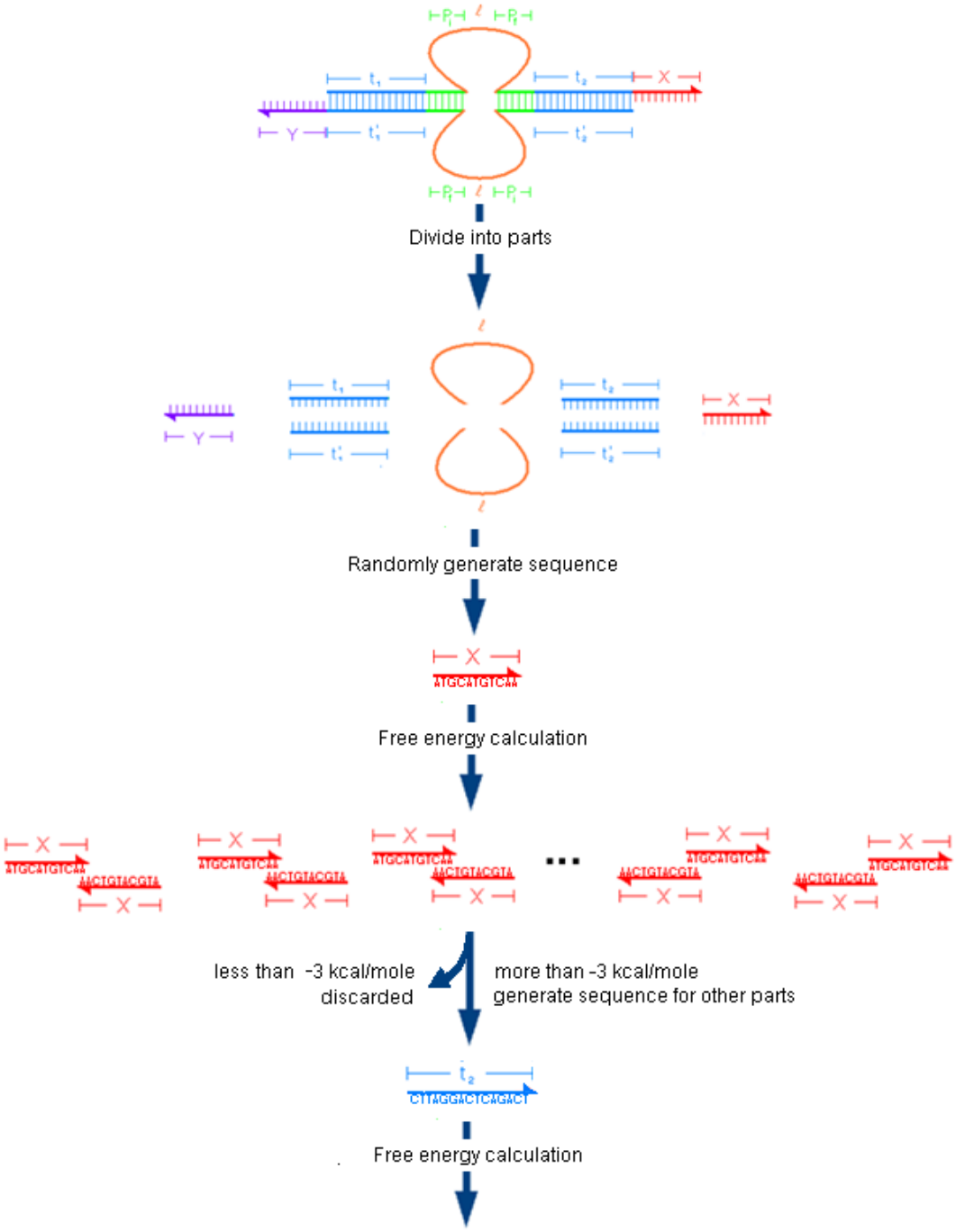

Figure 3.7 Overall process of DNACodeDesigner software for sequence design of DNA-based XOR logic gate.

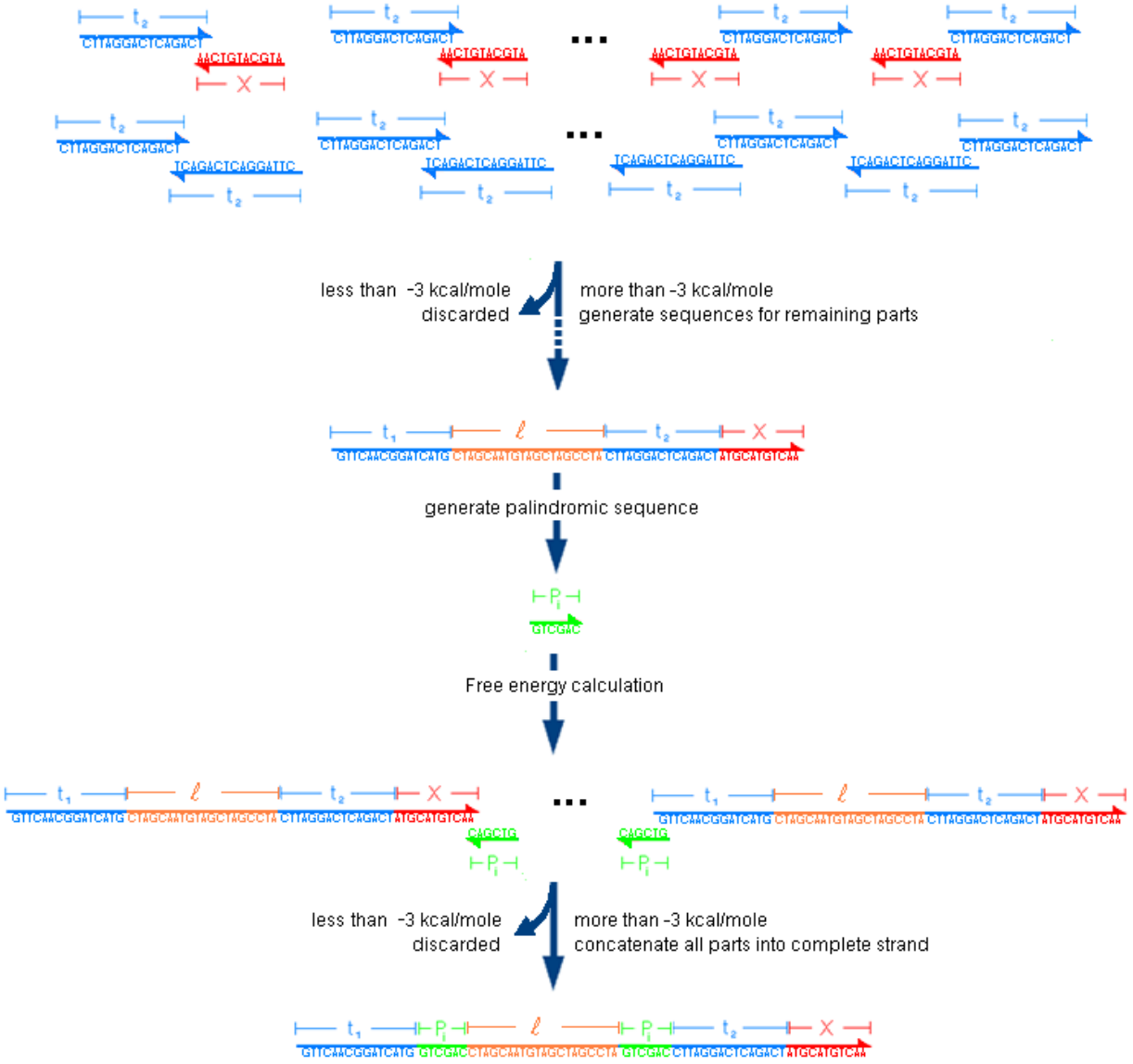

Figure 3.7 Overall process of DNACodeDesigner software for sequence design of DNA-based XOR logic gate (cont.).

The sequence of the complete strand was further verified for possibility of secondary structure formation by OligoAnalyzer 3.1 developed by Integrated DNA Technologies. Function “Hairpin” was selected for secondary structure formation, and conditions used were as follow; 0.25 μM oligo concentration, 5 mM Na^{+} concentration, 0 mM Mg^{2+} concentration, temperature 25 ^{o}C, Suboptimality 50% and Maximun folding 20.

If the result shows significant secondary structure formation, minimum free energy (MFE) algorithm will be used. The random MFE reduction is performed by randomly changed the sequence at the region which the unintended complex structure is formed. If the random changes results into lower free energy, the changed sequence will be memorized. The random MFE reduction process will be performed until the required secondary structure is the most stable structure. However, the constraints for MFE algorithm are varied from design to design. In this case, Guanine base was preferred to be mutated for point mutation process. The OligoAnalyzer 3.1 sequence analyzing process is demonstrated in Figure 3.8 and Figure 3.9.

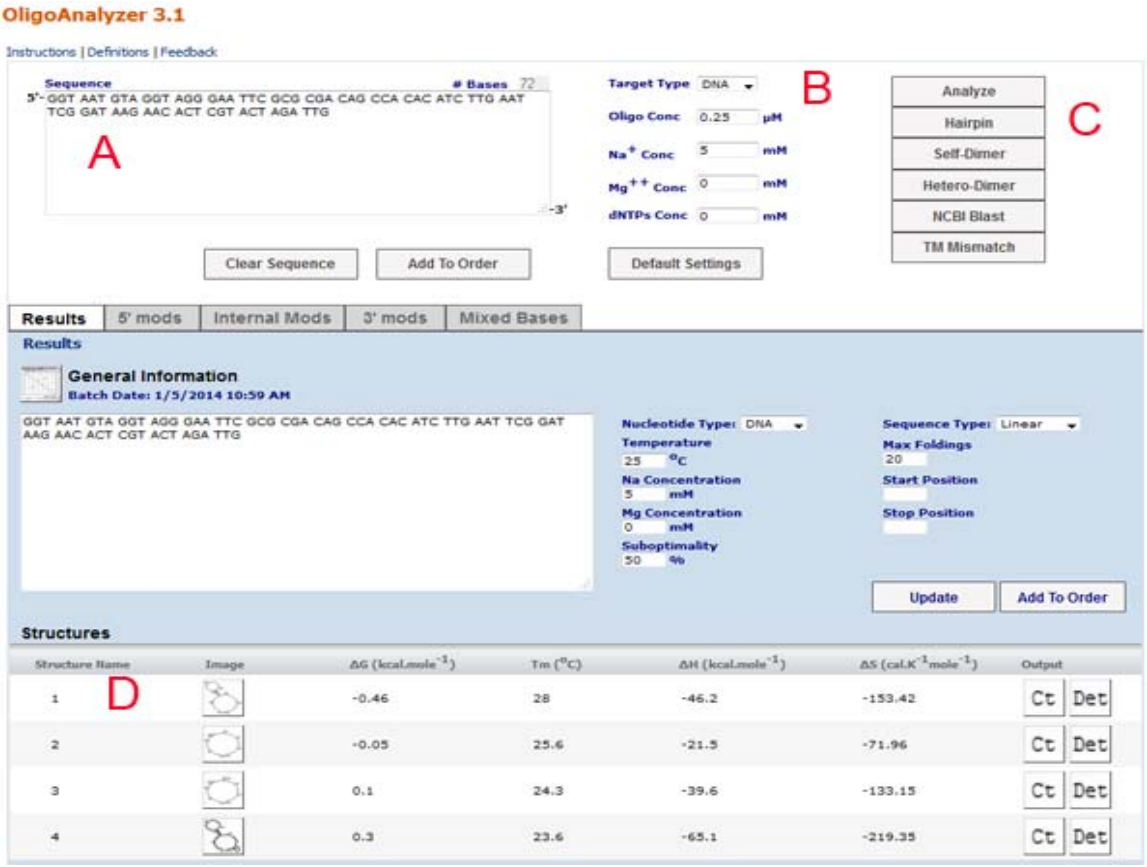

Figure 3.8 The software " OligoAnalyzer 3.1". First, put sequence of interest in box "A". Second, adjust the parameter involved in secondary structure formation at "B". Third, select "Hairpin" function at "C". The result of secondary structures are shown as structural image and data of thermodynamics parameters at "D".

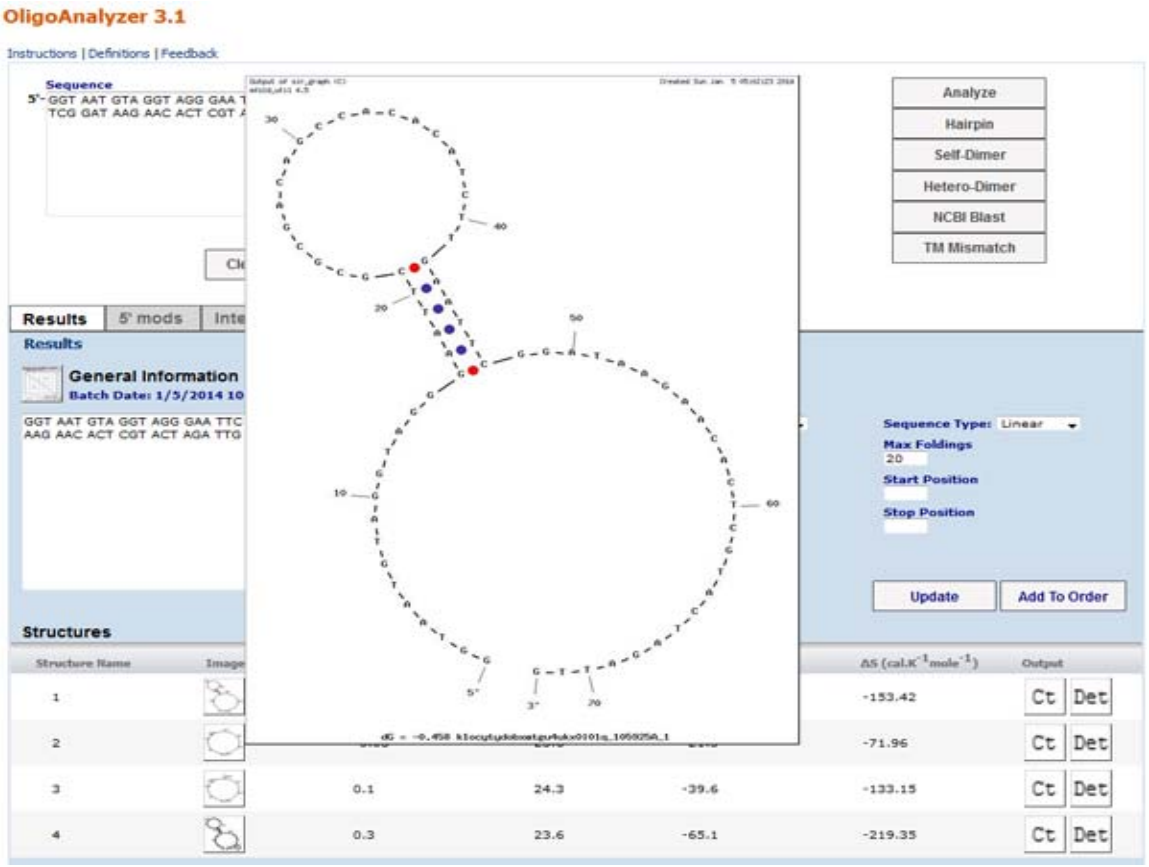

Figure 3.9 The example image of "strand X" of DNA-based XOR logic gate according to the design. The unintended secondary structure is not allowed. In case of unintended secondary structure, random MFE reduction process is applied.

3.4 Materials and methods of DNA-based XOR logic gate

Strand preparation: All DNA oligonucleotides are synthesized by Pacific Science Co., Ltd (Thailand). Oligonucleotides are purified by denaturing polyacrylamide gel electrophoresis (16% PAGE, 7 M Urea). The purified oligonucleotides are stored in TE buffer (0.04 M Tris base, 1 mM EDTA) as stock solution at 100 μM. The stock solutions are kept at - 20 ^{o}C. All DNA oligonucleotides sequence using in XOR DNA-based logic gate experiment are shown in Table 3.3.

Gate formation: The XOR logic gate single-stranded DNA (Gate strands X and Y) at concentration of 2.5 μM are incubated in TE buffer at total volume of 20 μL. The solution is heated up to 90 ^{o}C for 5 minutes and slowly cooled down with constant rate 1 ^{o}C/min to 15 ^{o}C. The formed logic gates can be stored at 4 ^{o}C for couple weeks with efficient function.

Gate purification: The well-formed DNA-based XOR logic gate is purified by using 3% agarose gel (Nusieve 3:1) with TAE buffer (0.04 M Tris Acetate, 1 mM EDTA). NucleoTrap® was used in order to obtain high purity product from agarose gel extraction.

Crush and soak is another method for gate purification process. The excised gel containing DNA-based logic gate was frozen in liquid nitrogen then centrifuged at 14,000 rpm for 5 minutes. Supernatant is collected and remaining gel was centrifuged for additional 5 minutes, then supernatant is collected. The collected supernatant is, then, precipitated by 95% alcohol. Crush and soak technique provides better gate structure recovery rate but fair purity compared to the kit extraction technique.

Gate function analysis: The DNA-based XOR logic gate and input strands are incubated at 25 ^{o}C for 15 minutes. Then, the reaction mixture is analyzed by non-denaturing polyacrylamide gels electrophoresis (non-denaturing PAGE; 10% acrylamide-bis 19:1). PAGE result shows gate structure and interaction between gate and input strands. The input X (X_{in}) and input Y (Y_{in}) concentration are 10 μM. At beginning, all inputs are added to the reactions and incubated for 10 minutes. Then, DNA-based XOR logic gate is added to the reactions and incubated for 5 minutes. PAGE was run in TAE buffer at 100 V for 2 hours. Gel is stained with ethidium bromide for imaging. The gel is visualized under UV light and photographed by G:box

(SYNGENE, UK). DNA Band intensity was measured by GENETOOLS software (SYNGENE, UK) and compared each other in relative value.

Ladder marker: GeneRuler Ultra Low Range DNA Ladder (Thermo Scientific) is used as marker in all experiments. The ladder contains the band of double-stranded DNA with length from 10-300 base pairs. The pattern of GeneRuler Ultra Low Range DNA Ladder is shown in Figure 2.3.

Table 3.3 The sequence of all DNA oligonucleotides using in DNA-based XOR logic gate experiment. The gray color indicates the complementary region of toehold regionin input strand and toehold binding region in logic gate strand. The underlined bases indicate palindromic sequences

Strand Name	Bases
X	5'-GGTAATGTAGGTAGGGAATTCGCGCGACAGCCACACATCTTGAATTCGGATAAGAACACTCGTACTAGATTG -3'
Y	5'-CGAGTGTTCTTATCCGAATTCGCGCGACAGCCACACATCTTGAATTC CCTACCTACATTACCCTATGACGGA -3'
X_{in}	5'-CAATCTAGTACGAGTGTTCTTATCCGAATTCGAATTCCCTACCTACATTACC -3'
X_{bin}	5'-CAATCTAGTACGAGTGTTCTTATCCGAATTCGAATTCCCTACCTACATTACCCTATGACGGA -3'
X_{cin}	5'-CCTTGACCAATCTAGTACGAGTGTTCTTATCCGAATTCGAATTCCCTACCTACATTACCCTATGACGGA CTGAGCA -3'
Y_{in}	5'-TCCGTCATAGGGTAATGTAGGTAGGGAATTCGAATTCGGATAAGAACACTCG -3'
Y_{bin}	5'-TCCGTCATAGGGTAATGTAGGTAGGGAATTCGAATTCGGATAAGAACACTCGTACTAGATTG -3'
Y_{cin}	5'-TGCTCAGTCCGTCATAGGGTAATGTAGGTAGGGAATTCGAATTCGGATAAGAACACTCGTACTAGATTG GTCAAGG -3'

3.5 Experimental results of DNA-based XOR logic gate

The PAGE was applied to observe the changes of DNA-based XOR logic gate structure. Since XOR logic gate has 2 inputs (X_{in} and Y_{in}), $2^2 = 4$ conditions will be observed. First, both input strands are absent (X = 0, Y = 0). Second, Input X is present but Input Y is absent (X = 1, Y = 0). Third, input Y is present but input X is absent (X = 0, Y = 1). Fourth, both input X and input Y are present (X = 1, Y = 1).

3.5.1 Overhang ends structure of $X_{in}Y_{in}$

At the beginning, the primitive design was observed. The XOR logic gate structure is merely detected in lane 1 (condition 1) but cannot be detected in lane 2-4 (condition 2-4). In the fourth lane, $X_{in}Y_{in}$ structure is barely detected but XX_{in} and YY_{in} structured can be detected. The disappearance of XOR logic gate band suggests the complete leakage due to cross activation between the XOR logic gate structure and $X_{in}Y_{in}$ structure. The result is shown in Figure 3.10.

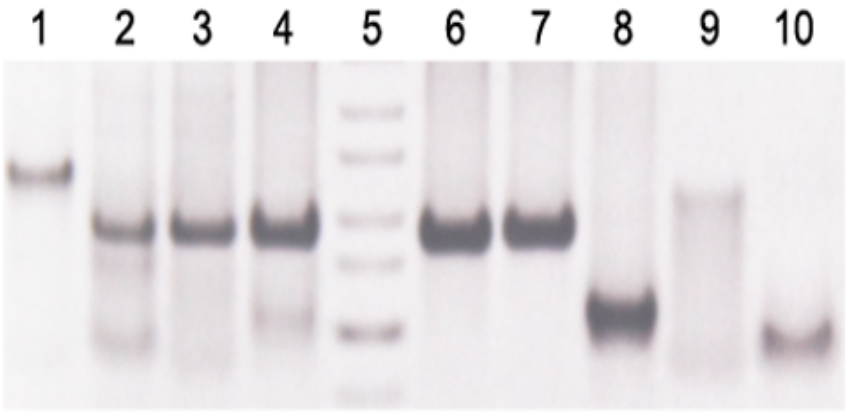

Figure 3.10 The electrophoretic pattern of primitive DNA-based XOR logic gate design with overhangs toehold binding region on both 3' ends with input strand X_{in} and Y_{in}. XOR gate concentration is 2.5 μM, X_{in} concentration is 10 μM, Y_{in} concentration is 10 μM, XX_{in} concentration is 10 μM, YY_{in} concentration is 10 μM and $X_{in}Y_{in}$ concentration is 10 μM. The gate-input ratio is 1:4.

1^{st} lane = XOR gate

2^{nd} lane = XOR gate + X_{in}

3^{rd} lane = XOR gate + Y_{in}

4^{th} lane = XOR gate + X_{in} + Y_{in}

5^{th} lane = Ladder Marker

6^{th} lane = XX_{in}

7^{th} lane = YY_{in}

8^{th} lane = $X_{in}Y_{in}$

9^{th} lane = X

10^{th} lane = X_{in}

3.5.2 Blunt end structure of $X_{bin}Y_{bin}$

In the second design, XOR logic gate contains the primitive sequences (X strand and Y strand) but the input strands have been changed into the longer strand. The new input strands or called "X_{bin} and Y_{bin}" contains extra 10 bases complementary to toehold binding region sequence for each other (Table 3.3). The extra 10 bases function as toehold blocking region to prevent the cross activation with XOR logic gate structure. The new input strand "X_{bin} and Y_{bin}" are shown in Figure 3.11. The XOR logic gate structure is merely detected in lane 2 (condition 1), barely detected in lane 5 (condition 4) but cannot be detected in lane 3-4 (condition 2-3). In the fifth lane, $X_{bin}Y_{bin}$ structure is clearly detected as well as XX_{bin} and YY_{bin} structures. The detection of fade XOR logic gate band in lane 5 (condition 4) suggests the better of blunt-end $X_{bin}Y_{bin}$ structure in order to prevent cross activation with XOR logic gate structure. The result of XOR gate with X_{bin} and Y_{bin} strand is shown in Figure 3.12.

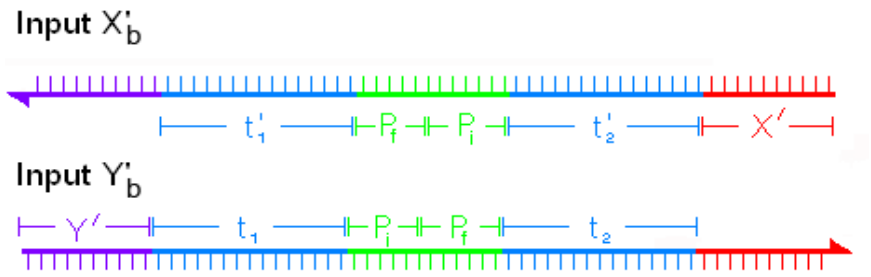

Figure 3.11 The illustration of Input X_b strand (X_{bin}) and Input Y_b strand (Y_{bin}).

The Input X_b strand and Input Y_b strand will bind each other and form into blunt double-stranded DNA.

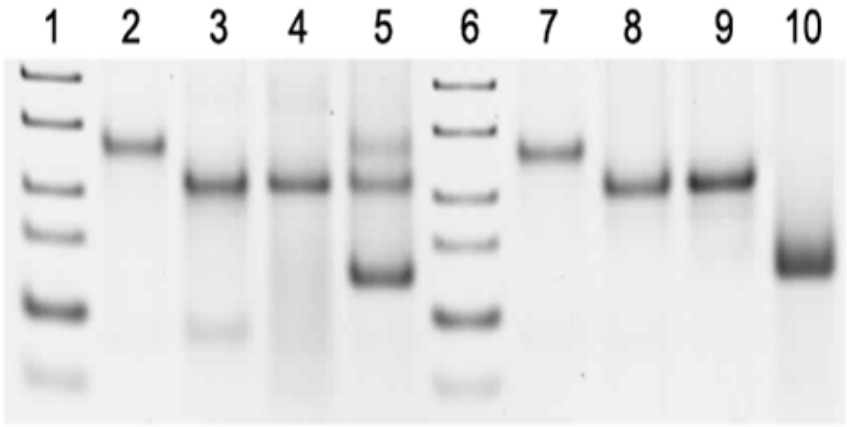

Figure 3.12 The electrophoretic pattern of primitive DNA-based XOR logic gate design with overhangs toehold binding region on both 3' ends with input strand X_{bin} and Y_{bin}. XOR gate concentration is 2.5 μM, X_{bin} concentration is 10 μM, Y_{bin} concentration is 10 μM, XX_{bin} concentration is 10 μM, YY_{bin} concentration is 10 μM and $X_{bin}Y_{bin}$ concentration is 10 μM. The gate-input ratio is 1:4.

1^{st} lane = Ladder marker

2^{nd} lane = XOR gate

3^{rd} lane = XOR gate + X_{bin}

4^{th} lane = XOR gate + Y_{bin}

5^{th} lane = XOR gate + X_{bin} + Y_{bin}

6^{th} lane = Ladder Marker

7^{nd} lane = XOR gate

8^{th} lane = XX_{bin}

9^{th} lane = YY_{bin}

10^{th} lane = $X_{bin}Y_{bin}$

3.5.3 Clamp end of $X_{cin}Y_{cin}$ structure with clamps

In the third design, XOR logic gate still contains the primitive sequences (X strand and Y strand) but the input strands have been changed into the even longer strand. The new input strands or called "X_{cin} and Y_{cin}" contains the extra 7 bases with complementary sequence for each other. The extra bases function as clamps at both ends of $X_{cin}Y_{cin}$ structure in order to reduce double-stranded fraying which reveal the toehold sequence of input strand. The new input strand "X_{cin} and Y_{cin}" are shown in Figure 3.13. The XOR logic gate structure is merely detected in lane 2 (condition 1) and lane 5 (condition 4). The XX_{cin} structure can be detected in lane 3 (condition 2) and YY_{cin} structure can be detected in lane 4 (condition 3). In lane 5, $X_{cin}Y_{cin}$ structure is clearly detected but the XX_{cin} and YY_{cin} structure cannot be detected (condition 4). The detection of XOR logic gate band in lane 5(condition 4) with nearly the same band intensity compare to control lane (lane2, condition 1) suggest the capability of 7 bases clamps in order to prevent cross activation between XOR logic gate structure and $X_{cin}Y_{cin}$ structure. The result of XOR gate with X_{cin} and Y_{cin} is shown in Figure 3.14.

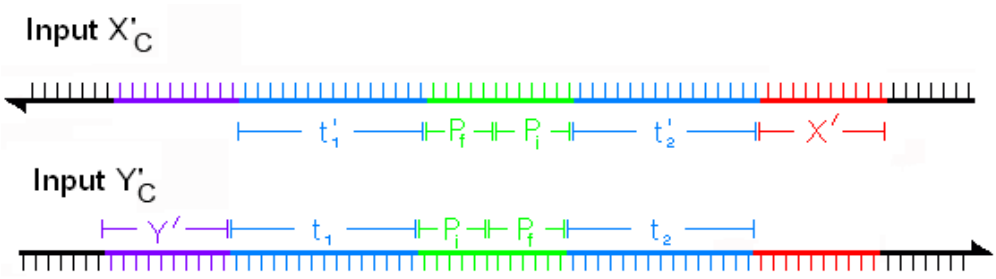

Figure 3.13 The illustration of Input X_c strand (X_{cin}) and Input Y_c strand (Y_{cin}).
The Input X_c strand and Input Y_c strand will bind each other and form into blunt double-stranded DNA with 7 base pairs clamps at both ends.

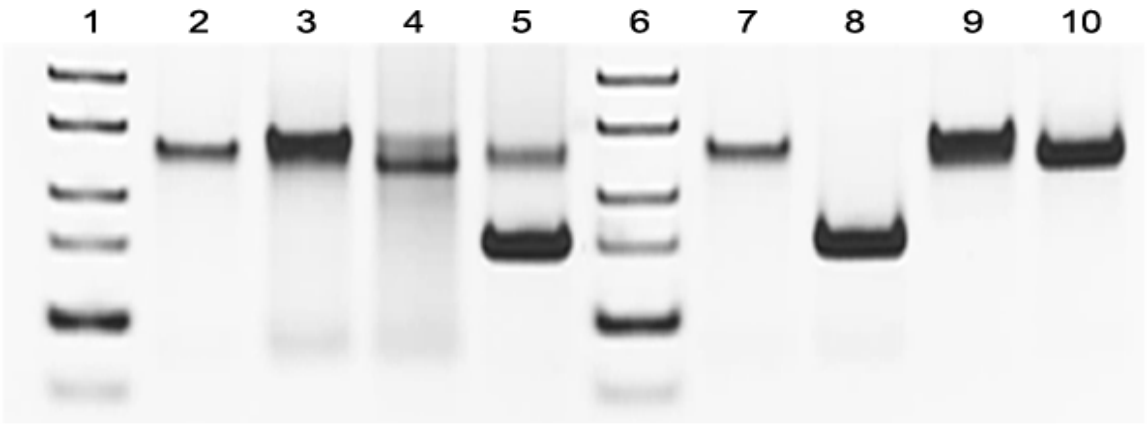

Figure 3.14 The electrophoretic pattern of primitive DNA-based XOR logic gate design with overhangs toehold binding region on both 3' ends with input strand X_{cin} and Y_{cin}. XOR gate concentration is 2.5 μM, X_{cin} concentration is 10 μM, Y_{cin} concentration is 10 μM, XX_{cin} concentration is 10 μM, YY_{cin} concentration is 10 μM and $X_{cin}Y_{cin}$ concentration is 10 μM. The gate-input ratio is 1:4.

1st lane = Ladder marker

2nd lane = XOR gate

3rd lane = XOR gate + X_{cin}

4th lane = XOR gate + Y_{cin}

5th lane = XOR gate + X_{cin} + Y_{cin}

6th lane = Ladder Marker

7th lane = XOR gate

8th lane = $X_{cin}Y_{cin}$

9th lane = XX_{cin}

10th lane = YY_{cin}

The band intensity of XOR logic gate structure of all experimental results are measured and compared in term of function. Since there is no input strand presented, the XOR logic gate structure should be intacted. This results in the maximum value of band intensity. In other words, relative band intensity value is 1.0 as the negative result control. The fourth condition of Boolean logic of XOR logic gate, X and Y input strands are presented, were measured for XOR logic gate structure band intensity and compared to the control. The stability of XOR logic gate with the common input strands, X_{in} and Y_{in}, compare to the control is 0.587. Since the input strands are modified in to X_{bin} and Y_{bin}, the XOR logic gate stability is increased to 0.850 and even more increased to 0.929 when the input strands are modified in to X_{cin} and Y_{cin}. The comparison of the XOR logic gate stability with different design of input strands is shown in Figure 3.15.

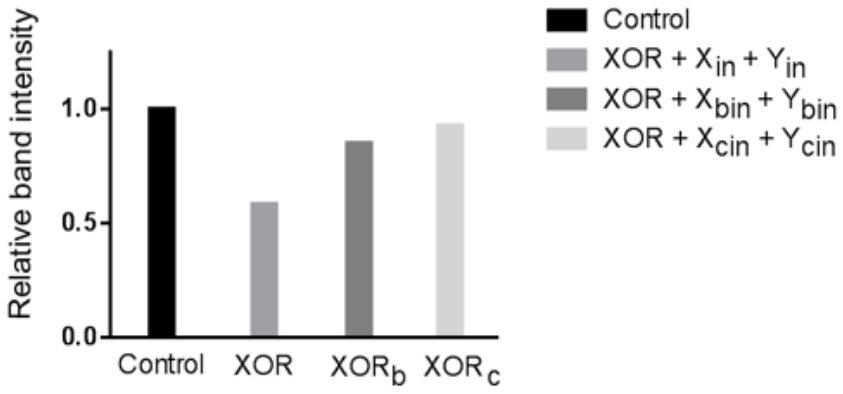

Figure 3.15 . The comparison of the XOR logic gate stability with different design of input strands. Control bar represents the condition which only XOR logic gate structure is presented in the solution. Relative band intensity value, therefore, is 1.0. The XOR, XOR_b and XOR_c bars represent the condition which primitive design strands X_{in} and Y_{in}, X_{bin} and Y_{bin} and X_{cin} Y_{cin} strands are used, respectively.

3.6 Discussion of the DNA-based XOR logic gate

Here we introduced the design of DNA-based XOR logic gate structure utilizing the palindrome sequence. In order to design the DNA-based logic gate structure function as XOR Boolean logic algebra, two input strands with distinctive sequence must produce an output strand in the condition which only one input, X or Y, is presented. However, we suggest an optional concept by producing 2 input strands with a part contains the same sequence which is the palindrome sequence. From the beginning, the DNA-based XOR logic gate system was designed by mainly focus on its function without concern of cross-activation. As the result, the experiment of first version shows the cross-activation between the XOR logic gate and $X_{in}Y_{in}$ structure. (Figure 3.10). However, the electrophoretic patterns surprisingly shows pattern of OR logic gate instead. Anyway, we further adjust the first design to function as XOR logic gate by increasing input strands length in order to prevent cross-activation. The extra bases of input strands, X_{bin} and $Y_{bin,}$ are completely complementary to toehold region of another input which form into blunt-end structure. The result shows reduction in cross-activation (Figure 3.12). We further improve the model by adding clamps at both ends of input complex. The X_{cin} and Y_{cin} strand are able to reduce cross-activation compare to the condition with X_{bin} and Y_{bin} (Figure 3.15).

Since we consider all results comparatively, we found an interesting aspect regard to the change of structure function from being OR logic gate to XOR logic gate due to the change of input length and design. According to this ability of designed XOR logic gate structure, computational detection system will be simplified since the same sequence of input strands are able to function into two optional ways, OR or XOR, by regulating the structure of input strands.

The success of DNA-based XOR logic gate compatible with cascading circuit allows us to construct the full-adder circuit. However, limitations according to the designed is needed to be solved. The problem of DNA-based XOR logic gate is considered in two aspects, which are logic gate error itself and circuit error.

The logic gate error is occurred due to structure defect during gate formation process. The malformation of DNA-based XOR logic gate is the result of inappropriate sequence design process which non-specific structures are formed. For example, dimer structure of DNA-based XOR logic gate. This problem, however, can

be solved by additional gate purification process. Environmental conditions also play roles. The improper temperature, too high or too low, could affect on thermodynamics of logic gate computation process. High salt concentration also increases stability of non-specific structure which cross-activation can be occurred.

The circuit error is another aspect to concern. As we know, DNA-based XOR logic gate has two input strands. Different patterns of inputs added result into different outputs. The DNA-based XOR logic gate requires exactly only one input (X or Y) but not both, to activate the XOR gate operation to produce an output. If two active inputs arrive at the XOR logic gate but at different times, the logic gate may be activated by the first input resulting in an incorrect operation as a fault positive result. Choosing the appropriate time is, therefore, necessary for the correct operation of the XOR logic gate.

As we concern about half-adder in term of circuit, the different input strands for different logic gate is necessary, XOR and AND in this case. That means four input strands with distinctive sequence related to each logic gate are needed. This problem results in high complexity of upstream circuit. In addition, the input strands are necessary to be incubated to form the double-stranded complex before the computation process with the XOR logic gate structure is begun. This problem has no effect on half-adder circuit construction but significantly impacts on full adder circuit design. Here we are going to introduce the new structure, only a structure for 1-bit full-adder operation, at next.

CHAPTER IV
DEVELOPMENT OF DNA-BASED FULL ADDER IN ENZYME-FREE BIOLOGICAL CIRCUIT

4.1 Design of full adder structure

Full adder logic circuit is an circuit with addition function utilizing three one-bit numbers summation operation. The full adder logic circuit takes three input strands (A, B and Carry in(C_{in})) and gives out two output which are SUM and $CARRY_{out}$. The truth table of full-adder logic circuit is shown in Table 3.1.

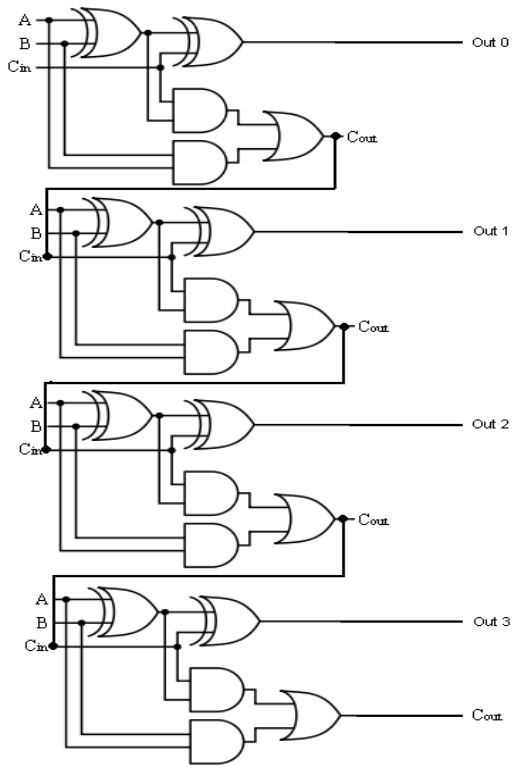

Figure 4.1 The 4-bit full adder circuit. SUM = (A XOR B) XOR C. CARRY = (A XOR B) ∧ C) ∨ (A ∧ B)

According to full adder logic circuit design in silicon-based computer, full adder DNA-based logic gate was designed to use three inputs in order to perform addition and release CARRY as output for next bit calculation. The design of full adder DNA-based logic gate structure was shown in Figure 4.1. As we concern each unit of full adder circuit, these smallest units comprise of 2 XOR logic gate, 2 AND logic gate and 1 OR logic gate. Although our success on XOR logic gate development, the full adder circuit based on common silicon-based circuit design seems to be very complex. In this chapter, we will focus on full adder circuit design with low complexity.

Our full adder DNA-based logic gate structure is composed of three single-stranded DNA with 80 bases long on each strand (A, B and C) which form into three-way junction structure (Figure 4.2). The full-adder DNA-based logic gate structure can be divided into five regions on each arm as follows.

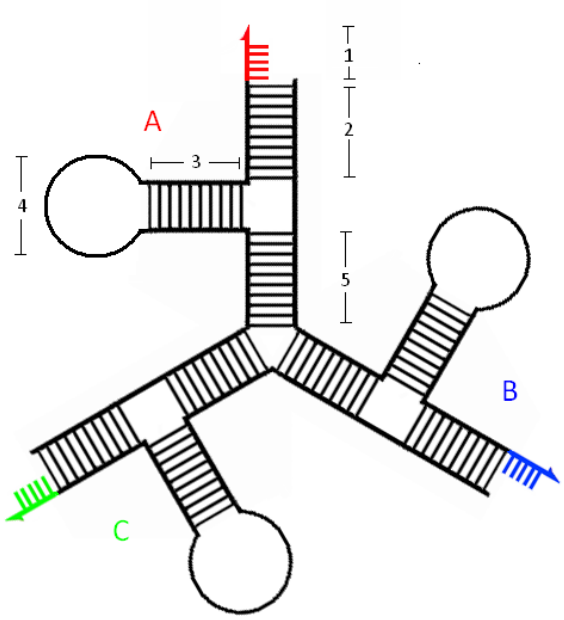

Figure 4.2 The illustration of full-adder DNA-based logic gate structure. The structure comprises of three DNA strands (A, B, and C) which form into "3-way junction" structure. 1 = Toehold region, 2 = Distal region, 3 = Stem region, 4 = Loop region, 5 = proximal region. red = toehold binding region of A_{in}, blue = toehold binding region of B_{in}, green = toehold binding region of C_{in}.

Toehold region: Toehold region has 5 bases long. This region functions as recognition region for specific input to activate computing process.

Distal region: Distal region has 10 bases long. This region functions as clamp for the structure and also increases specificity for the incoming input strand.

Stem region: Stem region has 10 bases long. This region functions as control device for sequences in loop region.

Loop region: Loop region has 10 bases long. This region functions as data for CARRY. This data is locked by stem region which needs the specific key to initiate the CARRY function.

Proximal region: Proximal region has 10 bases long. This region functions as clamp for the structure and also increases specificity for the incoming input strand.

Input for full adder DNA-based logic gate structure is single-stranded DNA with 45 bases long (Figure 4.3). These three inputs are named as A_{in}, B_{in} and C_{in}. The A_{in} strand and B_{in} strand represent two binary numbers in a binary digit while C_{in} represents the CARRY which is the output that was released from previous bit.

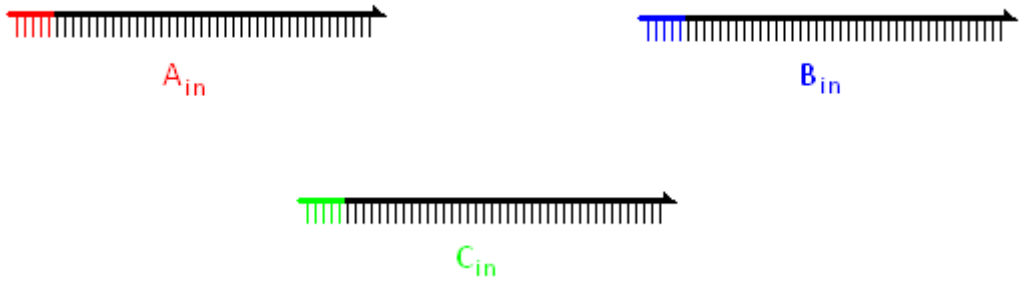

Figure 4.3 Input for full adder DNA-based logic gate. The colored regions represent toehold regions for input strands related to full adder structure in Figure 4.2.

Since full adder DNA-based logic gate uses three inputs to perform computing process, there are eight possible conditions.

1st condition: No input

No input is added. The full adder DNA-based logic gate structure is intact. No single-stranded DNA is released from the structure.

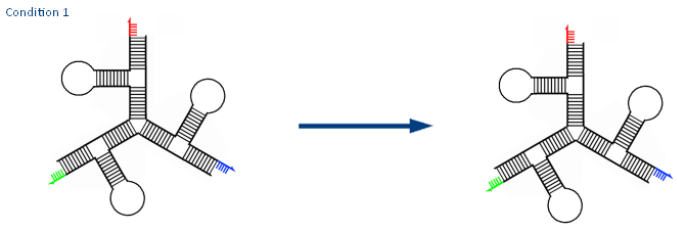

Figure 4.4 Schematic diagram of "1st condition" of DNA-based full adder structure.

2nd condition: A_{in}

A_{in} binds to the A toehold region, forming A-A_{in} complex.

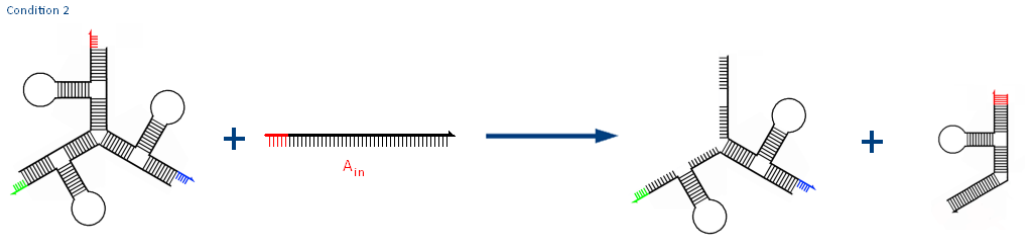

Figure 4.5 Schematic diagram of "2nd condition" of DNA-based full adder structure.

3rd condition: B_{in}

B_{in} binds to the B toehold region, forming B-B_{in} complex.

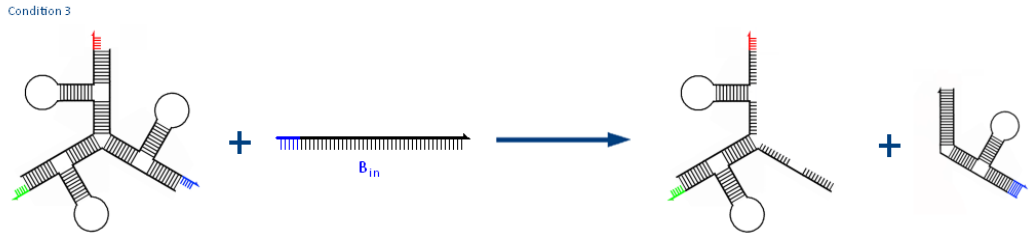

Figure 4.6 Schematic diagram of "3rd condition" of DNA-based full adder structure.

4th condition: C_{in}

C_{in} binds to the C toehold region, forming C-C_{in} complex.

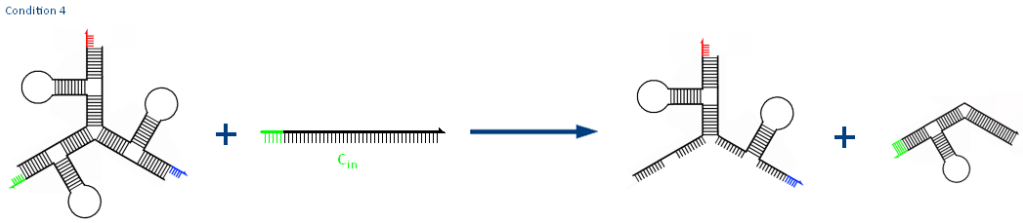

Figure 4.7 Schematic diagram of "4th condition" of DNA-based full adder structure.

5th condition: A_{in} and B_{in}

A_{in} binds to the A toehold region, forming A-A_{in} complex.

B_{in} binds to the B toehold region, forming B-B_{in} complex.

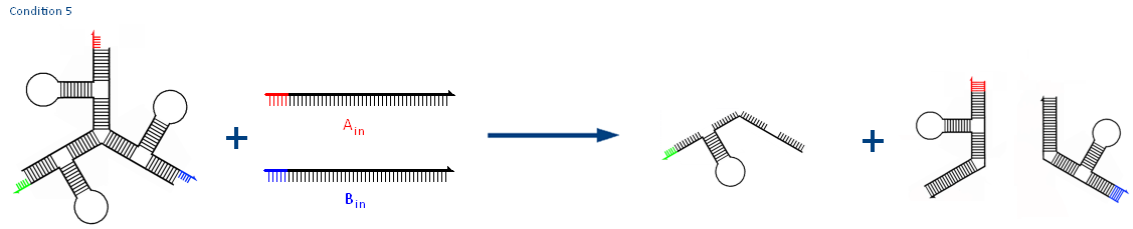

Figure 4.8 Schematic diagram of "5th condition" of DNA-based full adder structure.

6th condition: A_{in} and C_{in}

A_{in} binds to the A toehold region, forming A-A_{in} complex.

C_{in} binds to the C toehold region, forming C-C_{in} complex.

Figure 4.9 Schematic diagram of "6th condition" of DNA-based full adder structure.

7th condition: B_{in} and C_{in}

B_{in} binds to the B toehold region, forming B-B_{in} complex.

C_{in} binds to the C toehold region, forming C-C_{in} complex.

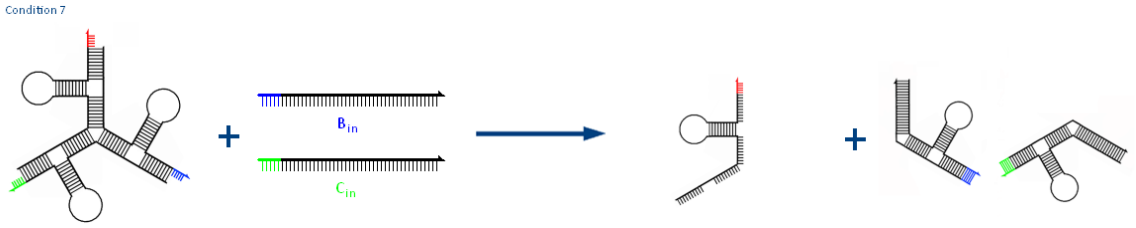

Figure 4.10 Schematic diagram of "7th condition" of DNA-based full adder structure.

8th condition: A_{in}, B_{in} and C_{in}

A_{in} binds to the A toehold region, forming A-A_{in} complex.

B_{in} binds to the B toehold region, forming B-B_{in} complex.

C_{in} binds to the C toehold region, forming C-C_{in} complex.

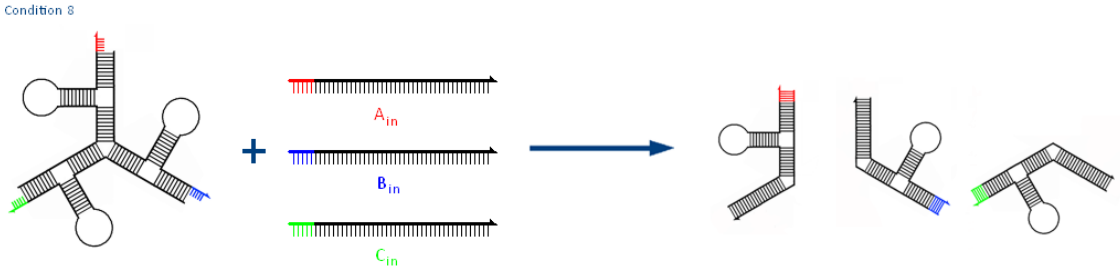

Figure 4.11 Schematic diagram of "8th condition" of DNA-based full adder structure.

4.2 Sequence design of full-adder structure

The sequence design of 3-way junction full-adder structure is designed with constraints. Two "GC" base pairs were placed at both of duplex ends and all junctions to reduce duplex fraying. Three base repetitions were avoided. Sequence of all nucleotides are primarily designed by “DNACodeDesigner” software and further optimized by Oligoanalyzer 3.1 software with MFE reduction method. The sequence of all oligonucleotides used in full-adder experiment are shown in Table 4.1.

4.3 Materials and methods of full-adder structure

Strand preparation: All DNA oligonucleotides are synthesized by Pacific Science Co., Ltd (Thailand). Oligonucleotides are purified by denaturing polyacrylamide gel electrophoresis (16% PAGE, 7 M Urea). The purified oligonucleotides are stored in TE buffer (0.04 M Tris base, 1 mM EDTA) as stock solution at 100 μM. The stock solutions are kept at -20 ^{o}C.

Gate formation: The single-stranded DNA of full-adder structure (Gate strands A, B and C) at concentration of 2.5 μM are incubated in TE buffer at total volume of 20 μL. The solution is heated up to 90 ^{o}C for 5 minutes and slowly cooled down with a constant rate of 1 ^{o}C/min to 15 ^{o}C. The formed logic gates can be stored at 4 ^{o}C for couple weeks with efficient function.

Gate function analysis: The DNA-based XOR logic gate and input strands are incubated at 25 ^{o}C for 15 minutes. Then, the reaction mixture is analyzed by non-denaturing polyacrylamide gels electrophoresis (non-denaturing PAGE; 10% acrylamide-bis 19:1). PAGE result shows gate structure and interaction between gate and input strands. The input A (A_{in}), B (B_{in}) and input C (C_{in}) concentration are 10 μM. The full-adder structure and all input strands are added to the reactions and incubated for 15 minutes. PAGE was run in TAE buffer at 100 V for 2 hours. Gel is stained with ethidium bromide for imaging. The gel is visualized under UV light and photographed by G:box (SYNGENE, UK). DNA band intensity was measured by GENETOOLS software (SYNGENE, UK) and compared each other in relative value.

Ladder marker: GeneRuler Ultra Low Range DNA Ladder (Thermo Scientific) is used as marker in all experiments. The ladder contains the band of double-stranded DNA with length from 10-300 base pairs. The pattern of GeneRuler Ultra Low Range DNA Ladder is shown in Figure 2.3.

Table 4.1 The sequence of all DNA oligonucleotides used in full adder structure experiment. The gray color indicates the complementary region of toehold region in input strand and toehold binding region in logic gate strand.

Strand Name	Bases
A	5'- GAGGTATAGGCTAATGCTGCGGATCAACACATCATCATGTG AGTACGC CAATTAGACATGATGATCCATGCAGTCCACTA -3'
B	5'- GACTGCATGGGTGTTGATCCGCGAATATCCTTACGGCTGTGA GTACGC CAATTAGACAGCCGTAACGGTACAGAGTGAGC -3'
C	5'- CTCTGTACCGGGATATTCGCGCAGCATTAGGAGAACTAACG AGTACGC CAATTAGGTTAGTTCTCCCTATACCTCGCAAT -3
A_{in}	5'- TAGTGGACTGCATGGGTGTTGATCCGCAGCATTAGCCTATAC CTC -3'
B_{in}	5'- GCTCACTCTGTACCGGGATATTCGCGGATCAACACCCATGCA GTC -3'
C_{in}	5'- ATTGCGAGGTATAGGCTAATGCTGCGCGAATATCCCGGTAC AGAG -3'
Ae4	5'- ATGGATCATACACCTGTCCGCTAAGTCAGATCGACAGGTGT ATGAT-3'
Be4	5'- CTACGTACGACACCTGTCCGCTAAGTCAGATCGACAGGTGTC GTAC -3'
Ce4	5'- ACTGCAATCACACCTGTCCGCTAAGTCAGATCGACAGGTGT GATTG -3'
S_{Ae4}	5'- AGCGGACAGGTGTCGTACGTAG -3'
S_{Be4}	5'- AGCGGACAGGTGTGATTGCAGTAAAA -3'
S_{Ce4}	5'- AGCGGACAGGTGTATGATCCATAAAAAAAA -3'
R_u	5'- ACACCTGTCGATCTGACTT -3'
R_d	5'- AAGTCAGATCGACAG -3'

4.4 Experimental results of full-adder structure

The PAGE was applied to observe the changes of DNA-based full-adder structure. Since the full-adder structure has 3 inputs, 2^3 = 8 conditions will be observed. First, all input strands are absent (A = 0, B = 0, C = 0). Second, only Input A is present (A = 1, B = 0, C = 0). Third, only Input B is present (A = 0, B = 1, C = 0). Fourth, only Input C is present (A = 0, B = 0, C = 1). Fifth, Input A and B are present (A = 1, B = 1, C = 0). Sixth, Input A and C are present (A = 1, B = 0, C = 1). Seventh, Input B and C are present (A = 0, B = 1, C = 1). Eighth, all Input A, B and C are present (A = 1, B = 1, C = 1).

4.4.1 Three-way junction full-adder structure

At the beginning, the primitive design of full-adder structure function is observed on 8 possible conditions. The result of three-way junction full-adder structure is shown in Figure 4.2. In the first condition (lane 2), the full-adder structure band is detected at approximately 300 bps position and also gate strand remnant (A, B and C strand) around at 75 bps position. The second condition (lane 3), AA_{in} band is detected at around 150 bps position. The gate strand A and A-A duplex are detected around 50 and 75 bps position, respectively. The third condition (lane 4), BB_{in} band is detected at around 150 bps position. The gate strand B and B-B duplex are detected around 50 and 75 bps position, respectively. The fourth condition (lane 5), CC_{in} band is clearly detected at around 150 bps position. The gate strand is barely detected around 300 bps position. The fifth condition (lane 6), AA_{in} and BB_{in} are detected. The $A_{in}B_{in}$ complex is clearly detected at around 75 bps position. The C strand is hardly detected. The sixth condition (lane 7), AA_{in} and CC_{in} are detected. $A_{in}C_{in}$ complex is clearly detected at around 75 bps position. The B strand is clearly detected. The seventh condition (lane 8), BB_{in} and CC_{in} are detected. The $B_{in}C_{in}$ complex is clearly detected at around 50 bps position. The A strand is hardly detected. The eighth condition (lane 9), AA_{in}, BB_{in} and CC_{in} are detected. The $A_{in}B_{in}C_{in}$ complex is clearly detected. The A and B strands can be detected. The result of the full adder structure is shown in Figure 4.12.

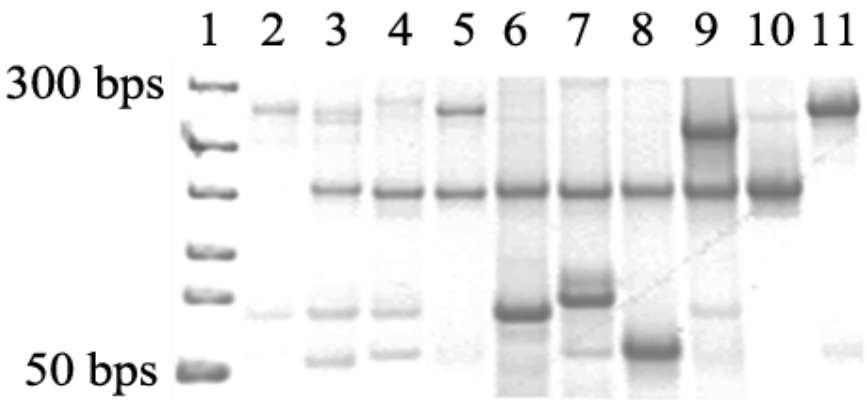

Figure 4.12 The electrophoretic pattern of primitive full-adder structure with input strands. Adder concentration is 2.5μM, A_{in} concentration is 10 μM, B_{in} concentration is 10 μM, C_{in} concentration is 10 μM, AA_{in} concentration is 10 μM and AB concentration is 10 μM. The gate-input ratio is 1:4. The full-adder structure is not purified.

1st lane = Ladder marker

2nd lane = Adder

3rd lane = Adder + A_{in}

4th lane = Adder + B_{in}

5th lane = Adder + C_{in}

6th lane = Adder + A_{in} + B_{in}

7th lane = Adder + A_{in} + C_{in}

8th lane = Adder + B_{in} + C_{in}

9th lane = Adder + A_{in} + B_{in} + C_{in}

10th lane = AA_{in}

11th lane = AB

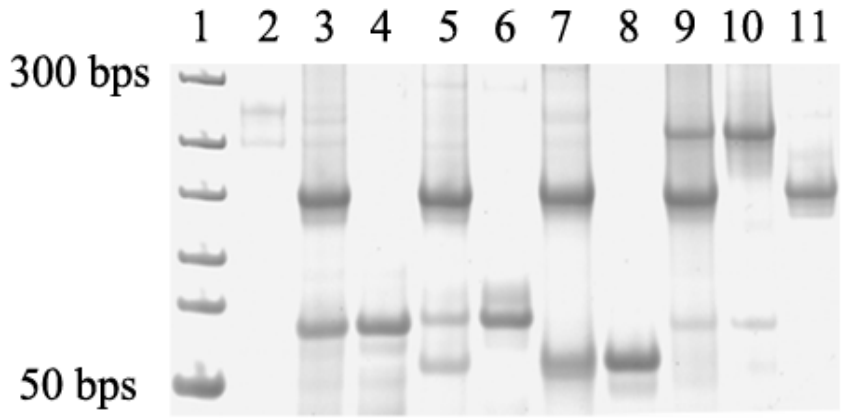

Figure 4.13 The electrophoretic result to confirm structure formation in 3-way-junction full-adder operation. Adder concentration is 2.5μM, A_{in} concentration is 10 μM, B_{in} concentration is 10 μM, C_{in} concentration is 10 μM, $A_{in}B_{in}$ complex concentration is 10 μM, $A_{in}C_{in}$ complex concentration is 10 μM, $B_{in}C_{in}$ complex concentration is 10 μM, $A_{in}B_{in}C_{in}$ complex concentration is 10 μM and AB concentration is 10 μM. The full-adder structure is not purified.

1st lane = Ladder marker

2nd lane = Adder

3rd lane = Adder +A_{in} + B_{in}

4th lane = $A_{in}B_{in}$ complex

5th lane = Adder +A_{in} + C_{in}

6th lane = $A_{in}C_{in}$ complex

7th lane = Adder +B_{in} + C_{in}

8th lane = $B_{in}C_{in}$ complex

9th lane = Adder +A_{in} + B_{in}+ C_{in}

10th lane = $A_{in}B_{in}C_{in}$ complex

11th lane = AB

According to the full adder structure result, the 8th condition, the presence of A_{in}, B_{in} and C_{in}, suggest the limitation of full adder circuit construction because of absent of output strand release. So, we further develop the new design in order to solve this issue.

4.4.2 Full-adder non-assembly system

Another system, non-assembly system, is developed to serve as the full-adder circuit. The full-adder non-assembly system is composed of 3 input strands, A_{e4} B_{e4} and $C_{e4,}$ which function distinctively. These input strands, A_{e4}, B_{e4} and C_{e4} strands, have 46 bases long with hairpin structure. The hairpin structure functions as container for CARRY input of the next bit which can be activated by short single-stranded DNA called "separator" (Figure 4.13). The hairpin structure of A_{e4}, B_{e4} and C_{e4} strands are unlocked by S_{Ce4}, S_{Ae4} and S_{Be4} respectively. The conditional addition of input strands and separator strands are matched into solution called "Solution A", "Solution B" and "Solution C" which represent Input A, Input B and Input C, respectively. The "Solution A" comprises of A_{e4} strand and S_{Ae4} strand. The "Solution B" comprises of B_{e4} strand and B_{Ae4} strand. The "Solution C" comprises of C_{e4} strand and C_{Ae4} strand. These matched solutions allow the non-assembly system to function as full-adder circuit. Illustration of components of Solution A, B and C is shown in Figure 4.14. The mechanism of non-assembly system as full-adder circuit is shown in Figure 4.15- 4.21.

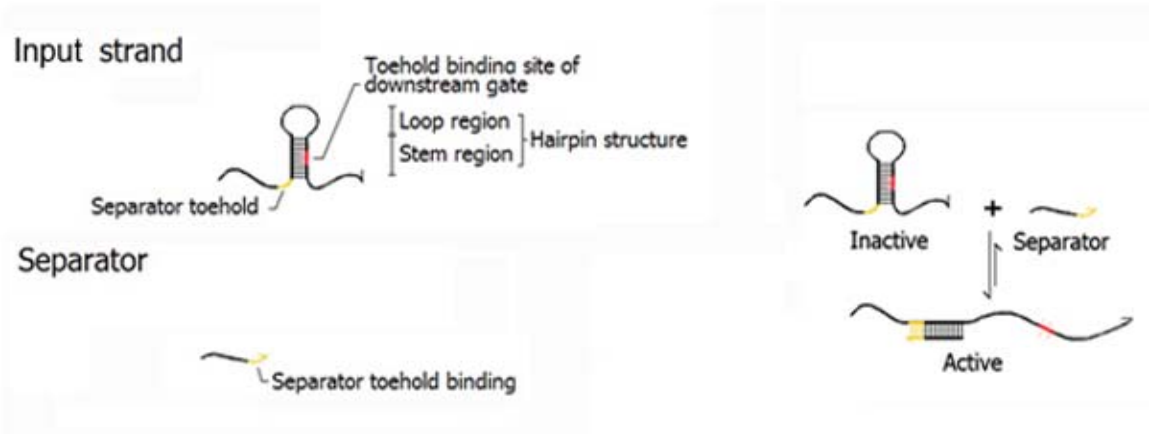

Figure 4.14 Illustration of full-adder non-assembly system component. The input strand with hairpin structure, 14-base pair stem and 14-base loop, with the CARRY.

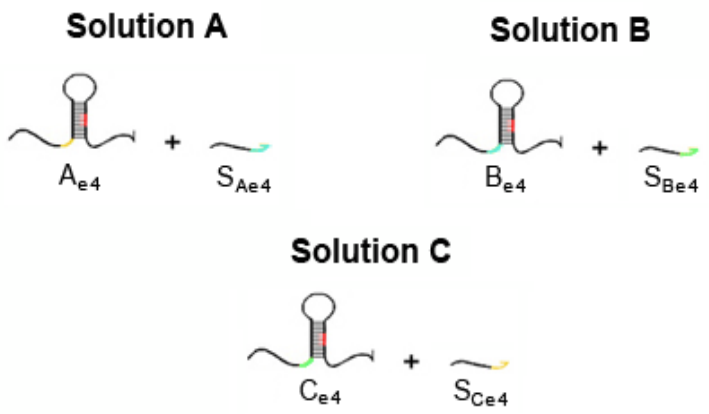

Figure 4.15 Illustration of components in Solution A, B and C. Solution A comprises of A_{e4} strand and S_{Ae4} separator strand. Solution B comprises of B_{e4} strand and S_{Be4} separator strand. Solution C comprises of C strand and S_{Ce4} separator strand.

Since the non-assembly full-adder system functions based on three inputs, so there are eight possible conditions to consider.

1st condition: No input

No input is added. The full adder DNA-based logic gate structure is intact. No single-stranded DNA is released from the structure.

2nd condition: Input A

No computation.

Figure 4.16 Schematic diagram of "2nd condition" of non-assembly full adder system.

3rd condition: Input B

No computation.

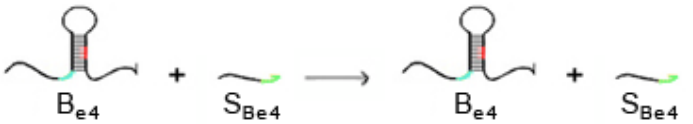

Figure 4.17 Schematic diagram of "3rd condition" of non-assembly full adder system.

4th condition: Input C

No computation.

Figure 4.18 Schematic diagram of "4th condition" of non-assembly full adder system.

5th condition: Input A and Input B

The S_{Ae4} strand of "Solution A" activates the B_{e4} strand of "Solution B"

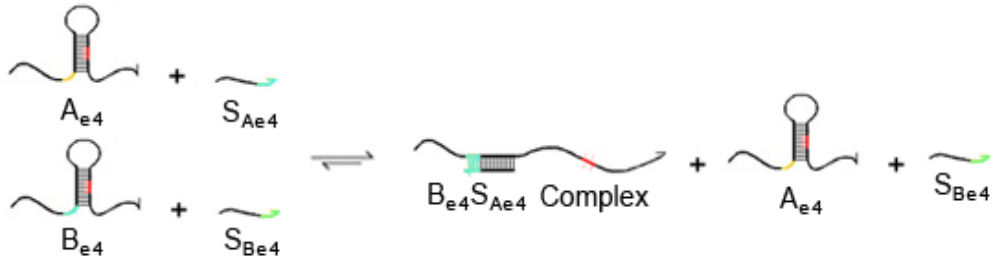

Figure 4.19 Schematic diagram of "5th condition" of non-assembly full adder system.

6th condition: Input A and Input C

The S_{Ce4} strand of "Solution C" activates the A_{e4} strand of "Solution A"

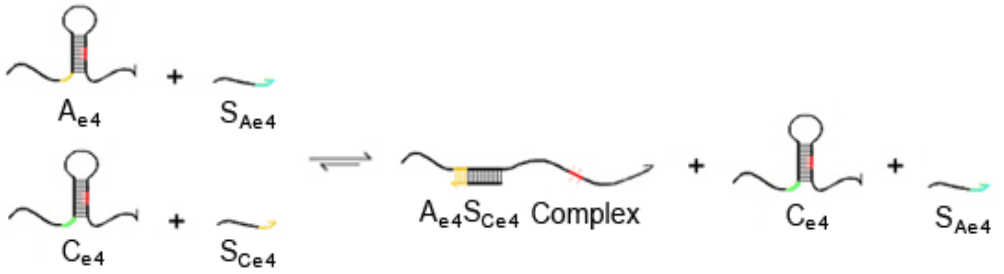

Figure 4.20 Schematic diagram of "6th condition" of non-assembly full adder system.

7th condition: Input B and Input C

The S_{Be4} strand of "Solution B" activates the C_{e4} strand of "Solution C"

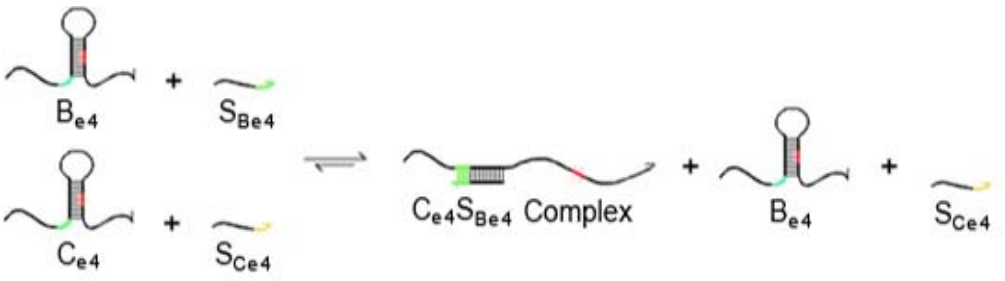

Figure 4.21 Schematic diagram of "7th condition" of non-assembly full adder system.

8th condition: Input A, Input B and Input C

The S_{Ae4} strand of "Solution A" activates the B_{e4} strand of "Solution B"

The S_{Ce4} strand of "Solution C" activates the A_{e4} strand of "Solution A"

The S_{Be4} strand of "Solution B" activates the C_{e4} strand of "Solution C"

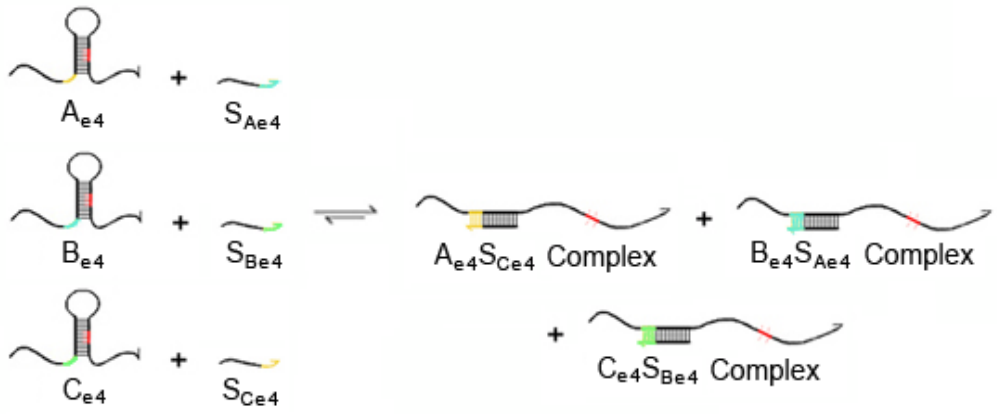

Figure 4.22 Schematic diagram of "8th condition" of non-assembly full adder system

The results of the non-assembly full-adder system are shown in Figure 4.23 and 4.24. Eight possible conditions were observed. For the first condition, no input has been added. Only reporter band is clearly detected. The second condition, reporter and Solution A were added to the computing process. A_{e4} band and S_{Ae4} band is clearly detected. The third condition, reporter and Solution B were added. B_{e4} band and S_{Be4} band is clearly detected. The fourth condition, reporter and Solution C were added. C_{e4} band and S_{Ce4} band is clearly detected. The fifth condition, reporter and Solution A and Solution B were added. Reduction of S_{Ae4} band was detected. The sixth condition, reporter and Solution A and Solution C were added. Reduction of reporter band and S_{Ce4} band were detected. The seventh condition, reporter and Solution B and Solution C were added. Reduction of reporter band and S_{Be4} band were detected. The eighth condition, reporter and Solution A, Solution B and Solution C were added. Reduction of reporter band S_{Ae4}, S_{Be4} and S_{Ce4} band were detected. The non-assembly full-adder system has been demonstrated in case of excess separator strand (R:C:S is 1:2:4) to observe the disturbance of S_{Be4} band on reporter gate band (Figure 4.24). The result shows the significant increase of reporter band intensity in the condition which S_{Be4} strand has been added to the computing solution (Figure 4.24, Lane 4, 5 and 8). The sequences of all oligonucleotides used in non-assembly full adder system are shown in Table 4.1.

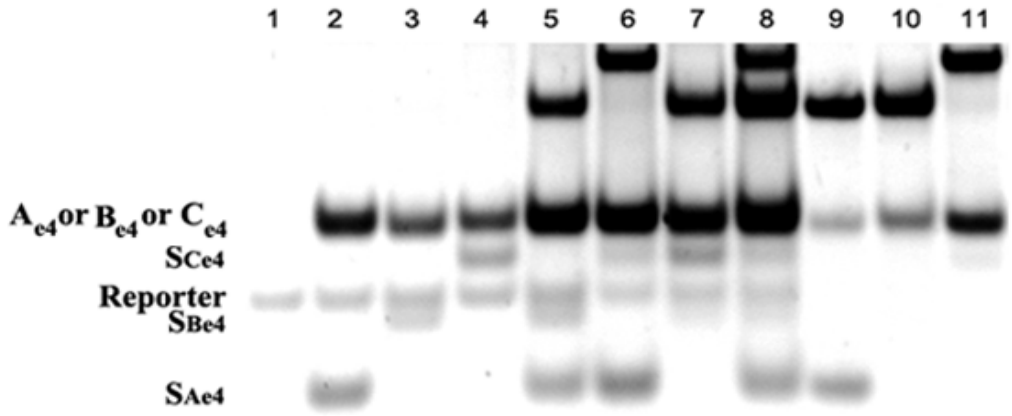

Figure 4.23 The electrophoretic pattern of non-assembly full-adder system with separator strands (1:2:2). Reporter concentration = 1 μM, A_{e4} concentration = 3μM, B_{e4} concentration = 3μM, C_{e4} concentration = 3μM, S_{Ae4} concentration = 6 μM, S_{Be4} concentration = 6 μM, S_{Ce4} concentration = 6 μM, $B_{e4}S_{Ae4}$ concentration = 6 μM, $C_{e4}S_{Be4}$ concentration = 6 μM, $A_{e4}S_{Ce4}$ concentration = 6 μM, Reporter-Input-Separator ratio is 1:2:2.

1st lane = Reporter

2nd lane = Reporter + A_{e4} + S_{Ae4}

3rd lane = Reporter + B_{e4} + S_{Be4}

4th lane = Reporter + C_{e4} + S_{Ce4}

5th lane = Reporter + A_{e4} + S_{Ae4} + B_{e4} + S_{Be4}

6th lane = Reporter + A_{e4} + S_{Ae4} + C_{e4} + S_{Ce4}

7th lane = Reporter + B_{e4} + S_{Be4} + C_{e4} + S_{Ce4}

8th lane = Reporter + A_{e4} + S_{Ae4} + B_{e4} + S_{Be4}+ C_{e4} + S_{Ce4}

9th lane = $B_{e4}S_{Ae4}$complex

10th lane = $C_{e4}S_{Be4}$ complex

11th lane = $A_{e4}S_{Ce4}$complex

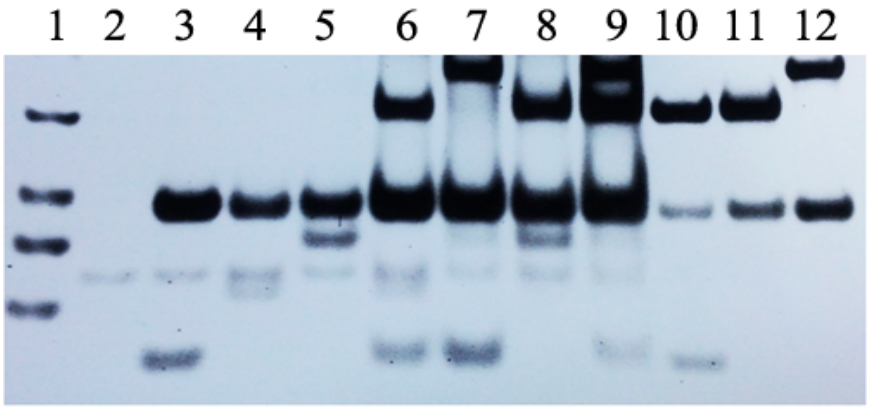

Figure 4.24 The electrophoretic pattern of non-assembly full-adder system with separator strands (1:2:4). Reporter concentration = 1 μM, A_{e4} concentration = 3μM, B_{e4} concentration = 3μM, C_{e4} concentration = 3μM, S_{Ae4} concentration = 6 μM, S_{Be4} concentration = 6 μM, S_{Ce4} concentration = 6 μM, $B_{e4}S_{Ae4}$ concentration = 6 μM, $C_{e4}S_{Be4}$ concentration = 6 μM, $A_{e4}S_{Ce4}$ concentration = 6 μM, Reporter-Input-Separator ratio is 1:2:4.

1st lane = Reporter

2nd lane = Reporter + A_{e4} + S_{Ae4}

3rd lane = Reporter + B_{e4} + S_{Be4}

4th lane = Reporter + C_{e4} + S_{Ce4}

5th lane = Reporter + A_{e4} + S_{Ae4} + B_{e4} + S_{Be4}

6th lane = Reporter + A_{e4} + S_{Ae4} + C_{e4} + S_{Ce4}

7th lane = Reporter + B_{e4} + S_{Be4} + C_{e4} + S_{Ce4}

8th lane = Reporter + A_{e4} + S_{Ae4} + B_{e4} + S_{Be4}+ C_{e4} + S_{Ce4}

9th lane = $B_{e4}S_{Ae4}$complex

10th lane = $C_{e4}S_{Be4}$ complex

11th lane = $A_{e4}S_{Ce4}$complex

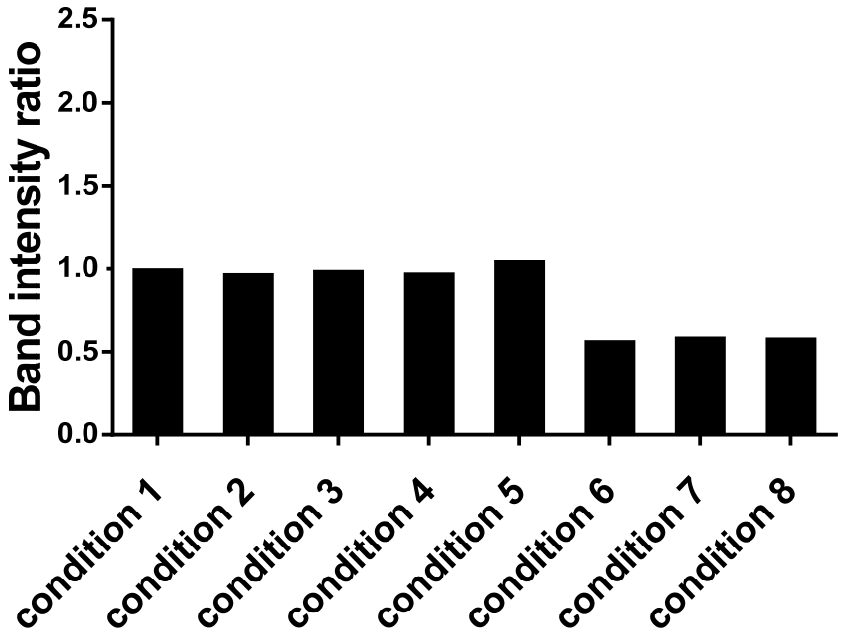

Figure 4.25 The comparison of CARRY function via band intensity ratio of reporter. The CARRY function is clearly detected in condition 6, 7 and 8 while CARRY is unable to function in condition 2, 3 and 4 compare to the control condition 1.

4.5 Discussion of the full-adder structure

Here we introduced the DNA-based full-adder circuit in two designs, the full-adder structure and non-assembly system. According to the first design, the full-adder structure is able to perform full-adder operation. Since this design produces no output strands, it is unable to function in term of cascading circuit, in other words, multi-bit addition operation is not possible. The second design, non-assembly system, is developed in order to deal with this problem. The non-assembly full-adder system is developed based on separator system (detail in Chapter 2). The non-assembly full-adder system is composed of three independent input strands with shared CARRY sequence inside the hairpin structure of each input strand. In the real situation, all inactive strands A_{e4}, B_{e4} and C_{e4} of all bits are ready to function in the computing solution. Only separator strands are added to the solution on demand. Whenever the CARRY data is activated by the added separator strand (condition 5-8), the sequence of CARRY data immediately functions as separator strand of "Inactive strand C" of next bit addition operation. According to these procedures, the non-assembly full-adder system is considered to perform multi-bit addition operation completely in enzyme-free cascading circuit.

CHAPTER V
CONCLUSION

5.1 Development of DNA signal synchronization system

The possibility of synchronizing DNA-based logic gate operations to resemble the use of clock signaling in conventional computer digital logic circuit was demonstrated in our work (Chapter 2). The Output signal from an upstream logic gate in cascading circuit (intending to be the input for the next downstream gate) will be encoded in a DNA strand that spontaneously fold into a hairpin structure that is in an inactive state (Figure 3.2). It will wait until a clock signal, the separator, is present and activates it by linearization of the hairpin structure. In this linearized complex form, the input data signal region for the downstream gate will be exposed which is concerned as activated state and ready to interact with downstream gates having toehold region matching the signal. Here we have observed the function of separator system in two aspects, data blockage and separator activation level. The experiments were demonstrated to observe the optimal length of stem and loop region. abd the result shows 14-base-stem structure is the optimal structure for both data blockage and separator function. To fully operate a complete conventional digital circuit, separators must be entered into the system at appropriate time in the manner similar to how clock crystal in silicon-based processor periodically regulates logic operation cycle (clock cycle). Possible benefits of our work include the construction of a robust XOR gate which requires an assurance that both input signals are present simultaneously. However, there is a limitation in the size of the output signal that our system can deliver and leakage can happen in some settings. Our findings show that the data size should not be greater than 14 bases (Figure 3.5 and 3.6) and the stem length should be about 14 bases long including the toehold binding region (Figure 3.4). The length of the separator strand can be extended to increase the stability of the linearized structure to improve the performance of our system

5.2 Development of DNA-based XOR logic gate

Here we introduce the DNA-based XOR logic gate design utilizing DNA palindromic sequence. Our design is compatible to enzyme-free cascading circuit design developed by Seelig et al. According to our logic gate design, two gate strands, X or Y, are able to function separately as output strand of XOR operation. As a consequence, the output strand, X or Y, will bind to toehold binding region of downstream logic gate with the palindromic motif. However, the first design of dangling end $X_{in}Y_{in}$ complex (Figure 2.4) results in 41.3% leakage via cross-activation between $X_{in}Y_{in}$ complex itself and the DNA-based XOR logic gate (Figure 2.16). In the second design, we attempted to reduce the cross-activation by adding the complementary sequence to the toehold binding region (Figure 2.12). The blunt-end $X_{in}Y_{in}$ complex design minimizes the cross-activation down to 15% (Figure 2.16). We further improved the design by clamping the $X_{in}Y_{in}$ complex with extra seven base pairs. The leakage of clamp-end $X_{in}Y_{in}$ complex slightly reduces to 7.1% (Figure 2.16). According to these designs, we succeed on developing XOR logic gate and accidentally OR logic gate. We, therefore, are able to apply the XOR logic gate, XY structure, into circuit to function as an alternative logic gate of XOR-OR logic gate relying on the conformation of input strands complex. The success of DNA-based XOR logic gate development would benefit various circuit designs for solving complex tasks, full-adder circuit for example.

5.3 Development of DNA-based full-adder operation

With the success on XOR DNA-based logic gate development, we further developed novel designs which are not rely on the cascading circuit design. We introduce two designs, the full-adder structure and non-assembly system circuit. The results of the first design, the full-adder structure, are the consistent result with the hypothesis of full-adder truth table. However, this design is incompatible to function in cascading circuit since there is no output strand. So, we further developed the second design, the non-assembly system, to solve the multi-bit addition operation. The non-assembly system is embedded with the separator system in order to control state of input strand, A_{e4} B_{e4} and C_{e4}, into an active or inactive form via the short single-

stranded DNA called separator. The systematically impletion of three separator strands with three input strands allow this system to function similar to 1-bit addition operation. Since the activation of input strand is considered as output of the system, this 1-bit addition system is able to link to other 1-bit addition systems and form into circuit with multi-bit addition operation. According to the success of DNA-based full-adder circuit development, the capability of multi-bit addition operation would suggest the possibility to develop even more complex circuit like multiplier circuit based on our full-adder design.

CHAPTER VI
FUTURE WORKS

6.1 Development of DNA-based multiplier circuit

According to our success on DNA-based full-adder system development, we further move forward to multiplier circuit development. Technically, basis of multiplier operation is repetition of addition operation. So, we apply this concept to the multiplier circuit design. As we consider the following digit multiplication,

$$3 \times 2 = 6$$

This digit multiplication can be converted into bit multiplication as the following equation,

$$11 \times 10 = 110$$

The equation can be shown as the factorizing equation of the bit multiplication operation as shown in the following equation,

$$(10 + 01) \times (10) = 110$$

$$(10 \times 10) + (01 \times 10) = 110$$

However, the equation can be solved by lattice multiplication technique shown in Figure 5.1.

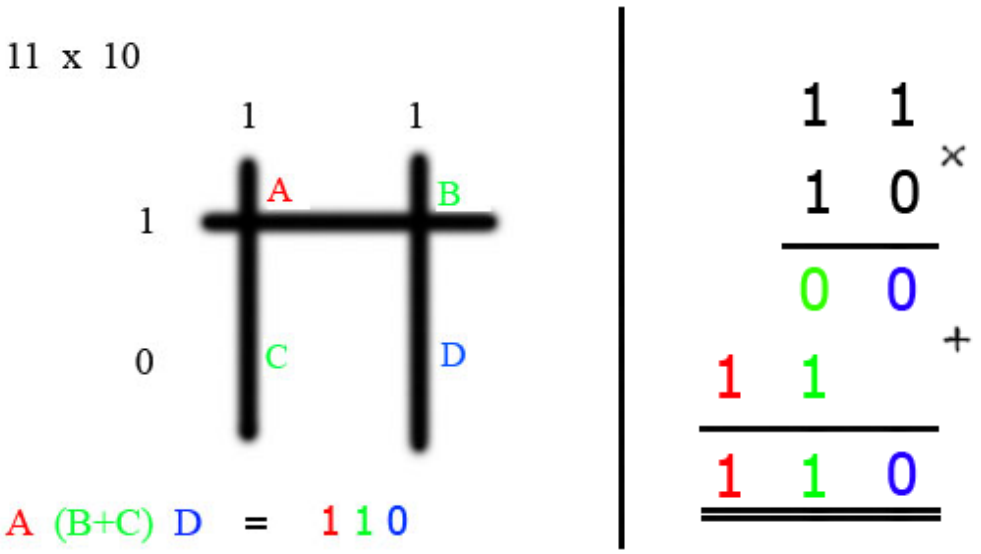

Figure 6.1 Schematic representation of 2-bit lattice multiplication technique. The different colors imply the relation between lattice multiplication (left) and common multiplication (right). The present of cross of vertical line and horizontal line or the present of intersection means "1" while an absence of intersection means "0" (left). The Common form of multiplication with underlying lattice multiplication technique. The multiplication of all binary numbers are matched one by one. All 1-bit multiplication results is summed up as the last computing process in order to give out the final result (right).

The lattice multiplication technique comprises of 2 parts: 1-bit multiplication operation and multi-bit summation operation. If we look at pattern of the 1-bit multiplication operation, there are four possible conditions;

$$0 \times 0 = 0$$
$$0 \times 1 = 0$$
$$1 \times 0 = 0$$
$$1 \times 1 = 1$$

The pattern of 1-bit multiplication operation shows the same pattern as the AND Boolean logic operation. In other words, the application of DNA-based AND logic gate is possible for the 1-bit multiplication operation. The multi-bit summation

operation is another point to concern. Since we have developed the non-assembly DNA-based full-adder system which is able to perform full-adder operation, the system can be applied as a part of the multiplier circuit.

According to these principles, it suggests possibility to design the multi-bit multiplier circuit based on AND logic gate and non-assembly DNA-based full-adder system.

6.2 Development of DNA-based NOT logic gate

Our success on separator system development allows researchers to design variety of synchronizing circuits. As we consider about the function of separator system, the system has partial function of NOT logic gate which turns the inactive input strand (OFF) into activated input strand (ON). We, therefore, are interested in developing the NOT logic gate with underlying mechanism of the separator system. Since the mechanism of DNA binding in the separator system is based on thermodynamics, it is impossible to design the circuit with only separator strand and controlled strand to function in two ways, turns ON and OFF. We, therefore, come up with the idea of competitor strand. Actually, competitor strand has been introduced by scientists for long time known as "fuel" [38, 41, 44].

As its name, the fuel strand functions on competitive binding to the intermediate structure of the enzyme-free DNA-based recycling circuit, resulting in the release of the initial workable input strand that is compatible with the main circuit. Here, we are going to apply the "fuel" to the separator system. According to the design of the separator system, the activated controlled strand is the complex of separator strand and controlled strand itself. When we want to switch the signal from ON to OFF, we would have to add the fuel strand with highly competitive capability to bind with the separator strand against the controlled strand. As the separator strand is sequestrated from the controlled strand, the controlled strand will form the hairpin structure and the toehold binding region is concealed. We might consider this process as "ON into OFF". The development of NOT logic gate compatible to cascading circuit suggests the variety of circuit designs for complex tasks.

REFERENCES

[1] Dahm R. Discovering DNA: Friedrich Miescher and the early years of nucleic acid research. Hum Genet 2008;122:565-81.

[2] Jones ME. Albrecht Kossel, a biographical sketch. Yale J Biol Med 1953;26:80-97.

[3] Levene PA. The structure of yeast nucleic acid: IV. Ammonia hydrolysis. J Biol Chem 1919;40:415-24.

[4] Watson JD, Crick FHC. A structure for deoxyribose nucleic acid. Nature 1953;171:737-8.

[5] Wilkins MHF, Stokes AR, Wilson HR. Molecular structure of deoxypentose nucleic acids. Nature 1953;171:738-40.

[6] Franklin RE, Gosling RG. Molecular configuration in sodium thymonucleate. Nature 1953;171:740-1.

[7] Watson JD, Crick FHC. Genetical implications of the structure of deoxyribonucleic acid. Nature 1953;171:964-7.

[8] Franklin RE, Gosling RG. Evidence for 2-chain helix in crystalline structure of sodium deoxyribonucleate. Nature 1953,172:156-7.

[9] Avery OT, MacLeod CM, McCarty M. Studies on the chemical nature of the substance inducing transformation of Pneumococcal types. J Exp Med 1944;79:137-58.

[10] Kuure-Kinsey M, McCooey B. The basics of recombinant DNA [Internet]. 2000 [cited 2014 March 27]. Available from: http://www.rpi.edu/dept/chem-eng/Biotech-Environ/Projects00/rdna/rdna.html

[11] Wikipedia. DNA chemical structure [Internet]. 2013 [cited 2014 March 27]. Available from: http://en.wikipedia.org/wiki/File:DNA_chemical_structure.svg

[12] Muller M. BIOS 100 Summer 2010 [Internet]. 2010 [cited 2014 March 27]. Available from: http://www.uic.edu/classes/bios/bios100/lectures/n-bases.jpg

[13] Wikipedia. A-DNA, B-DNA and Z-DNA [Internet]. 2012 [cited 2014 March 27]. Available from: http://en.wikipedia.org/wiki/File:A-DNA,_B-DNA_and_Z-DNA.png

[14] Krylov A. [Internet]. California: Department of Chemistry, University of Southern California [updated 2014; cited 2014 March 27]. Available from: http://chem.usc.edu/faculty/Krylov.html

[15] Citrus College Online Learning Center. Biology [Internet]. California: Citrus College [updated 2014, cited 2014 March 27]. Available from: http://www.citruscollege.edu/lc/archive/biology/PublishingImages/0243l.jpg

[16] Breslauer KJ, Frank R, Blöcker H, Marky LA. Predicting DNA duplex stability from the base sequence. Proc Natl Acad Sci USA 1986;83:3746-50.

[17] SantaLucia J Jr, Hicks D. The thermodynamics of DNA structural motifs. Annu Rev Biophys Biomol Struct 2004;33:415-40.

[18] Jaeger JA, SantaLucia J Jr, Tinoc I Jr. Determination of RNA structure and thermodynamics. Annu Rev Biochem 1993;62:255-87.

[19] Frank-Kamenetskii MD, Mirkin SM. Triplex DNA structures. Annu Rev Biochem 1995;64:65-95.

[20] Wikipedia. Stem-loop [Internet]. 2006 [cited 2014 March 27]. Available from: http://en.wikipedia.org/wiki/File:Stem-loop.svg

[21] Barleyworld.org [Internet]. Oregon: Oregon State University; c2014 [cited 2014 Match 27]. Available from: http://barleyworld.org/plantgen/from-rna-to-protein-3

[22] Wikipedia. Holliday Junction [Internet]. 2007 [cited 2014 March 27]. Available from: http://en.wikipedia.org/wiki/File:Holliday_junction_coloured.png

[23] Sciencedaily.com [Internet]. Maryland: ScienceDaily, c2014 [cited 2014 March 27]. Available from: http://images.sciencedaily.com/2012/04/120418095315-large.jpg

[24] Wikipedia. Hoogsteen [Internet]. 2011 [cited 2014 March 27]. Available from: http://en.wikipedia.org/wiki/File:Hoogsteen.png

[25] Monchaud D, Teulade-Fichou MP. A hitchhiker's guide to G-quadruplex ligands. Org Biomol Chem 2008;6:627-36.

[26] Mass Spectrometry Research at WU [Internet]. St. Louis: Department of Chemistry, Washington University [updated 2014; cited 2014 March 27]. Available from:

http://www.chemistry.wustl.edu/~coursedev/Online%20tutorials/Atomic%20Mass/masspec.htm

[27] Adleman LM. Molecular computation of solutions to combinatorial problems. Science 1994;266:1021-4.

[28] Lipton RJ. DNA solution of hard computational problems. Science 1995;268:542-5.

[29] Sakamoto K, Gouzu H, Komiya K, Kiga D, Yokoyama S, Yokomori T, et al. Molecular computation by DNA hairpin formation. Science 2000;288:1223-6.

[30] Braich RS, Chelyapov N, Johnson C, Rothemund PWK, Adleman LM. Solution of a 20-variable 3-SAT problem on a DNA computer. Science 2002;296:499-502.

[31] Stojanovic MN, Mitchell TE, Stefanovic D. Deoxyribozyme-based logic gates. J Am Chem Soc 2002;124:3555-61.

[32] Fedichkin L, Katz E, Privman V. Error correction and digitalization concepts in biochemical computing. J Comput Theor Nanosci 2008;5:36-43.

[33] Voelcker NH, Guckian KM, Saghatelian A, Ghadiri MR. Sequence-addressable DNA logic. Small 2008;4:427-31.

[34] Lee CS, Davis RW, Davidson N. A Physical study by electron microscopy of the terminally repetitious, circularly permuted DNA from the coliphage particles of *Escherichia coli* 15. J Mol Biol 1970;48:1-22.

[35] Reynaldo LP, Vologodskii AV, Neri BP, Lyamichev VI. The kinetics of oligonucleotide replacements. J Mol Biol 2000;297:511-20.

[36] Quartin RS, Plewinska M, Wetmur JG. Branch migration mediated DNA labeling and cloning. Biochemistry 1989;28:8676-82.

[37] Wong DM, Weinstock PH, Wetmur JG. Branch capture reactions: displacers derived from asymmetric PCR. Nucleic Acids Res 1991;19:2251-9.

[38] Yurke B, Turberfield AJ, Mills AP Jr, Simmel FC, Neumann JL. A DNA-fuelled molecular machine made of DNA. Nature 2000;406:605-8.

[39] Yurke B, Mills AP Jr. Using DNA to power nanostructures. Genet Program Evol M 2003;4:111-22.

[40] Zhang DY, Winfree E. Control of DNA strand displacement kinetics using toehold exchange. J Am Chem Soc 2009;131:17303-14.

[41] Turberfield AJ, Mitchell JC, Yurke B, Mills AP Jr, Blakey MI, Simmel FC. DNA fuel for free-running nanomachines. Phys Rev Lett 2003;90:118102.

[42] Dirk RM, Pierce NA. Triggered amplification by hybridization chain reaction. Proc Natl Acad Sci USA 2004;101:15275-8.

[43] Yin P, Choi HMT, Calvert CR, Pierce NA. Programming biomolecular self-assembly pathways. Nature 2008;451:318-22.

[44] Seelig G, Soloveichik D, Zhang DY, Winfree E. Enzyme-free nucleic acid logic circuits. Science 2006;314:1585-8.

[45] Qian L, Winfree E. A simple DNA gate motif for synthesizing large-scale circuits. J R Soc Interface 2011;8:1281-97.

[46] Qian L, Winfree E. Scaling up digital circuit computation with DNA strand displacement cascades. Science 2011;332:1196-201.

BIOGRAPHY

NAME	Mr. Peerapat Intaluck
DATE OF BIRTH	March 13, 1987
PLACE OF BIRTH	Chonburi, Thailand
INSTITUTIONS ATTENDED	Mahidol University, 2009: Bangkok, Thailand Bachelor of Science (Medical Science) Mahidol University, 2009-2013 Doctor of Philosophy (Biotechnology)
SCHORLARSHIP RECEIVED	Medicals Scholars Program (MSP) Year 2009-2013 Mahidol University
HOME ADDRESS	27/52 Sukhumvit Road, Bansuan, Muang Chonburi, Thailand 20000 Tel: 081-771-2252 E-mail: valkyrie_patt@yahoo.com
PRESENTATION	Oral presentation: “Gate Formation in DNA Computing” in “The Tenth Science Project Exhibition” March 13, 2009, Mahidol University, Bangkok, Thailand.